

2005

Modifications of spacetime and particle physics beyond the standard model

Justin M. Conroy
College of William & Mary - Arts & Sciences

Follow this and additional works at: <https://scholarworks.wm.edu/etd>



Part of the [Physics Commons](#)

Recommended Citation

Conroy, Justin M., "Modifications of spacetime and particle physics beyond the standard model" (2005). *Dissertations, Theses, and Masters Projects*. Paper 1539623481. <https://dx.doi.org/doi:10.21220/s2-314k-w853>

This Dissertation is brought to you for free and open access by the Theses, Dissertations, & Master Projects at W&M ScholarWorks. It has been accepted for inclusion in Dissertations, Theses, and Masters Projects by an authorized administrator of W&M ScholarWorks. For more information, please contact scholarworks@wm.edu.

NOTE TO USERS

This reproduction is the best copy available.

UMI[®]

MODIFICATIONS OF SPACETIME AND PARTICLE PHYSICS BEYOND
THE STANDARD MODEL

A Dissertation

Presented to

The Faculty of the Department of Physics
The College of William and Mary in Virginia

In Partial Fulfillment

Of the Requirements for the Degree of
Doctor of Philosophy

by

Justin M. Conroy

2005

UMI Number: 3201114

INFORMATION TO USERS

The quality of this reproduction is dependent upon the quality of the copy submitted. Broken or indistinct print, colored or poor quality illustrations and photographs, print bleed-through, substandard margins, and improper alignment can adversely affect reproduction.

In the unlikely event that the author did not send a complete manuscript and there are missing pages, these will be noted. Also, if unauthorized copyright material had to be removed, a note will indicate the deletion.

UMI[®]

UMI Microform 3201114

Copyright 2006 by ProQuest Information and Learning Company.

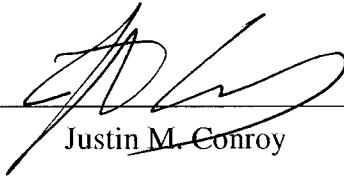
All rights reserved. This microform edition is protected against unauthorized copying under Title 17, United States Code.

ProQuest Information and Learning Company
300 North Zeeb Road
P.O. Box 1346
Ann Arbor, MI 48106-1346

APPROVAL SHEET


This dissertation is submitted in partial fulfillment of
the requirements for the degree of

Doctor of Philosophy




Justin M. Conroy


Approved by the Committee, August 2005



Christopher D. Carone, Chair



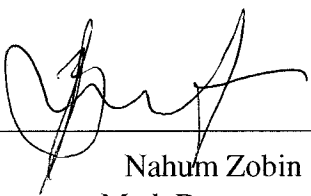
Carl E. Carlson



Joshua Erlich



Marc Sher



Nahum Zobin
Math Department

DEDICATION

I present this dissertation in honor of my parents, James and Sharonlee Conroy.

Table of Contents

Acknowledgments	vi
List of Tables	vii
List of Figures	viii
Abstract	x
CHAPTER	
1 Introduction	2
1.1 The Standard Model: Successes and Shortcomings	2
1.2 Going Beyond the Standard Model	6
2 Phenomenology of Lorentz-Conserving Noncommutative QED	14
2.1 Introduction	14
2.2 Algebra and QED Formulation	16
2.3 Collider Signatures	22
2.3.1 Dilepton Production, $e^+e^- \rightarrow l^+l^-$	23
2.3.2 Møller Scattering	25
2.3.3 Diphoton Production, $e^+e^- \rightarrow \gamma\gamma$	26
2.4 Bounds on Λ_{NC} from colliders	28
2.5 Conclusion	31
3 Universal Extra Dimensions and Kaluza-Klein Bound States	32
3.1 Introduction	32
3.2 UED	35

3.3	Bound States	39
3.3.1	Decay widths and branching ratios	40
3.3.2	Production cross-sections	44
3.3.3	Mass Splittings	45
3.4	Detection	48
3.5	Conclusions	51
3.6	Decay Width Formulae	52
4	Higgsless GUT Breaking and Trinification	54
4.1	Introduction	54
4.2	Framework	57
4.3	Symmetry Breaking	61
4.4	Gauge Unification	68
4.5	Other Possibilities	71
4.6	Conclusions	75
5	Improved Trinification in 5D	76
5.1	Introduction	76
5.2	$SU(3)^3 \times Z_3$	77
5.3	$SU(9) \times SU(3)^3$	86
5.4	Conclusions	88
	Bibliography	90
	Vita	100

ACKNOWLEDGMENTS

It is with great pleasure that I thank my advisor Christopher D. Carone for always providing inspiration and exciting research topics. I'd like to thank him for his guidance over the past five years.

I would like to thank my wonderful wife Jen for her infinite amount of patience, love, and support.

I would also like to thank my collaborators and the entire Particle Theory Group for making my work over the past five years such an enjoyable experience.

Four friends and fellow graduate students deserve special mention. I want to thank Herry Kwee, Josh Moss, Jeff Secrest, and Keoki Seu for their friendship and the many physics discussions over the years.

I'd also like to thank my undergraduate advisor, Bulent Atalay, for inspiring me to go into this field.

Finally, I would like to express my gratitude to my parents for their unconditional love and encouragement.

LIST OF TABLES

2.1	Bhabha Scattering: Data from L3 experiment and SM Prediction[1] . . .	29
2.2	$e^+e^- \rightarrow \mu^+\mu^-$: Data from L3 experiment and SM Prediction [1]	30
3.1	The partial decay width of $V \rightarrow e^+e^-$ for both isodoublet and isosinglet KK-quark bound states	45
3.2	Energy shifts and radial wave functions at the origin computed numerical assuming the potential in Eq. (3.28). The parameter a_0 here is $1/(\mu\alpha_s)$, where $\mu = M_{KK}/2$ is the reduced mass. The last two columns show the result obtained when neglecting the linear term in the potential.	48
4.1	$SU(3)^3$ reps in the product of two trinified 27 -plets containing Standard Model singlet components, with hypercharge defined as in Eq. (4.33). Parentheses delimit indices that are symmetric.	66
4.2	Contributions to the beta function coefficients from the zero modes (b_i) and the KK levels (\tilde{b}_i) in our minimal scenario. Here Φ represents a chiral multiplet in the adjoint rep.	69
5.1	Contributions to the beta function coefficients from the zero modes (b_i) and the KK levels (\tilde{b}_i). Here the Φ represent chiral multiplets in the adjoint representation. Results in the second and third lines represent sums over all fields with the stated quantum numbers.	85

LIST OF FIGURES

1.1	Spectrum of the first massive KK modes in the UED model [2]	12
2.1	2-fermions-1-photon vertex.	24
2.2	Bhabha Scattering.	24
2.3	Two fermions - two photon vertex.	27
2.4	Feynman diagrams for $e^+e^- \rightarrow \gamma\gamma$	27
3.1	The mass splitting between KK-quarks and the LKP, $\gamma^{(1)}$, as well as the splitting between the weak KK-gauge bosons and the LKP, as a function of $1/R$ for $\Lambda R = 20$. Here, Q_L stands for all isodoublet KK-quarks except top, u_R for up and charm isosinglet KK-quarks, and d_R for down, strange and bottom isosinglet KK-quarks	39
3.2	The production and decay chains of $q_R^{(1)}$ and $q_L^{(1)}$ pairs. Note that all of the decays in the $q_L^{(1)}$ decay chain are two-body, leading to monochromatic quarks and leptons.	40
3.3	The total decay width of $n = 1$ isosinglet and isodoublet down KK-quarks as a function of R^{-1} for fixed $\Lambda R = 5, 10, 20$. The solid lines represent the total decay widths of isodoublet down KK-quarks for each corresponding ΛR value, respectively. The dashed lines are for the isosinglet case. The isodoublet up KK-quark total decay width is equal to that of the down and the isosinglet up KK-quark's width is four times larger than that of the isosinglet down.	42

3.4	The resonance production cross section for isodoublet KK-quarkonia states, except KK-toponium, as a function of R^{-1} for $\lambda R = 5, 20$. The solid lines represent down type KK-quarkonia states and the dashed ones represent up-type KK-quarkonia states, and the upper (lower) lines correspond to $\lambda R = 5$ (20).	46
3.5	The same as Fig. 3.4 but for isosinglet KK-quarkonia states. Here the upper (lower) lines correspond to $\lambda R = 20$ (5).	47
3.6	The cross section for KK-quarkonia formed by isosinglet KK-quarks as a function of \sqrt{s} for $1/R = 500$ GeV and $\Lambda R = 20$. The labels V^D refer to the bound states of isosinglet KK-down, KK-strange and KK-bottom quarks, while V^U refers to the bound states of isosinglet KK-up and KK-charm quarks.	49
3.7	The cross section for KK-quarkonia formed by isodoublet KK-quarks as a function of \sqrt{s} for $1/R = 500$ GeV and $\Lambda R = 20$. The label V^Q refers to all of the isodoublet KK-quarks, except for the KK-top.	50
3.8	The cross section for KK-quarkonia formed by isosinglet KK-quarks as a function of \sqrt{s} for $1/R = 300$ GeV and $\Lambda R = 20$. The labels are the same as in the previous figures.	51
3.9	The cross section for KK-quarkonia formed by isodoublet KK-quarks as a function of \sqrt{s} for $1/R = 300$ GeV and $\Lambda R = 20$. The labels are the same as in the previous figures.	52
4.1	Gauge unification for $M_c = 4 \times 10^{15}$ GeV.	70
4.2	Unification and 5D Planck scales as functions of M_c . For definitions of scales, see the text.	71

ABSTRACT

In this dissertation we consider spacetime modifications that result in new physics beyond the standard model. We investigate various collider implications of a particular Lorentz-conserving formulation of QED in which spacetime coordinates are noncommuting. We also consider collider implications of Universal Extra Dimensions. Specifically, we address the possible formation of bound states involving the first quark KK-modes, *i.e.* KK-quarkonium. In addition, we consider the use of boundary conditions in extra dimensions to break gauge symmetries in unified theories. These boundary conditions can be related to a boundary Higgs sector that decouples from the theory. This technique of “Higgsless” symmetry breaking is applied to several models based on the trinified gauge group $G_T = SU(3)_C \times SU(3)_L \times SU(3)_R$. In addition, we analyze various phenomenological issues such as coupling unification and proton decay.

MODIFICATIONS OF SPACETIME AND PARTICLE PHYSICS BEYOND THE
STANDARD MODEL

CHAPTER 1

Introduction

1.1 The Standard Model: Successes and Shortcomings

The Standard Model of particle physics has proven to be a remarkably successful theory. Its predictions have matched experimental results with unprecedented accuracies and with few, if any, discrepancies. This high level of success is particularly true with regard to accelerator-based experiments making it clear that the Standard Model is the correct theory of nature from the length scales of atomic physics down to roughly 10^{-18} m.

One area which has demonstrated remarkable agreement between standard model theory and experiment has been the precision tests of QED, in particular the precise measurements of the Lamb shift and the anomalous magnetic moment of the electron [3]. In addition, some of the most notable accomplishments of the standard model have been the prediction and discovery of the W and Z bosons, as well as the precision measurements of their masses and decay widths [4].

Although the standard model has been remarkably successful, there is little reason to believe it to be the ultimate theory of nature. One shortcoming of the standard model is the numerous parameters such as couplings, masses, and mixing angles that must be

inserted by hand. One would hope that a complete theory would uniquely determine most or all of these parameters.

The standard model is also incapable of accommodating massive neutrinos, if the theory is defined such that lepton number is conserved. However, results over the last several years on solar and atmospheric neutrino oscillations convincingly demonstrate that neutrinos are in fact massive although extremely light. There are simple extensions of the standard model which allow for neutrino masses, but they are extensions nonetheless and cannot be attributed to the standard model itself. Besides the issue of how to give mass to the neutrinos, one also has to explain why they are so light. This is typically attributed to a new large mass scale. Clearly, neutrino physics requires there to be some new physics beyond the standard model.

There are also several cosmological issues that cannot be reconciled with the standard model. For example, recent data suggests the existence of dark matter, which cannot be explained using standard model particle content and interactions. Other cosmological issues that lie beyond the standard model are the baryon asymmetry in the Universe and Dark Energy [5].

More generally, an unattractive feature of the standard model is that it does not take gravity into account. One would expect that a fundamental theory of nature would accommodate gravity as well. String theory, which appears to be a promising candidate for such a Theory of Everything, suggests many specific ideas of what physics might exist beyond the standard model. As we will discuss later, many of the ideas that are investigated in this thesis are motivated by string theory:

Perhaps the most troubling issue of the standard model is that of Electroweak symmetry breaking (EWSB), which we briefly review. In the standard model, EWSB is gen-

erated by an $SU(2)$ weak Higgs doublet

$$H = \begin{pmatrix} H^+ \\ H^0 \end{pmatrix} \quad (1.1)$$

with hypercharge $Y = +1/2$. For the potential

$$V = m^2 H^\dagger H + \frac{\lambda}{2} (H^\dagger H)^2, \quad (1.2)$$

with $m^2 < 0$ the Higgs doublet develops a vacuum expectation value (vev)

$$\langle H^\dagger H \rangle = -\frac{m^2}{\lambda} \equiv \frac{v^2}{2} \quad (1.3)$$

which breaks the standard model gauge symmetry $SU(2)_w \times U(1)_Y$ down to $U(1)_{EM}$.

The parameters m and λ cannot be determined by the standard model. Rather, the vev v is obtained from the experimentally measured values of the W and Z masses which gives

$v = 246$ GeV. In other words, the standard model does not determine the scale of EWSB.

In addition, the individual parameters λ and m remain free parameters of the theory. No experiment has yet to find the Higgs boson and its mass is not predicted by the standard model. Current bounds place its mass to lie in the range $114 \text{ GeV} < m_h < 300 \text{ GeV}$ [4].

In 2007, the Large Hadron Collider (LHC) will turn on and probe energies between 1 and 10 TeV, which offers the promising possibility of discovering the Higgs boson. One might wonder if it is most likely then that the LHC will simply reveal this minimal model of the standard model gauge group spontaneously broken by a Higgs doublet, and that no new physics beyond the standard model will be discovered. However, the EWSB sector itself not only offers reasons to believe that there is new physics beyond the standard model, but that this new physics should be detectable within the energy range probed by the LHC.

This reasoning follows directly from the mass of the Higgs boson. Consider the addition of the following mass term for the Higgs doublet to the standard model Lagrangian,

$$\mathcal{L} \supset -m_h^2 H^\dagger H. \quad (1.4)$$

This term is invariant under all the symmetries of the standard model and can easily accommodate a Higgs mass in the allowed range given above. On the other hand, what prevents m_h from being at the Planck scale $\sim 10^{18}\text{GeV}$? Even if the Higgs mass is set to zero the Higgs will still receive a mass contribution from radiative corrections. These contributions arise from one-loop diagrams the most significant of which come from the top quark, the standard model gauge bosons, and the Higgs itself. These one-loop diagrams are all quadratically divergent and require the introduction of a cutoff scale Λ signifying the appearance of new physics. The contribution from these one-loop diagrams is

$$\delta m_h^2 = \frac{3}{64\pi^2}(-8y_t^2 + 3g_2^2 + g_1^2 + \lambda)\Lambda^2 \quad (1.5)$$

where y_t is the top quark yukawa coupling, g_1 and g_2 are the weak SU(2) and U(1) hypercharge couplings respectively, and λ is the Higgs self-coupling [6]. If the standard model is correct up to the Planck scale (or even the GUT scale) a tremendous fine-tuning must occur in order to cancel the bare mass and radiative corrections and give a Higgs mass of $\mathcal{O}(100 \text{ GeV})$. This is known as the gauge hierarchy problem. The hierarchy problem is perhaps the most compelling reason for why there must be physics beyond the standard model.

Observe from Eq. (1.5) that if the cutoff scale were taken as $\Lambda \sim 1 \text{ TeV}$ an electroweak scale Higgs mass is naturally obtained. This suggests that beyond the standard model physics should reveal itself not far above the electroweak scale.

The most well known solution to the hierarchy problem is supersymmetry. In supersymmetric theories one introduces a new symmetry that associates every fermion with a boson (and vice versa) having the same quantum numbers except spin. In this case particles that contribute to the one-loop diagrams now have a superpartner also contributing to the one-loop diagrams but with a minus sign due to their opposite spin. Therefore all quadratically divergent loop diagrams cancel at each order of perturbation theory thus eliminating the hierarchy problem.

1.2 Going Beyond the Standard Model

It is clear that there are well-motivated reasons to consider physics beyond the standard model. There are two fundamentally different methods of introducing new physics. The first is to assume that spacetime is ordinary four-dimensional (4D) Minkowski space and to add new symmetries and interactions. Alternatively, one can modify the structure and characteristics of spacetime itself and study the consequences that these modifications have on particle physics. Modifying spacetime provides interesting solutions to many of the problems discussed in the previous section. For instance, we will discuss shortly how a particular modification of spacetime can offer a solution to the hierarchy problem. Finally, it should be emphasized that a realistic theory of nature could require changes in particle content, symmetries, and spacetime structure.

A well known example of new physics in ordinary spacetime is Grand Unification. In grand unified theories (GUT) one embeds the gauge structure and matter content of the standard model into a larger symmetry group. The best known example of a GUT is SU(5), which is the group of smallest rank that can contain the standard model as a subgroup [7]. One motivation for GUT's is the behavior of the standard model gauge couplings at high energies. The running of the gauge couplings is dictated by the renormalization group equations and for nonsupersymmetric standard model particle content one finds that they almost meet at a single value at an energy of $\sim 10^{14}$ GeV. It is clear that these models still suffer from the hierarchy problem with M_{Planck} being replaced by M_{GUT} . This leads one to consider supersymmetric GUT's which unify the standard model gauge groups and stabilize the hierarchy. Adding supersymmetry also yields the profound result that the couplings do in fact unify at a single point (up to threshold corrections) at $M_{GUT} \sim 2 \times 10^{16}$ GeV.

As mentioned, besides introducing physics beyond the standard model by enlarging the symmetries, particle content, and interactions of the standard model within ordinary

4D Minkowski space, it is interesting to consider what physical effects might result from the modification of spacetime itself. String theory provides several motivations for doing so. For instance, constructing a consistent string theory requires that the Universe contain extra spatial dimensions, typically 6 or 7 of them. This motivates one to consider what effect adding extra dimensions would have on particle physics. In string theory the extra dimensions can be compactified on orbifolds (defined below) whose radii are small. These extra dimensions are undetectable if their radii are smaller than the best experimental resolution. However, recent advances have suggested that modifying spacetime through additional spatial dimensions can not only provide solutions to long-standing problems of the standard model, but that these extra dimensions need not be far beyond our current experimental resolution.

In 1997, Arkani Hamed, Dimopoulos, and Dvali (ADD) [8, 9, 10] suggested the idea that there are such extra dimensions, but that only gravity can propagate into the higher-dimensional space, referred to as the “bulk”. Standard model fields are restricted to a 4D subspace called a “brane” which corresponds to the typical Minkowski space. From Gauss’ law an immediate consequence of this is that the actual higher-dimensional Planck scale is related to the measured 4D Planck scale by

$$\bar{M}_{Planck}^2 = V_n M_*^{n+2}, \quad (1.6)$$

where V_n is the volume of the n -dimensional space. From this point of view, the 4D measured Planck scale is a derived quantity whose value can be much larger than the fundamental scale M_* due to the volume of the higher-dimensional space. One can then ask whether the fundamental scale of gravity could arise at the TeV scale. In fact, assuming $M_* \sim \mathcal{O}(1 \text{ TeV})$ implies that two extra dimensions should have radii as large as $R \sim 100 \mu\text{m}$, which is just below the current distance scales probed by table top experiments that look for deviations from Newtonian gravity [11, 12].

Although extra dimensions were motivated earlier by string theory, the ADD model

offers the possibility that extra dimensions could be of value purely from a particle physics perspective ¹. In addition, the idea that certain fields could exist in a higher-dimensional space, while restricting other particles to a brane suggests a wide range of model-building possibilities, several of which are considered in this thesis.

To illustrate some of the generic consequences of an extra spatial dimension, consider a massless scalar field Φ propagating along an extra dimension y . The bulk action is

$$\mathcal{S} = \int dx^\mu \int dy \frac{1}{2} \partial_M \Phi(x^\mu, y) \partial^M \Phi(x^\mu, y), \quad (1.7)$$

where $M=0,1,2,3,y$. By imposing a periodic boundary condition along the extra dimension $\Phi(y) = \Phi(y + 2\pi R)$, the field may be expanded in a complete set of states

$$\Phi(x^\mu, y) = \sum_n \phi_n(x^\mu) e^{iny/R}. \quad (1.8)$$

Varying the bulk action gives the 5D massless Klein Gordon equation $\partial_M \partial^M \Phi = 0$. Substituting in the expansion Eq.(1.8)yields

$$(\partial_\mu \partial^\mu - \frac{n^2}{R^2}) \phi_n(x^\mu) = 0. \quad (1.9)$$

Therefore, in the effective 4D theory the extra dimension reveals itself as a tower of particles with mass $\sim n/R$. These towers of Kaluza Klein (KK) modes are a generic consequence of a compactified extra dimension. For a small enough extra dimension, the mass of the first KK-mode could be large enough so as to avoid experimental detection.

Extra dimensions can also be compactified into more complicated spaces that can provide a wider range of choices for model building. Viable models are most often compactified on an orbifold. A simple example is a single extra dimension compactified on a S^1/Z_2 orbifold. This is obtained by first imposing the periodic boundary condition under the translation $y \rightarrow y + 2\pi R$ and then identifying points related by the reflection

¹We mention for completeness an alternative solution to the hierarchy problem first proposed by Randall and Sundrum which utilizes a warped extra dimension. However, the details of this model lie beyond the scope of this thesis [13, 14].

$y \rightarrow -y$. The physical region along the extra dimension is then the interval $[0, \pi R]$ with the two endpoints, so called fixed points, being invariant under these operations. By compactifying on an orbifold, the KK expansion in Eq. (1.8) now will only be a function of sine's or cosine's depending on whether the field is odd or even under the Z_2 parity transformation. This provides a wealth of new options for model building. Consider a generic gauge theory in one extra dimension. In this case the 5D action contains gauge bosons which are Lorentz 5-vectors, A^M . In 4D this reduces to an ordinary 4-vector A^μ and a scalar A^5 (and associated KK-towers). By assigning A^μ to be even and A^5 to be odd under the Z_2 parity, their wavefunctions become

$$\begin{aligned} A^\mu(x^\mu, y) &= \sum_n A^\mu(x^\mu) \cos(ny/R), \\ A^5(x^\mu, y) &= \sum_n A^5(x^\mu) \sin(ny/R). \end{aligned} \quad (1.10)$$

The result of the orbifold projection is that although both fields acquire a tower of KK-modes, only A^μ contains a massless zero mode. In other words, the adjoint scalar has been projected out of the low energy spectrum. Clearly, orbifold projections offer a large range of possibilities for model building in extra dimensions.

Rather than only permitting gravity to propagate in the bulk, one could also imagine a universe in which all fields propagate in the bulk. This model of Universal Extra Dimensions (UED) was proposed by Appelquist, Cheng, and Dobrescu [15]. Since all fields propagate in the bulk, all fields develop associated KK-towers of particles. An immediate consequence of this is that KK-mode number is conserved simply due to conservation of (discrete) momentum along the extra dimension. By compactifying on an orbifold, translational invariance along the extra dimension is broken since two special points are now distinguished. However, after compactification a discrete KK-parity remains unbroken. This renders the lightest KK-mode stable, making it a possible dark matter candidate [16, 17, 18, 19]. For standard model fields propagating in the bulk, the tightest bounds on

the possible size of an extra dimension are most severely constrained by Z-pole observables. Due to the parity conservation in the UED model, KK-modes of gauge bosons can only be pair-produced. This results in a bound on the mass of the first KK-mode to be as light as 300 GeV [20], thus offering the prospect of their detection in the next generation of experiments.

There are other ways in which the modification of spacetime can lead to new physics beyond the standard model. One simple idea is to make spacetime noncommutative. This is accomplished by promoting the spacetime coordinates to operators satisfying the following commutation relations

$$[\hat{x}^\mu, \hat{x}^\nu] = \theta^{\mu\nu}. \quad (1.11)$$

In the canonical formulation of noncommutative field theory, $\theta^{\mu\nu}$ is simply an antisymmetric c -number. This idea of noncommutative spacetime is motivated by string theory, where one finds that for an open string propagating in an antisymmetric background field the endpoints of the string are described by noncommuting coordinates [21, 22, 23].

Rather than construct a field theory based on these noncommutative coordinate operators, one would clearly prefer to use ordinary commuting coordinates. This is accomplished by introducing a modified multiplication rule

$$(f \star g)(x) = f(x) \exp\left[\frac{i}{2} \overleftarrow{\partial}_\mu \theta^{\mu\nu} \overrightarrow{\partial}_\nu\right] g(x), \quad (1.12)$$

known as the star or Moyal-product. By promoting all multiplication to the star-product, a field theory action can be constructed from fields that are functions of ordinary commuting coordinates. In other words, the star-product encapsulates the noncommutativity of spacetime. An immediate consequence of this form of spacetime noncommutativity is that Lorentz invariance is broken. For example, $\epsilon^{ijk}\theta^{ij}$ defines a preferred direction in a given Lorentz frame. Experiments looking for Lorentz violation place tight bounds on the possible scale of noncommutativity in this simple version [24, 25, 26, 27].

Carlson, Carone, and Zobin (CCZ) have proposed a Lorentz-conserving version of noncommutative QED [28]. This was accomplished by promoting $\theta^{\mu\nu}$ to an antisymmetric Lorentz tensor satisfying the Lie algebra

$$\begin{aligned} [\hat{x}^\mu, \hat{x}^\nu] &= i\hat{\theta}^{\mu\nu}, \\ [\hat{\theta}^{\mu\nu}, \hat{x}^\lambda] &= 0, \\ [\hat{\theta}^{\mu\nu}, \hat{\theta}^{\alpha\beta}] &= 0. \end{aligned} \tag{1.13}$$

Fields are then functions of both \hat{x} and $\hat{\theta}^{\mu\nu}$. This lead CCZ to introduce a new star-product

$$(f \star g)(x, \theta) = f(x, \theta) \exp\left[\frac{i}{2} \overleftarrow{\partial}_\mu \theta^{\mu\nu} \overrightarrow{\partial}_\nu\right] g(x, \theta), \tag{1.14}$$

where the difference from the star-product of canonical noncommutativity is the functional dependence on θ . The QED action is then obtained by promoting all multiplication to this modified star product. In this case, the fields are still functions of x and θ . CCZ demonstrated how to obtain interactions involving fields that are only functions of x . This was accomplished using a particular field redefinition and an expansion in powers of θ . This results in a new version of QED containing new Lorentz-invariant interactions that are a direct result of spacetime noncommutativity.

It is interesting to note that the Lie algebra of Eq. (1.13) proposed by CCZ is the same as the Lie algebra proposed by Doplicher, Fredenhagen, and Roberts (DFR)[29, 30]. DFR arrived at this Lie algebra by considering the general properties of a theory combining the Heisenberg uncertainty principle with classical gravity, i.e. a quantum theory of gravity.

The first two chapters of this thesis deal with different collider signatures that are the result of a modified spacetime. In Chapter 2, we consider the phenomenological implications of the model of Lorentz-conserving Noncommutative QED proposed by CCZ. We calculate modifications to the differential and total cross sections for Bhabha, Møller, and $e^+e^- \rightarrow \mu^+\mu^-$ scattering, as well as $e^+e^- \rightarrow \gamma\gamma$ up to second order in the noncommutative parameter. From this we extract bounds on the noncommutativity scale from

LEP data and consider whether this form of noncommutativity may be probed by a Next Linear Collider (NLC).

In models of UED all SM fields propagate in the bulk and therefore have KK towers with the tree level mass

$$m_{KK}^2 = m_{SM}^2 + \frac{n^2}{R^2}. \quad (1.15)$$

Even for a relatively small compactification radius, these masses are nearly degenerate at each KK level. In this case, radiative corrections are important and lead to a breaking of this degeneracy. Fig. 1.1 shows the mass splittings for the first KK modes for a typical

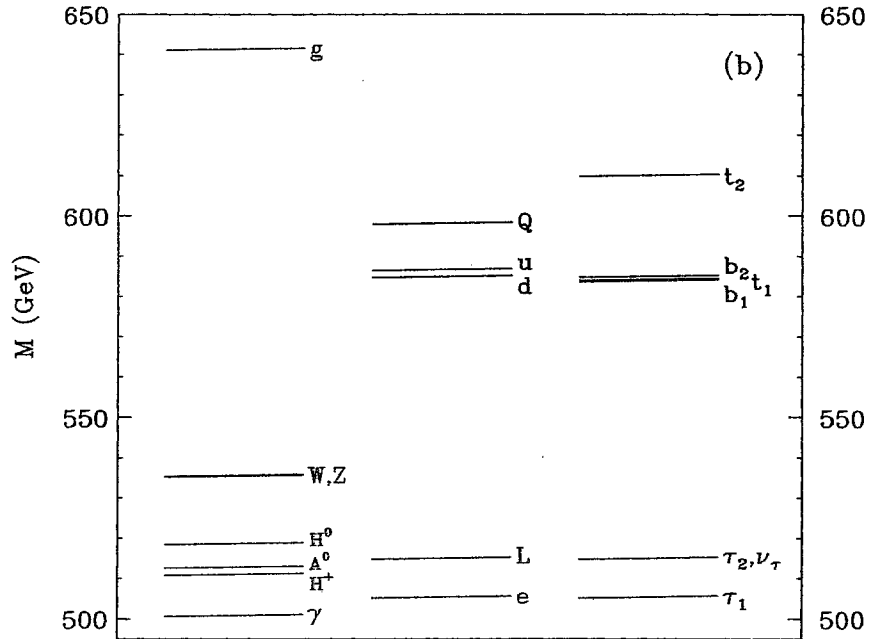


FIG. 1.1: Spectrum of the first massive KK modes in the UED model [2]

choice of parameters. For a reasonable choice of parameters, one finds a small mass difference between the lightest KK particle (LKP) and the first quark KK modes. In Chapter 3 we consider the implications of this mass spectrum on the possible formation of KK-quark bound states, *i.e.* KK-quarkonium.

Extra dimensions also offer new ways of constructing theories that, although are not directly testable at colliders, can explain the unity of fundamental forces. For instance,

orbifold parity on an extra-dimensional interval can be chosen such that only some components of a gauge multiplet retain a massless zero mode, thus reducing the gauge symmetry. However, this procedure does not allow a reduction in group rank. On the other hand more generalized boundary conditions may be imposed on the group generators allowing group rank to be reduced. These generalized boundary conditions can be thought of as arising from the vev of a brane-localized Higgs field. In the limit that the vev is taken to infinity, the symmetry breaking Higgs field completely decouples from the theory, and the mass of the KK modes is set by the size of the extra dimension.

In Chapter 4, we apply this technique, called “Higgsless” symmetry breaking, toward the breaking of GUT gauge symmetries, and in particular to the trinified group $G_T = SU(3)_C \times SU(3)_L \times SU(3)_R$. In Trinification, the Higgs fields are placed in a 27 of G_T , which leads to a complicated and rather undesirable Higgs sector. We introduce boundary breaking Higgs fields that break G_T , leaving the MSSM particle spectrum in the low-energy theory. Exotic fermions couple to these boundary fields and are decoupled from the theory (along with the symmetry breaking Higgs fields) in the Higgsless limit. We also show that unification is delayed and can coincide with the 5D Planck scale.

In Chapter 5 we construct improved models of Trinification utilizing a single extra dimension. In these models the GUT gauge symmetry is broken by a combination of orbifold parities and generalized boundary conditions. For the boundary conditions, we explicitly give the corresponding boundary Higgs representations needed to break Trinification down to the MSSM. The two MSSM Higgs doublets are identified with some of the higher-dimensional components of the gauge fields in an approach called gauge-higgs unification [31, 32, 33, 34, 35]. We discuss various phenomenological issues such as gauge coupling unification and proton decay.

CHAPTER 2

Phenomenology of Lorentz-Conserving Noncommutative QED

2.1 Introduction

It is interesting to consider the possibility that the structure of space-time is nontrivial. In one of the most popular scenarios position four-vectors are promoted to operators that do not commute at short distance scales [36, 37, 38, 39, 40, 41, 42, 43, 44, 45, 46, 47, 48, 49, 50, 51, 52, 53, 54, 55, 56, 57, 58, 59, 28, 60, 61, 29, 30, 62]. There has been a lot of work on field theories with an underlying noncommutative space-time structure. Jurčo *et al.* [42] have presented a formalism on how to construct non-Abelian gauge theories in noncommutative spaces from a consistency relation. Using a similar approach Carlson, Carone and Zobin (CCZ) [28] have formulated noncommutative Lorentz-conserving QED based on a contracted Snyder [62] algebra, thus offering a general prescription as how to formulate noncommutative Lorentz-conserving gauge theories. In this algebra the selfadjoint spacetime coordinate operators satisfy the following commutation relation,

$$[\hat{x}^\mu, \hat{x}^\nu] = i\hat{\theta}^{\mu\nu}. \quad (2.1)$$

Here $\hat{\theta}^{\mu\nu} = -\hat{\theta}^{\nu\mu}$ transforms as a Lorentz tensor and is in the same algebra with \hat{x}^μ . This algebra is Lorentz covariant.

The Lie algebra considered by CCZ is the same as the Lie algebra of Doplicher, Fredenhagen, and Roberts (DFR) [29, 30]. Interestingly enough DFR came to the formulation of their algebra by considering modifications of spacetime structure in theories that are designed to quantize gravity. The DFR algebra places limitations on the precision of localization in spacetime. As noted in [29, 30], quantum spacetime can be regarded as a novel underlying geometry for a quantum field theory of gravity.

Interest in noncommutative spacetime originated with the work of Connes and collaborators [63, 64, 65, 66] and has gained more attention due to developments in string theory [21], where noncommutative spacetime has been shown to arise in a low energy limit. In string theories $\theta^{\mu\nu}$ is just an antisymmetric c-number. Theories involving noncommutative spacetime structure based on algebras with c-number $\theta^{\mu\nu}$ suffer from Lorentz-violating effects. Such effects are severely constrained [46, 47, 48, 49, 50, 51, 52, 53, 54] by a variety of low energy experiments [24, 25, 26, 27]. Lorentz-violating effects appear in field theories as a consequence of θ^{0i} and $\epsilon^{ijk}\theta^{ij}$ defining preferred direction in a given Lorentz frame. In contrast to this the noncommutative QED (NCQED) formulated by CCZ based on Eq. (2.1) is free from Lorentz-violating effects.

Carlson, Carone and Zobin have connected the DFR Lie algebra Eq. (2.1), and the antisymmetric tensor $\hat{\theta}^{\mu\nu}$ to experimental observables, by showing how to formulate a quantum field theory on this noncommutative spacetime. Similar issues have been discussed by Morita *et al.* [60, 61]. These theories make it possible to study phenomenological consequences of Lorentz-conserving noncommutative spacetime. As a beginning, CCZ have studied light-by-light elastic scattering and obtained contributions that can be significant with respect to the standard model background.

In this chapter we calculate other phenomenological consequences of Lorentz-conserving NCQED formulated by CCZ. We consider various collider processes such as Bhabha and

Møller scattering, $e^+e^- \rightarrow \mu^+\mu^-$ and $e^+e^- \rightarrow \gamma\gamma$. The experiments at planned colliders will provide means of testing the properties and the structure of space-time at smaller distance scales. We note that any property prescribed to space-time, if confirmed experimentally, must affect all interactions.

In the following section we discuss the underlying formalism of noncommutative Lorentz-conserving gauge theories, with emphasis on NCQED. In Section 2.3 we study the Lorentz-conserving NCQED by considering various collider processes. In Section 2.4 we obtain bounds on the noncommutativity scale from Bhabha scattering, $e^+e^- \rightarrow \mu^+\mu^-$ and $e^+e^- \rightarrow \gamma\gamma$ experiments. We summarize our discussion in Section 2.5 with some concluding remarks.

2.2 Algebra and QED Formulation

The simplest construction of a Lorentz-conserving noncommutative theory involves promoting the position four-vector to an operator which satisfies the DFR Lie algebra

$$\begin{aligned} [\hat{x}^\mu, \hat{x}^\nu] &= i\hat{\theta}^{\mu\nu}, \\ [\hat{\theta}^{\mu\nu}, \hat{x}^\lambda] &= 0, \\ [\hat{\theta}^{\mu\nu}, \hat{\theta}^{\alpha\beta}] &= 0, \end{aligned} \tag{2.2}$$

where $\theta^{\mu\nu}$ is antisymmetric and transforms as a Lorentz tensor.

On the other hand, CCZ took as the starting point Snyder's algebra,

$$\begin{aligned} [\hat{x}^\mu, \hat{x}^\nu] &= i\alpha^2 \hat{M}^{\mu\nu}, \\ [\hat{M}^{\mu\nu}, \hat{x}^\lambda] &= i(\hat{x}^\mu g^{\nu\lambda} - \hat{x}^\nu g^{\mu\lambda}), \\ [\hat{M}^{\mu\nu}, \hat{M}^{\alpha\beta}] &= i(\hat{M}^{\mu\beta} g^{\nu\alpha} + \hat{M}^{\nu\alpha} g^{\mu\beta} - \hat{M}^{\mu\alpha} g^{\nu\beta} - \hat{M}^{\nu\beta} g^{\mu\alpha}). \end{aligned} \tag{2.3}$$

Snyder's algebra (which is the same as the algebra of $SO(4,1)$) describes a Lorentz-

invariant noncommutative discrete spacetime characterized by a fundamental length scale a . By constructing an explicit representation for \hat{x} and \hat{M} in terms of differential operators, the Lorentz invariance of Eq. (2.3) was demonstrated [62]. CCZ then extracted the DFR Lie algebra by performing a particular contraction on Eq. (2.3). Specifically, by rescaling $M^{\mu\nu} = \hat{\theta}^{\mu\nu}/b$ and holding the ratio $a^2/b = 1$ fixed, the limit $b \rightarrow 0$, $a \rightarrow 0$ yields the DFR Lie algebra. Thus, the Lorentz covariance of Snyder's Lie algebra implies the Lorentz covariance of Eq. (2.2) [28]. The commutator of $\hat{\theta}^{\mu\nu}$ and $\hat{M}^{\mu\nu}$ is

$$[\hat{M}^{\mu\nu}, \hat{\theta}^{\alpha\beta}] = i(\hat{\theta}^{\mu\beta} g^{\nu\alpha} + \hat{\theta}^{\nu\alpha} g^{\mu\beta} - \hat{\theta}^{\mu\alpha} g^{\nu\beta} - \hat{\theta}^{\nu\beta} g^{\mu\alpha}), \quad (2.4)$$

as one would expect if $\hat{\theta}^{\mu\nu}$ is a Lorentz tensor. Note that the contraction also implies that the eigenvalues of the position operator of the DFR algebra are continuous.

To develop a field theory on a noncommutative spacetime, one defines a one-to-one mapping which associates functions of the noncommuting coordinates with functions of the typical c-number coordinates. In the canonical noncommutative theory this is achieved via a Fourier transform

$$\hat{f}(\hat{x}) = \frac{1}{2\pi^n} \int d^n k e^{-ik\hat{x}} \int d^n x e^{ikx} f(x). \quad (2.5)$$

In the Lorentz-conserving case the presence of the operator $\hat{\theta}^{\mu\nu}$ requires that the mapping involve a new c-number coordinate $\theta^{\mu\nu}$ (no hat). Functions of the noncommuting coordinates are then related to functions of c-number coordinates by

$$\hat{f}(\hat{x}, \hat{\theta}) = \int \frac{d^4 \alpha}{(2\pi)^4} \frac{d^6 B}{(2\pi)^6} e^{-i(\alpha_\mu \hat{x}^\mu + \frac{B_{\mu\nu} \hat{\theta}^{\mu\nu}}{2})} \tilde{f}(\alpha, B), \quad (2.6)$$

where

$$\tilde{f}(\alpha, B) = \int d^4 x d^6 \theta e^{i(\alpha_\mu x^\mu + \frac{B_{\mu\nu} \theta^{\mu\nu}}{2})} f(x, \theta). \quad (2.7)$$

Lorentz invariance requires that B transform as a two-index Lorentz tensor.

To ensure that operator multiplication be preserved; $\widehat{fg} = \widehat{f \star g}$, one finds that the

rule for ordinary multiplication must be modified:

$$(f \star g)(x, \theta) = f(x, \theta) \exp\left[\frac{i}{2} \overleftarrow{\partial}_\mu \theta^{\mu\nu} \overrightarrow{\partial}_\nu\right] g(x, \theta). \quad (2.8)$$

The θ dependence of the functions distinguishes this result from the \star -product of the canonical noncommutative theory. Eqs. (2.6) and (2.7) allow one to work solely with functions of classical coordinates x and θ , provided that all multiplication be promoted to a \star -product.

The introduction of a Lorentz invariant weighting function $W(\theta)$ allows for the following generalization of the operator trace:

$$\text{Tr} \hat{f} = \int d^4x d^6\theta W(\theta) f(x, \theta). \quad (2.9)$$

In [28] CCZ took the normalization to be

$$\int d^6\theta W(\theta) = 1. \quad (2.10)$$

It is straightforward to demonstrate the cyclic property of Eq. (2.9), *i.e.* $\text{Tr} \hat{f} \hat{g} = \text{Tr} \hat{g} \hat{f}$. One requires that for large $|\theta^{\mu\nu}|$, $W(\theta)$ dies off sufficiently fast in order that all integrals be well defined [28]. Lorentz-invariance requires that W be an even function of θ , which yields

$$\int d^6\theta W(\theta) \theta^{\mu\nu} = 0. \quad (2.11)$$

As will be seen, this restriction has interesting consequences on possible collider signatures of the theory.

Field theory interactions are extracted by performing the $d^6\theta$ integral, resulting in the action

$$\mathcal{S} = \text{Tr} \hat{\mathcal{L}} = \int d^4x d^6\theta W(\theta) \mathcal{L}(\phi, \partial\phi)_\star, \quad (2.12)$$

where the notation in $\mathcal{L}(\phi, \partial\phi)_\star$ indicates \star -product multiplication.

As was mentioned, in the Lorentz-conserving noncommutative theory the initial “fields” are generally functions of x and θ , and must be related to ordinary quantum fields

which are only functions of x . CCZ showed how this can be done for NCQED using a nonlinear field redefinition and an expansion in θ . Since the phenomenology of NCQED is the topic of this chapter, all developments will be directed toward a U(1) gauge theory. For completeness the formalism presented in [28] is reviewed.

In Lorentz-conserving NCQED, one has a matter field ψ and gauge field A . For a U(1) gauge transformation characterized by a parameter $\Lambda(x, \theta)$, the fields transform as

$$\psi(x, \theta) \rightarrow U \star \psi(x, \theta), \quad (2.13)$$

and

$$A_\mu(x, \theta) \rightarrow U \star A_\mu(x, \theta) \star U^{-1} + \frac{i}{e} U \star \partial_\mu U^{-1}, \quad (2.14)$$

where

$$\begin{aligned} U &= (e^{i\Lambda})_\star \\ &= 1 + i\Lambda(x, \theta) + \frac{1}{2!} i\Lambda(x, \theta) \star i\Lambda(x, \theta) + \dots \end{aligned} \quad (2.15)$$

A U(1) gauge invariant Lagrangian is

$$\mathcal{L} = \int d^6\theta W(\theta) \left[-\frac{1}{4} F_{\mu\nu} \star F^{\mu\nu} + \bar{\psi} \star (i \not{D} - m) \star \psi \right], \quad (2.16)$$

where

$$D_\mu = \partial_\mu - ieA_\mu, \quad (2.17)$$

and the field strength is

$$F_{\mu\nu} = \partial_\mu A_\nu - \partial_\nu A_\mu - ie[A_\mu \star A_\nu]. \quad (2.18)$$

In demonstrating the gauge invariance of Eq. (2.16) and the cyclic property of Eq. (2.9), the following identity is useful

$$\int d^4x f \star g = \int d^4x f g. \quad (2.19)$$

Eqs. (2.16), (2.17), and (2.18) are similar in form to those obtained in the canonical NC-QED case, the difference again being the θ dependence of the fields $\psi(x, \theta)$ and $A(x, \theta)$ in Eq. (2.16). One must have a way of relating ψ and A to ordinary quantum fields which are only functions of x . This is accomplished by utilizing the behavior of the weighting function Eq. (2.9), which allows an expansion of the fields and gauge parameter in powers of θ . A similar technique involving field expansions was first used in constructing a noncommutative $SU(N)$ gauge theory in [42]. The coefficients of the power series are thus only functions of x and correspond to ordinary quantum fields. From requirements of gauge invariance and noncommutativity, these coefficients can be determined order by order in θ .

The matter field, gauge field, and gauge parameter of NCQED are expanded as:

$$\Lambda_\alpha(x, \theta) = \alpha(x) + \theta^{\mu\nu} \Lambda_{\mu\nu}^{(1)}(x; \alpha) + \theta^{\mu\nu} \theta^{\eta\sigma} \Lambda_{\mu\nu\eta\sigma}^{(2)}(x; \alpha) + \dots, \quad (2.20)$$

$$A_\rho(x, \theta) = A_\rho(x) + \theta^{\mu\nu} A_{\mu\nu\rho}^{(1)}(x) + \theta^{\mu\nu} \theta^{\eta\sigma} A_{\mu\nu\eta\sigma\rho}^{(2)}(x) + \dots, \quad (2.21)$$

$$\psi(x, \theta) = \psi(x) + \theta^{\mu\nu} \psi_{\mu\nu}^{(1)}(x) + \theta^{\mu\nu} \theta^{\eta\sigma} \psi_{\mu\nu\eta\sigma}^{(2)}(x) + \dots. \quad (2.22)$$

The lowest order term in each expansion corresponds to the ordinary QED term. Thus, ordinary QED can be extracted by taking the commutative limit, $\theta^{\mu\nu} \rightarrow 0$.

Consider an infinitesimal transformation of a matter field $\psi(x)$ in an ordinary $U(1)$ gauge theory:

$$\delta_\alpha \psi(x) = i\alpha(x)\psi(x). \quad (2.23)$$

For a Lorentz-conserving noncommutative theory, this is generalized to

$$\delta_\alpha \psi(x, \theta) = i\Lambda_\alpha(x, \theta) \star \psi(x, \theta). \quad (2.24)$$

In an Abelian gauge theory two successive gauge transformations must then satisfy the relation

$$(\delta_\alpha \delta_\beta - \delta_\beta \delta_\alpha) \psi(x, \theta) = 0. \quad (2.25)$$

For Eq.(2.25) to hold, Λ must satisfy

$$i\delta_\alpha\Lambda_\beta - i\delta_\beta\Lambda_\alpha + [\Lambda_\alpha * \Lambda_\beta] = 0. \quad (2.26)$$

The parameter Λ can then be determined at each order in θ . Specifically, it can be shown that

$$\Lambda_{\mu\nu}^{(1)}(x; \alpha) = \frac{e}{2}\partial_\mu\alpha(x)A_\nu(x) \quad (2.27)$$

and

$$\Lambda_{\mu\nu\eta\sigma}^{(2)}(x; \alpha) = -\frac{e^2}{2}\partial_\mu\alpha(x)A_\eta(x)\partial_\sigma A_\nu(x) \quad (2.28)$$

satisfy the condition of Eq. (2.26). The gauge and matter fields are treated in a similar manner.

The restriction of a gauge field transforming infinitesimally as

$$\delta_\alpha A_\sigma = \partial_\sigma\Lambda_\alpha + i[\Lambda_\alpha * A_\sigma], \quad (2.29)$$

is satisfied by the following expressions for $A^{(1)}$ and $A^{(2)}$:

$$A_{\mu\nu\rho}^{(1)}(x) = -\frac{e}{2}A_\mu(\partial_\nu A_\rho + F_{\nu\rho}^0), \quad (2.30)$$

$$A_{\mu\nu\eta\sigma\rho}^{(2)}(x) = \frac{e^2}{2}(A_\mu A_\eta \partial_\sigma F_{\nu\rho}^0 - \partial_\nu A_\rho \partial_\eta A_\mu A_\sigma + A_\mu F_{\nu\eta}^0 F_{\sigma\rho}^0), \quad (2.31)$$

where

$$F_{\mu\nu}^0 = \partial_\mu A_\nu - \partial_\nu A_\mu \quad (2.32)$$

is the ordinary QED field strength tensor.

Likewise, one can show that for a matter field transforming infinitesimally as Eq. (2.24), the appropriate forms of $\psi^{(1)}$ and $\psi^{(2)}$ are

$$\psi_{\mu\nu}^{(1)}(x) = -\frac{e}{2}A_\mu\partial_\nu\psi \quad (2.33)$$

and

$$\begin{aligned} \psi_{\mu\nu\eta\sigma}^{(2)}(x) = & \frac{e}{8}(-i\partial_\mu A_\eta \partial_\nu \partial_\sigma \psi + eA_\mu A_\eta \partial_\nu \partial_\sigma \psi + 2eA_\mu \partial_\nu A_\eta \partial_\sigma \psi \\ & + eA_\mu F_{\nu\eta}^0 \partial_\sigma \psi - \frac{e}{2}\partial_\mu A_\eta \partial_\nu A_\sigma \psi + ie^2 A_\mu A_\sigma \partial_\eta A_\nu \psi). \end{aligned} \quad (2.34)$$

Interactions are extracted by substituting Eqs. (2.27), (2.28), (2.30), (2.31), (2.33), (2.34) into the Lagrangian Eq. (2.16). We expand the Lagrangian through θ^2 and evaluate the $d^6\theta$ integral using the weighted average

$$\int d^6\theta W(\theta)\theta^{\mu\nu}\theta^{\eta\rho} = \frac{\langle\theta^2\rangle}{12}(g^{\mu\eta}g^{\nu\rho} - g^{\mu\rho}g^{\eta\nu}), \quad (2.35)$$

where the expectation value is defined as

$$\langle\theta^2\rangle \equiv \int d^6\theta W(\theta)\theta_{\mu\nu}\theta^{\mu\nu}. \quad (2.36)$$

It is natural to define $\Lambda_{NC} = (12/\langle\theta^2\rangle)^{1/4}$ which characterizes the energy scale where noncommutative effects become relevant. The restriction on W from Eq. (2.11) demands that only terms containing even powers of θ will result in interaction vertices. Thus, for example, the three-photon vertex of canonical NCQED is not present. The next section focuses on the phenomenology of a U(1) theory whose spacetime coordinate operators obey the DFR Lie algebra. Possible collider signatures are considered and bounds on the energy scale Λ_{NC} are obtained.

2.3 Collider Signatures

The Lagrangian for QED with Lorentz-invariant noncommutative spacetime Eq. (2.16) can be written as an expansion in θ order by order using the nonlinear field redefinition described above. The zeroth order in θ will give the ordinary QED Lagrangian. The first order is zero due to the evenness of the weighting function $W(\theta)$. The first nontrivial contributions come from the second order, they include:

1. the 4-photon vertex, which has been discussed extensively in [28],
2. the correction to 2-fermion-1-photon vertex (ordinary QED vertex),
3. the 2-fermion-2-photon vertex.

The lowest order correction to the ordinary QED vertex comes from the following terms in Lagrangian density:

$$\begin{aligned} & \bar{\psi}^{(2)}(i \not{\partial} - m)\psi^{(0)} + \bar{\psi}^{(0)}(i \not{\partial} - m)\psi^{(2)} \\ & + \frac{e}{2}\{(\bar{\psi}^{(0)} \star \mathcal{A}^{(0)})\psi^{(0)} + \bar{\psi}^{(0)}(\mathcal{A}^{(0)} \star \psi^{(0)})\}, \end{aligned} \quad (2.37)$$

where we retain only the second order term in contributions to the \star -product shown in the last two terms. The first two terms will go to zero if both fermion fields are on shell. And the 2-fermion-2-photon vertex comes from:

$$\begin{aligned} & \bar{\psi}^{(2)}(i \not{\partial} - m)\psi^{(0)} + \bar{\psi}^{(0)}(i \not{\partial} - m)\psi^{(2)} + \bar{\psi}^{(1)}(i \not{\partial} - m)\psi^{(1)} \\ & + e\{\bar{\psi}^{(2)} \mathcal{A}^{(0)}\psi^{(0)} + \bar{\psi}^{(0)} \mathcal{A}^{(0)}\psi^{(2)}\} \\ & + e\{(\bar{\psi}^{(0)} \star \mathcal{A}^{(0)})\psi^{(1)} + \bar{\psi}^{(1)}(\mathcal{A}^{(0)} \star \psi^{(0)}) + (\bar{\psi}^{(0)} \star \mathcal{A}^{(1)})\psi^{(0)}\}, \end{aligned} \quad (2.38)$$

where this time we retain only the first order in the \star -product shown.

2.3.1 Dilepton Production, $e^+e^- \rightarrow l^+l^-$

First we consider processes in which all fermions are on shell, *i.e.* dilepton production $e^+e^- \rightarrow l^+l^-$. For processes up to tree level Feynman diagram, only

$$\frac{e}{2}\{(\bar{\psi}^{(0)} \star \mathcal{A}^{(0)})\psi^{(0)} + \bar{\psi}^{(0)}(\mathcal{A}^{(0)} \star \psi^{(0)})\}$$

will contribute to the vertex correction since all the fermions are on shell. This Lagrangian term reduces to:

$$\frac{e}{2} \frac{\langle \theta^2 \rangle}{96} \{ \bar{\psi}(\partial_\mu \partial_\nu \mathcal{A})(\partial^\mu \partial^\nu \psi) + (\partial^\mu \partial^\nu \bar{\psi})(\partial_\mu \partial_\nu \mathcal{A})\psi \}. \quad (2.39)$$

From this we obtain the following Feynman rule for the 2-fermion-1-photon vertex with all fermions on shell and with momenta labeled as in Fig. 2.1:

$$ie\{1 + \frac{\langle \theta^2 \rangle}{384}(p_3)^4\}\gamma^\mu, \quad (2.40)$$

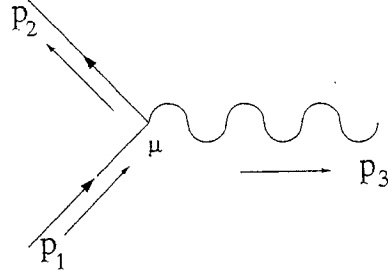


FIG. 2.1: 2-fermions-1-photon vertex.

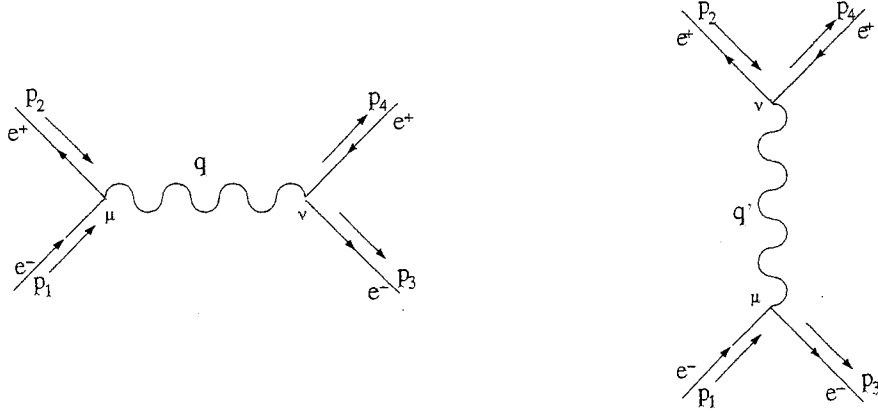


FIG. 2.2: Bhabha Scattering.

where we have not made the assumption that the fermions are massless (although we do set $m = 0$ in the cross section formula).

We will consider the following processes which are affected by this vertex correction: Bhabha scattering, $e^+e^- \rightarrow \mu^+\mu^-$ and Møller scattering. The matrix element with vertex correction for Bhabha scattering (Fig. 2.2) is:

$$\begin{aligned}
 i\mathcal{M} = & \bar{u}(p_3)(ie\gamma^\nu)(1 + \frac{\langle\theta^2\rangle}{384}q^4)v(p_4)\frac{-ig_{\mu\nu}}{q^2 + i\epsilon} \\
 & \times \bar{v}(p_2)(ie\gamma^\mu)(1 + \frac{\langle\theta^2\rangle}{384}q^4)u(p_1) \\
 & - \bar{v}(p_2)(ie\gamma^\nu)(1 + \frac{\langle\theta^2\rangle}{384}q'^4)v(p_4)\frac{-ig_{\mu\nu}}{q'^2 + i\epsilon} \\
 & \times \bar{u}(p_3)(ie\gamma^\mu)(1 + \frac{\langle\theta^2\rangle}{384}q'^4)u(p_1). \tag{2.41}
 \end{aligned}$$

Squaring the matrix element and summing(averaging) over the final(initial) fermion

spin states will give:

$$|\overline{\mathcal{M}}|^2 = 2e^4 \left\{ F_s^2 \left(\frac{t^2 + u^2}{s^2} \right) + 2F_s F_t \frac{u^2}{st} + F_t^2 \left(\frac{u^2 + s^2}{t^2} \right) \right\}, \quad (2.42)$$

where we define $F_s = \left\{ 1 + \frac{\langle \theta^2 \rangle}{96} \frac{s^2}{4} \right\}^2$ with s, t and u are the Mandelstam variables. To first order in $\langle \theta^2 \rangle / 12$ this will give us the center of mass (CM) differential cross section:

$$\frac{d\sigma}{d \cos \theta} = \left(\frac{d\sigma}{d \cos \theta} \right)_{QED} + \frac{\pi \alpha^2 \langle \theta^2 \rangle}{s \cdot 96} \left\{ s^2 + t^2 + 2u^2 + u^2 \left(\frac{t}{s} + \frac{s}{t} \right) \right\}, \quad (2.43)$$

where θ is the CM scattering angle.

The same results for $e^+e^- \rightarrow \mu^+\mu^-$ can be obtained easily by just throwing away the t channel in the Bhabha scattering calculation, assuming the muons are massless. The spin average square matrix element is:

$$|\overline{\mathcal{M}}|^2 = 2e^4 F_s^2 \left(\frac{t^2 + u^2}{s^2} \right). \quad (2.44)$$

And to first order in $\langle \theta^2 \rangle / 12$ this will give us:

$$\frac{d\sigma}{d \cos \theta} = \left(\frac{d\sigma}{d \cos \theta} \right)_{QED} \left(1 + \frac{\langle \theta^2 \rangle}{96} s^2 \right). \quad (2.45)$$

2.3.2 Møller Scattering

For Møller scattering, the spin average square matrix element is obtained by using crossing symmetry from Bhabha scattering:

$$|\overline{\mathcal{M}}|^2 = 2e^4 \left\{ F_t^2 \left(\frac{u^2 + s^2}{t^2} \right) + 2F_t F_u \frac{s^2}{tu} + F_u^2 \left(\frac{s^2 + t^2}{u^2} \right) \right\}. \quad (2.46)$$

To first order in $\langle \theta^2 \rangle / 12$ this gives us the CM differential cross section:

$$\frac{d\sigma}{d \cos \theta} = \left(\frac{d\sigma}{d \cos \theta} \right)_{QED} + \frac{\pi \alpha^2 \langle \theta^2 \rangle}{s \cdot 96} \left\{ t^2 + u^2 + 2s^2 + s^2 \left(\frac{u}{t} + \frac{t}{u} \right) \right\}. \quad (2.47)$$

2.3.3 Diphoton Production, $e^+e^- \rightarrow \gamma\gamma$

In order to calculate the cross section for $e^+e^- \rightarrow \gamma\gamma$, we first need to calculate the full correction to ordinary QED vertex, not just the case when all fermions are on shell. This requirement comes from the fact that in diphoton production we have fermion propagators in the Feynman diagrams. By using the non-linear field redefinition for $\psi^{(2)}$, the Lagrangian for the full correction can be written as:

$$\begin{aligned}
ie \frac{\langle \theta^2 \rangle}{96} & [(\partial_\mu A^\mu) \{(\partial^2 \bar{\psi})(i \not{\partial} - m)\psi + \{(i\partial_\alpha + m)\bar{\psi}\}\gamma^\alpha(\partial^2 \psi)\} \\
& - (\partial_\mu A_\nu) \{(\partial^\mu \partial^\nu \bar{\psi})(i \not{\partial} - m)\psi + \{(i\partial_\alpha + m)\bar{\psi}\}\gamma^\alpha(\partial^\mu \partial^\nu \psi)\} \\
& - \frac{i}{2} \{ \bar{\psi}(\partial_\mu \partial_\nu A)(\partial^\mu \partial^\nu \psi) + (\partial^\mu \partial^\nu \bar{\psi})(\partial_\mu \partial_\nu A)\psi \}]. \quad (2.48)
\end{aligned}$$

Then the Feynman rule for the 2-fermion-1-photon vertex with all fermions and photons possibly off-shell is (Fig. 2.1):

$$\begin{aligned}
ie \{ \gamma^\mu + \frac{\langle \theta^2 \rangle}{96} & [(\not{p}_1 - m)p_2^\mu p_3^\mu - (\not{p}_2 - m)p_1^\mu p_3^\mu \\
& + (\not{p}_2 - m)(p_1 \cdot p_3)p_1^\mu - (\not{p}_1 - m)(p_2 \cdot p_3)p_2^\mu \\
& + \frac{1}{2} \{ (p_1 \cdot p_3)^2 + (p_2 \cdot p_3)^2 \} \gamma^\mu \}]. \quad (2.49)
\end{aligned}$$

Next we need to calculate the contribution from the new vertex, *i.e.*, 2-fermion-2-photon vertex. The Lagrangian for this vertex is:

$$\begin{aligned}
ie^2 \frac{\langle \theta^2 \rangle}{96} & [A_\mu (\partial_\alpha A_\nu) \{(\partial^\mu \bar{\psi})\gamma^\alpha(\partial^\nu \psi) - (\partial^\nu \bar{\psi})\gamma^\alpha(\partial^\mu \psi)\} \\
& - (\partial_\mu A_\nu) \{(\partial^\mu \partial^\nu \bar{\psi}) A\psi - \bar{\psi} A(\partial^\mu \partial^\nu \psi)\} \\
& + 2A_\mu F_{\nu\alpha} \{(\partial^\mu \bar{\psi})\gamma^\alpha(\partial^\nu \psi) - (\partial^\nu \bar{\psi})\gamma^\alpha(\partial^\mu \psi)\}], \quad (2.50)
\end{aligned}$$

and we put all the fermions and photons on shell to simplify the calculation. This simplification is possible since in the calculation for diphoton production up to second order in θ for the 2-fermion-2-photon vertex all fermions and photons are on shell. Labeling momenta as in Fig. 2.3, we obtain the Feynman rule for the 2-fermion-2-photon vertex

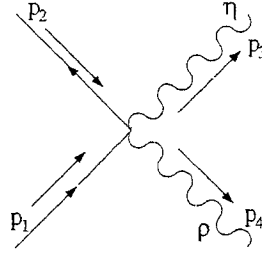
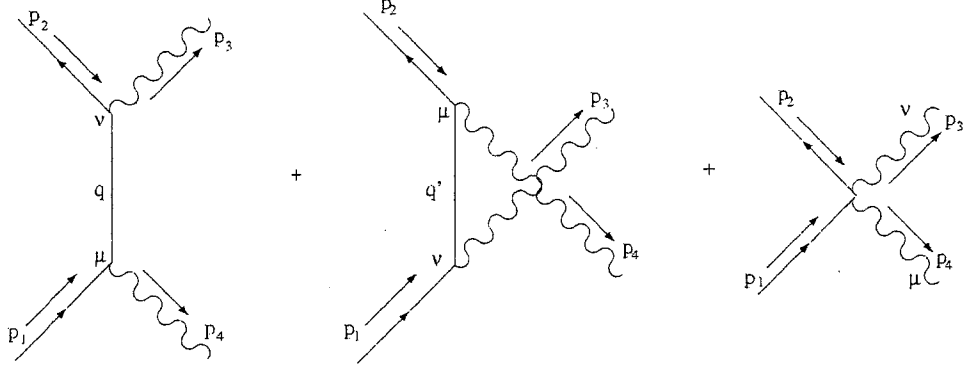


FIG. 2.3: Two fermions - two photon vertex.

FIG. 2.4: Feynman diagrams for $e^+e^- \rightarrow \gamma\gamma$

with all fermions and photons on shell:

$$\begin{aligned}
 & ie^2 \frac{\langle \theta^2 \rangle}{96} [(p_1 \cdot p_3) \{p_2^\rho \gamma^\eta - p_1^\eta \gamma^\rho\} \\
 & \quad + (p_1 \cdot p_4) \{p_2^\eta \gamma^\rho - p_1^\rho \gamma^\eta\} \\
 & \quad + (\not{p}_3 - \not{p}_4) \{p_1^\rho p_2^\eta - p_1^\eta p_2^\rho\}]. \tag{2.51}
 \end{aligned}$$

Putting all these rules together, the cross section up to first order in $\langle \theta^2 \rangle/12$ for diphoton production can be calculated (Fig. 2.4). The matrix element for diphoton production can be written as the sum of the three diagrams: $i\mathcal{M} = i\mathcal{M}_1 + i\mathcal{M}_2 + i\mathcal{M}_3$, with each matrix element defined below:

$$\begin{aligned}
 i\mathcal{M}_1 &= -ie^2 \epsilon_\mu^*(p_3) \epsilon_\nu^*(p_4) \bar{v}(p_2) \left[\frac{\gamma^\nu \not{q} \gamma^\mu}{t} + \frac{\langle \theta^2 \rangle}{96} \right. \\
 & \quad \left. \times \frac{t}{2} \{ \gamma^\nu \not{q} \gamma^\mu + p_2^\nu \gamma^\mu - p_1^\mu \gamma^\nu \} \right] u(p_1), \tag{2.52}
 \end{aligned}$$

$$\begin{aligned}
i\mathcal{M}_2 &= -ie^2\epsilon_\mu^*(p_3)\epsilon_\nu^*(p_4)\bar{v}(p_2) \left[\frac{\gamma^\mu \not{p}_1 \gamma^\nu}{u} + \frac{\langle\theta^2\rangle}{96} \right. \\
&\quad \left. \times \frac{u}{2} \{ \gamma^\mu \not{p}_1 \gamma^\nu + p_2^\mu \gamma^\nu - p_1^\nu \gamma^\mu \} \right] u(p_1), \tag{2.53}
\end{aligned}$$

$$\begin{aligned}
i\mathcal{M}_3 &= ie^2\epsilon_\mu^*(p_3)\epsilon_\nu^*(p_4)\frac{\langle\theta^2\rangle}{192}\bar{v}(p_2) \\
&\quad \times [t\{p_1^\mu \gamma^\nu - p_2^\nu \gamma^\mu\} + u\{p_1^\nu \gamma^\mu - p_2^\mu \gamma^\nu\} \\
&\quad + 2(\not{p}_3 - \not{p}_4)(p_1^\nu p_2^\mu - p_1^\mu p_2^\nu)] u(p_1). \tag{2.54}
\end{aligned}$$

It is easy to show that if either one of the polarization vectors is replaced with its momentum, the matrix element will be zero as we expect from gauge invariance. Next it is straightforward to show that the spin average square matrix element is:

$$|\overline{\mathcal{M}}|^2 = 2e^4 \left[\frac{t}{u} + \frac{u}{t} - \frac{\langle\theta^2\rangle}{96}(t^2 + u^2) \right]. \tag{2.55}$$

To first order in $\langle\theta^2\rangle/12$ this gives the following CM differential cross section:

$$\frac{d\sigma}{d\cos\theta} = \left(\frac{d\sigma}{d\cos\theta} \right)_{QED} \left[1 - \frac{\langle\theta^2\rangle}{192} \frac{s^2}{2} \sin^2\theta \right]. \tag{2.56}$$

2.4 Bounds on Λ_{NC} from colliders

Møller scattering experiments do not provide data at high enough energy to set a bound comparable to the one obtained from Bhabha scattering. For Bhabha scattering the bound can be extracted from a series of LEP experiments [1]. The total cross section integrated between θ_0 and $180^\circ - \theta_0$ predicted by our calculation can be written as:

$$\sigma = \sigma_{SM} + \frac{\pi\alpha^2 s}{8\Lambda_{NC}^4} \left\{ \frac{25}{4}a + \frac{7}{12}a^3 + 2 \ln \frac{1-a}{1+a} \right\}, \tag{2.57}$$

with $a = \cos\theta_0$. This matches the cut introduced by the L3 experiment where $\theta_0 = 44^\circ$ is the angle relevant to the L3 detector. Here we use σ_{SM} instead of σ_{QED} to take into account the weak interaction and radiative corrections. We have neglected the noncommutative correction to higher order QED and weak interactions. We use the

$\sqrt{s}(\text{GeV})$	$\sigma_{exp} \pm \Delta_{stat} \pm \Delta_{sys}(\text{pb})$	$\sigma_{SM}(\text{pb})$
130.10	$51.10 \pm 2.90 \pm 0.20$	56.50
136.10	$49.30 \pm 2.90 \pm 0.20$	50.90
161.30	$34.00 \pm 1.90 \pm 1.00$	35.10
172.30	$30.80 \pm 1.90 \pm 0.90$	30.30
182.70	$27.60 \pm 0.70 \pm 0.20$	26.70
188.70	$25.10 \pm 0.40 \pm 0.10$	24.90

TABLE 2.1: Bhabha Scattering: Data from L3 experiment at LEP and SM Prediction [1]

numerical values of the data above (TABLE 2.1) [1], and for the theoretical prediction we add the correction due to noncommutativity obtained in the previous section to the listed SM cross section. The χ^2 function is defined as follows:

$$\chi^2 = \sum_i \left(\frac{\sigma_{exp}^i - \sigma_{theor}^i}{\Delta_{exp}^i} \right)^2 \quad (2.58)$$

with $\Delta_{exp}^2 = \Delta_{stat}^2 + \Delta_{sys}^2$ and i sums over the energy range. Performing the χ^2 analysis over the energy range shown in TABLE 2.1, we obtain the bound $\Lambda_{NC} \geq 137$ GeV (95% C.L.).

A similar analysis can be performed on $e^+e^- \rightarrow \mu^+\mu^-$ using the data from the same experiment at LEP [1]. The total cross section integrated between θ_0 and $180^\circ - \theta_0$ is:

$$\sigma = \sigma_{SM} + \frac{\pi \alpha^2 s}{8 \Lambda_{NC}^4} \frac{a^3}{3}, \quad (2.59)$$

with a defined above and $\theta_0 = 44^\circ$. Fitting our theoretical prediction to LEP data (TABLE 2.2) [1] using χ^2 fit will set the bound for $\Lambda_{NC} \geq 86$ GeV (95% C.L.) Note that the correction term arising in the differential cross section can be written as $\frac{s^2}{8 \Lambda_{NC}^4}$, which is larger than one for $\sqrt{s} = 188.7$ GeV. Therefore this bound cannot be trusted. However, the other bounds obtained in this section are perturbatively valid and are much stronger than this result.

For diphoton production, the bound can be extracted from a series of experiments at LEP [67, 68, 69, 70, 71, 72]. The total cross section integrated between θ_0 and $180^\circ - \theta_0$

$\sqrt{s}(\text{GeV})$	$\sigma_{exp} \pm \Delta_{stat} \pm \Delta_{sys}(\text{pb})$	$\sigma_{SM}(\text{pb})$
130.10	$21.00 \pm 2.30 \pm 1.00$	20.90
136.10	$17.50 \pm 2.20 \pm 0.90$	17.80
161.30	$12.50 \pm 1.40 \pm 0.50$	10.90
172.30	$9.20 \pm 1.30 \pm 0.40$	9.20
182.70	$7.34 \pm 0.59 \pm 0.27$	7.90
188.70	$7.28 \pm 0.29 \pm 0.19$	7.29

TABLE 2.2: $e^+e^- \rightarrow \mu^+\mu^-$: Data from L3 experiment and SM Prediction [1]

predicted by our calculation can be written as:

$$\sigma = \sigma_{SM} - \frac{\pi\alpha^2 s}{16\Lambda_{NC}^4} \left\{ a + \frac{a^3}{3} \right\}, \quad (2.60)$$

with $a = \cos\theta_0$. This time the bound is obtained from an analysis done by the experimenters themselves for the purpose of bounding a generic contribution for ‘new physics.’ The bound set from diphoton production experiments at LEP, as obtained by the DELPHI collaboration and translated to our definition of noncommutativity scale is $\Lambda_{NC} \geq 160$ GeV [67, 68, 69, 70, 71, 72]. A similar analysis by the L3 collaboration yields a similar bound [67, 68, 69, 70, 71, 72].

A next linear collider (NLC) with a luminosity $3.4 \times 10^{34} \text{ cm}^{-2} \text{ s}^{-1}$ and center of mass energy 1.5 TeV will set a better bound for Λ_{NC} . We calculated the number of events predicted by ordinary QED at 1.5 TeV and took the statistical uncertainty from the square root of the number of events. By requiring the ‘new physics’ effect to be significant only if it can produce an effect at least 2 standard deviations away from this predicted value, a prediction for the bound that could be set for the noncommutative scale can be obtained. Our calculation for Bhabha scattering predicts a reach for $\Lambda_{NC} \approx 2.0$ TeV, for $e^+e^- \rightarrow \mu^+\mu^-$ $\Lambda_{NC} \approx 1.7$ TeV, for Møller scattering $\Lambda_{NC} \approx 2.7$ TeV and for diphoton production $\Lambda_{NC} \approx 2.0$ TeV. From this we can conclude that the bound obtained from these experiments will be about ≈ 2 TeV and is comparable to the energy scales where the experiments are performed.

2.5 Conclusion

We have considered the phenomenology of a Lorentz-conserving version of noncommutative QED. In this theory, spacetime coordinates are promoted to operators satisfying the DFR Lie algebra. As opposed to the Lorentz-violating canonical noncommutative theory, field theory variables have an additional dependence on the operator θ which characterizes the noncommutativity. This is handled by expanding the fields in powers of θ , and using gauge invariance and noncommutativity restrictions to determine the fields order by order in θ . Lorentz-invariance restricts interaction vertices to contain only even powers of θ , which has distinct consequences on the phenomenology of the theory. We considered various e^+e^- and e^-e^- collider processes. The cross section was calculated to second order in θ for Bhabha, Møller, and $e^+e^- \rightarrow \mu^+\mu^-$ scattering, as well as $e^+e^- \rightarrow \gamma\gamma$. Results were then compared to LEP 2 data, and bounds on the energy scale of noncommutativity, Λ_{NC} , were obtained. The tightest bound came from diphoton production which yielded $\Lambda_{NC} > 160$ GeV at the 95% confidence level. We also determined that an NLC running at 1.5 TeV with a luminosity of $3.4 \times 10^{34} \text{ cm}^{-2} \text{ s}^{-1}$ will be able to probe Λ_{NC} up to ~ 2 TeV.

CHAPTER 3

Universal Extra Dimensions and Kaluza-Klein Bound States

3.1 Introduction

The possibility of large extra dimensions has met considerable scrutiny in recent years. Sub-millimeter sized extra dimensions, in which only gravity can propagate in the bulk, allows for a reinterpretation of the hierarchy problem [73, 8, 9]. TeV-scale extra dimensions allow gauge and matter fields to propagate in the bulk as well, and have the virtue of allowing for an accelerated gauge unification [74, 75]. These and related scenarios are well-motivated by string theory, where the existence of extra spatial dimensions is necessary for the consistency of the theory.

The notion that the propagation of gauge and matter fields in the bulk implies compactification radii of order a TeV^{-1} follows from consideration of precision electroweak constraints [76, 77, 78, 79, 80, 81, 82]. In the first types of models studied, at least one Higgs field was assumed to be confined to an orbifold fixed point. The vacuum expectation value (vev) of such a field necessarily results in mixing between the Z boson and

its Kaluza-Klein (KK) excitations. One's intuition from models with extra Z' bosons and Z - Z' mixing suggests that the bounds on the first KK excitation will be of order a TeV, with some reduction if the vev of the Higgs responsible for this mixing is particularly small.

Universal extra dimensions (UED) were proposed as a way of avoiding such tree-level contributions to precision electroweak observables altogether [15]. In UED, all fields propagate in the bulk. Conservation of KK number prevents mixing between KK and zero-mode electroweak gauge bosons, so that the bounds described earlier are avoided. In the case of one extra dimension compactified on a Z_2 orbifold, a residual Z_2 symmetry of the effective four-dimensional (4D) Lagrangian allows interactions only between even numbers of the odd numbered KK modes. This renders the lightest KK particle (LKP) exactly stable. Typical bounds on the scale of compactification, $1/R$, are weakened to the collider bounds for the pair production of KK states, or approximately 300 GeV [20]. The possibility that the LKP is a dark matter candidate has also been investigated [16, 17, 83, 19, 18].

In the absence of radiative corrections and electroweak symmetry breaking, all KK modes at a given level would be exactly degenerate, with masses given by n/R , where n is a non-negative integer. Electroweak symmetry breaking introduces small corrections to this spectrum, with perhaps the exception of the KK excitations of the top quark, since m_{top} is not necessarily much smaller than $1/R$. A more sizable effect results from loop corrections to the KK mass spectrum, which can be divided into two types [2]. There are finite corrections, resulting from the propagation of bulk fields around the compact dimension, which are insensitive to momentum scales above $1/R$. There are also logarithmically divergent contributions that are localized at the orbifold fixed points. These renormalize the possible 5D Lorentz-violating interactions that exist at the fixed points and alter the KK mass spectrum. If we think of these interactions as counterterms, a renormalization condition must be chosen to fix their finite parts. Corrections to KK masses

are thus determined by $1/R$, the ultraviolet cutoff of the theory Λ , and the renormalization condition that determines the finite parts of the fixed-point-localized counterterms. Although in the most general case, these finite parts are undetermined (and the scenario is devoid of predictivity) one can adopt a minimal assumption that they vanish at the cutoff Λ . This boundary condition is no worse than, for example, the assumption of universal soft masses at the unification scale in the minimal supersymmetric standard model. We will adopt this assumption for the present purpose, and will show later that our results do not strictly depend on it.

A consequence of an otherwise degenerate mass spectrum corrected by loop effects is the possibility that some approximate degeneracies may remain. In particular, we note in the present work that the mass difference between the Kaluza-Klein excitations of the quarks (which we will refer to as KK-quarks, for brevity) and the LKP can be relatively small, for reasonable choices of R and Λ . The implication that we explore is the possible formation of KK-quark bound states, and we investigate whether they may be discerned at future electron-positron and muon colliders. In the case of heavy standard model quarks, it is well known that toponium bound states do not form because the lifetime of the top quark is short compared to the time scale associated with hadronization. It is usually said that this is a consequence of the heaviness of the top quark, but more precisely, it is a consequence of the large top-bottom mass difference. In the UED scenario of interest, the lightest KK quarks must decay to the (stable) LKP, and the phase space suppression leads to a different conclusion, for a wide range of model parameters. An investigation of KK bound states is not merely a topic of academic interest. It is possible that the pair production of KK modes of the first level may be accessible at colliders while that of the second level may be kinematically out of reach. Then the search for bound states of the first KK modes via a threshold scan may be the quickest approach to discovering additional interesting physics.

This chapter is organized as follows. In the next section we give a detailed review

of UED, including the topic of radiative corrections to the mass spectrum. In Section 3, we discuss the criterion for the formation of bound states, determine the model parameter space that is consistent with this constraint, and compute the bound state spectrum. In Section 4, we discuss the production and detection of “KK-quarkonia” at electron-positron, and at muon colliders. In particular, we show that the bound state decays have a distinctive signature that should allow easy discrimination from backgrounds. In the final section we summarize our conclusions.

3.2 UED

In this section we review the derivation of the 4D Lagrangian assuming one universal extra dimension. We begin by considering the simplified example of a U(1) gauge theory and then immediately generalize to the full standard model gauge group. We focus on results that will be used in the phenomenological analysis that follows.

Consider a 5D U(1) gauge theory with a fermion of unit charge e_{5D} propagating in the bulk. In 5D, the Clifford algebra is given by

$$\{\Gamma^M, \Gamma^N\} = 2g^{MN}, \quad (3.1)$$

where $\Gamma^\mu = \gamma^\mu$ and $\Gamma^5 = -i\gamma^5$. Here Roman indices run over all dimensions, while Greek indices run over the familiar four. It follows that the 5D spinor fields Ψ have four components, like their four-dimensional counterparts. However, since γ^5 no longer purely anticommutes with the 5D Dirac operator $i\Gamma^M\partial_M$, no chirality can be assigned to a massless 5D spinor field.

We now compactify the theory on the orbifold S^1/Z_2 . Four-dimensional chirality is obtained by imposing the boundary conditions $\Psi(x^\mu, y) = \Psi(x^\mu, y + 2\pi R)$ and $\Psi(x^\mu, y) = -\gamma^5\Psi(x^\mu, -y)$. This implies that there is a Z_2 even field Ψ_+ that is left-

handed, and an odd field Ψ_- that is right handed,

$$\Psi_+(x^M) = \sum_{n=0}^{\infty} \Psi_+^{(n)}(x^\mu) \cos(ny/R) , \quad \Psi_-(x^M) = \sum_{n=1}^{\infty} \Psi_-^{(n)}(x^\mu) \sin(ny/R) . \quad (3.2)$$

Since Ψ_- has no $n = 0$ component, only a left-handed zero-mode remains, while each higher KK level is composed of a vector-like pair. A 5D gauge field may be similarly decomposed

$$\mathcal{A}_\mu(x^M) = \sum_{n=0}^{\infty} \mathcal{A}_\mu^{(n)}(x^\nu) \cos(ny/R) , \quad \mathcal{A}_5(x^M) = \sum_{n=1}^{\infty} \mathcal{A}_5^{(n)}(x^\nu) \sin(ny/R) . \quad (3.3)$$

This choice of Z_2 parities assures that an unwanted scalar photon zero mode is also projected away by the orbifold boundary conditions.

The 4D Lagrangian may be obtained by substituting these expansions into the 5D action

$$S = \int d^5x \left(\bar{\Psi} i\Gamma^M D_M \Psi - \frac{1}{4} F_{MN} F^{MN} + \mathcal{L}_{\text{gauge fixing}} \right) , \quad (3.4)$$

where $D^M = \partial^M - ie_{5D} A^M$, and integrating over the extra dimension y . Terms quadratic in the n^{th} mode $\Psi^{(n)}$ or $\mathcal{A}_\mu^{(n)}$ in the 4D theory are then found to be multiplied by a factor of $2\pi R$ if $n = 0$, or πR if $n = k > 0$. Thus, properly normalized kinetic terms are obtained only after the rescalings

$$\mathcal{A}_\mu^{(0)} = \frac{1}{\sqrt{2\pi R}} A_\mu^{(0)} , \quad \mathcal{A}_M^{(k)} = \frac{1}{\sqrt{\pi R}} A_M^{(k)} , \quad \Psi_+^{(0)} = \frac{1}{\sqrt{2\pi R}} \psi_+^{(0)} , \quad \Psi_\pm^{(k)} = \frac{1}{\sqrt{\pi R}} \psi_\pm^{(k)} . \quad (3.5)$$

Notice that the fields Ψ and \mathcal{A}_μ have mass dimensions 2 and 3/2, respectively, while the rescaled fields ψ and A_μ have their usual 4D mass dimensions. Taking these rescalings into account, and that derivatives with respect to y become factors of n/R in the 4D theory, one may easily find the tree-level masses

$$m_{\psi^{(n)}} = m_{A^{(n)}} = n/R . \quad (3.6)$$

The gauge field fermion interactions for the Z_2 -even fermion fields follow from the 5D term

$$e_{5D} \bar{\Psi}_+ \mathcal{A}_\mu \gamma^\mu \Psi_+ . \quad (3.7)$$

Integrating over y , one finds

$$e_{5D} \left(2\pi R \bar{\Psi}_+^{(0)} \mathcal{A}^{(0)} \Psi_+^{(0)} + \sum_{n>0} \pi R \bar{\Psi}_+^{(0)} \mathcal{A}^{(n)} \Psi_+^{(n)} \right. \\ \left. + \sum_{m>0, n, r} (\delta_{m, |n-r|} + \delta_{m, n+r}) \frac{\pi R}{2} \bar{\Psi}_+^{(m)} \mathcal{A}^{(n)} \Psi_+^{(r)} \right) . \quad (3.8)$$

Of relevance to our investigation of KK quark decays later are the gauge interactions involving $n = 0$ and $n = 1$ modes. With the field rescalings described above, and including the Z_2 odd fermion field one finds

$$\mathcal{L} = e \left(\bar{\psi}_+^{(0)} \mathcal{A}^{(0)} \psi_+^{(0)} + \bar{\psi}_+^{(1)} \mathcal{A}^{(0)} \psi_+^{(1)} + \bar{\psi}_-^{(1)} \mathcal{A}^{(0)} \psi_-^{(1)} + [\bar{\psi}_+^{(0)} \mathcal{A}^{(1)} \psi_+^{(1)} + h.c.] \right) , \quad (3.9)$$

where the 4D gauge coupling $e = e_{5D}/\sqrt{2\pi R}$. Note that the 5D gauge coupling e_{5D} has mass dimension $-1/2$, while e is dimensionless, as we expect. This expression may be written more compactly by embedding the left- and right-handed modes ψ_+ and ψ_- into Dirac spinors ψ

$$\mathcal{L}_{\text{LH}} = e \left(\bar{\psi}^{(0)} \mathcal{A}^{(0)} P_L \psi^{(0)} + \bar{\psi}^{(1)} \mathcal{A}^{(0)} \psi^{(1)} + [\bar{\psi}^{(0)} \mathcal{A}^{(1)} P_L \psi^{(1)} + h.c.] \right) . \quad (3.10)$$

Here $P_L = (1 - \gamma^5)/2$, and the right-handed component of the zero-mode Dirac spinor is arbitrary. A similar expression for a fermion with a right-handed zero-mode can be obtained from Eq. (3.10) by replacing P_L by P_R . If radiative corrections render $m_{\psi^{(1)}} > m_{\mathcal{A}^{(1)}} + m_{\psi^{(0)}}$ then the last term can lead to KK fermion decay.

The field rescalings and the KK mode numbers in Eq. (3.10) are all independent of the chosen gauge group. We therefore may immediately generalize to the standard model. The interaction terms relevant to the KK-quark decays that we consider later are

as follows:

$$\begin{aligned}
\mathcal{L} = & \frac{2}{3}e \left[\frac{\sin(\theta_W + \theta_1) - \frac{1}{2}\sin(\theta_W - \theta_1)}{\sin 2\theta_W} \bar{u}^{(0)} \not{A}^{(1)} P_L u_L^{(1)} + \frac{\cos \theta_1}{\cos \theta_W} \bar{u}^{(0)} \not{A}^{(1)} P_R u_R^{(1)} \right] \\
& + \frac{1}{3}e \left[\frac{\cos(\theta_W - \theta_1) + 2\cos(\theta_W + \theta_1)}{\sin 2\theta_W} \bar{u}^{(0)} \not{Z}^{(1)} P_L u_L^{(1)} - 2\frac{\sin \theta_1}{\cos \theta_W} \bar{u}^{(0)} \not{Z}^{(1)} P_R u_R^{(1)} \right] \\
& - \frac{1}{3}e \left[\frac{\sin(\theta_W + \theta_1) - 2\sin(\theta_W - \theta_1)}{\sin 2\theta_W} \bar{d}^{(0)} \not{A}^{(1)} P_L d_L^{(1)} + \frac{\cos \theta_1}{\cos \theta_W} \bar{d}^{(0)} \not{A}^{(1)} P_R d_R^{(1)} \right] \\
& - \frac{1}{3}e \left[\frac{2\cos(\theta_W - \theta_1) + \cos(\theta_W + \theta_1)}{\sin 2\theta_W} \bar{d}^{(0)} \not{Z}^{(1)} P_L d_L^{(1)} - \frac{\sin \theta_1}{\cos \theta_W} \bar{d}^{(0)} \not{Z}^{(1)} P_R d_R^{(1)} \right] \\
& + \frac{1}{\sqrt{2}}e \left[\frac{1}{\sin \theta_W} \bar{u}^{(0)} \not{W}^{(1)} P_L d_L^{(1)} \right] + h.c. \tag{3.11}
\end{aligned}$$

Note that the $n = 1$ fields above are complete Dirac spinors (with both left- and right-handed components), and the subscript indicates only the chirality of the associated zero mode. In addition, θ_W is the zero-mode weak mixing (Weinberg) angle, while θ_1 is the corresponding angle for the $n = 1$ modes. In the absence of radiative corrections, the electroweak symmetry conserving contributions to the $B^{(1)}-W^{(1)}$ mass squared matrix are precisely diagonal (and equal to $1/R^2$), so that we expect $\theta_W = \theta_1$. In that limit, the photon and Z couplings in Eq. (3.11) have the same values as their couplings to either left- or right-handed up or down quarks. However, radiative corrections lead to much smaller values of θ_1 . For example, for $\Lambda R = 20$ and $R^{-1} = 500$ GeV, $\sin^2 \theta_1 \approx 10^{-2}$ [2]. In the following section, we omit the dependence on θ_1 to streamline our analytical expressions. The full dependence on θ_1 has been taken into account in all our numerical results, and complete analytical expressions are provided in the Appendix.

Radiative corrections to the KK-gauge boson and KK-quark masses allow for two-body decays via the interactions in Eq. (2.11). Over the range of ΛR and R^{-1} that we consider, the LKP is the first KK excitation of the photon, $\gamma^{(1)}$ [2]. The radiative corrections to the KK-quark and the KK-gauge boson masses were calculated by Cheng, Matchev and Schmaltz [2]. Adopting their assumption that the finite parts of counter terms vanish at the cutoff scale Λ , we plot the mass splitting between the KK-quarks and the LKP, as well as the splitting between the weak KK-gauge bosons and the LKP, as a

function of $1/R$, in Fig. 3.1, setting the value of $\Lambda R = 20$. Complete expressions for the radiative corrections that are taken into account in this figure can be found in Ref. [2]. As a consequence of the smallness of the $n = 1$ mixing angle θ_1 , the LKP, $\gamma^{(1)}$, is almost entirely a KK- B boson, while the KK- W and KK- Z are virtually degenerate in mass. As we will see in the next section, the values of ΔM in Fig. 3.1 are small enough to lead to KK-quark bound state formation.

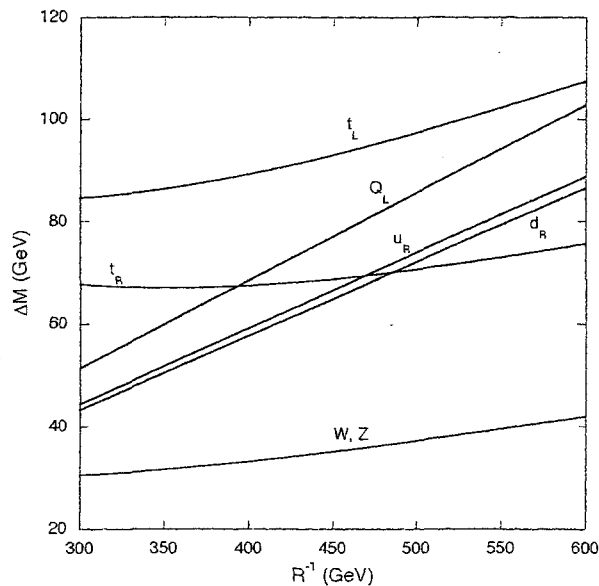


FIG. 3.1: The mass splitting between KK-quarks and the LKP, $\gamma^{(1)}$, as well as the splitting between the weak KK-gauge bosons and the LKP, as a function of $1/R$ for $\Lambda R = 20$. Here, Q_L stands for all isodoublet KK-quarks except top, u_R for up and charm isosinglet KK-quarks, and d_R for down, strange and bottom isosinglet KK-quarks

3.3 Bound States

From Fig. 3.1, one finds that radiative corrections to the KK masses in UED are typically in the 10-100 GeV range. We will show that this is numerically small enough to allow for the formation of bound states of KK quarks. The smaller phase space available for KK-quark decay renders the bound states narrower than the spacing between adjacent KK-quarkonia levels, at least for the first few levels. In this section, the decay widths

and branching ratios of the KK-quarks are calculated and discussed, as well as the mass splittings of the different KK-quarkonia energy levels and the production cross sections at lepton colliders.

3.3.1 Decay widths and branching ratios

With the Lagrangian and mass splittings given in the previous section, it is straightforward to determine the decay widths and branching ratios of the KK-quarks. We will begin by considering the weak isosinglet KK-quarks (except the KK-top), then the weak isodoublet KK-quarks, and finally the unusual case of the isosinglet KK-top quark. While the partial decay widths of KK-quarkonia through annihilation are typically tens of keV, we will see that the decay widths of the KK-quarks (except the KK-top) are typically close to a hundred MeV. Thus, the decay width of a KK-quarkonium state will be twice the decay width of the KK-quark.

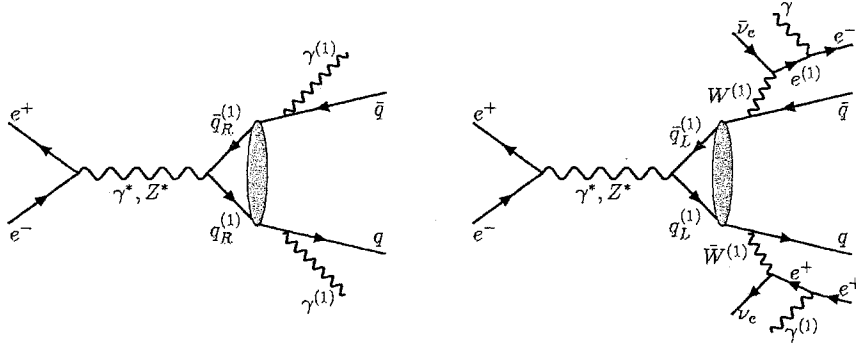


FIG. 3.2: The production and decay chains of $q_R^{(1)}$ and $q_L^{(1)}$ pairs. Note that all of the decays in the $q_L^{(1)}$ decay chain are two-body, leading to monochromatic quarks and leptons.

Isosinglet KK-quarks

Isosinglet KK-quarks cannot decay into KK-W bosons and their decay into KK-Z bosons is suppressed by a factor of $\sin^2 \theta_1$. In addition, their decay into KK-Higgs bosons is suppressed by small Yukawa couplings. As a result, the dominant decay mode

is $q^{(1)} \rightarrow q^{(0)} \gamma^{(1)}$, as shown in Fig. 3.2. Since the LKP is stable, the decay signature will be a monochromatic quark and missing energy. The one exception is the isosinglet KK-top quark, which cannot decay into a top quark and the LKP; we will discuss that case shortly. Including the small coupling to the KK-Z boson, we find that the branching ratio into a quark and a KK- γ is over 98 percent (consistent with the results in [84]). Neglecting the mass of the light quark and $\sin^2 \theta_1$, we find the decay width

$$\Gamma(d_R^{(1)} \rightarrow d_R \gamma^{(1)}) = \frac{e^2 m_{d_R^{(1)}}}{288\pi \cos^2 \theta_W} \left(1 - \frac{m_{\gamma^{(1)}}^2}{m_{d_R^{(1)}}^2}\right)^2 \left(2 + \frac{m_{d_R^{(1)}}^2}{m_{\gamma^{(1)}}^2}\right). \quad (3.12)$$

An exact expression is given in the Appendix. The decay width for the $u_R^{(1)}$ is larger by a factor of four. Given values for $1/R$ and ΛR , this width is completely determined. The results are shown in Fig. 3.3. We see that the widths are typically within a factor of two of 10 MeV. As noted above, the decay signature is a monochromatic quark and missing energy; for $1/R = 500$ GeV and $\Lambda R = 20$, the quark energy is 67 GeV.

Isodoublet KK-quarks

For the isodoublet KK-quarks, decay channels into KK-W and KK-Z bosons are available. Although there is less phase space into these than into the KK- γ boson, the couplings are substantially larger, and the KK-W and KK-Z modes dominate. The decay width into a KK-W is given by

$$\Gamma(d_L^{(1)} \rightarrow u_L W^{(1)}) = \frac{e^2 m_{d_L^{(1)}}}{64\pi \sin^2 \theta_W} |V_{ij}|^2 \left(1 - \frac{m_{W^{(1)}}^2}{m_{d_L^{(1)}}^2}\right)^2 \left(2 + \frac{m_{d_L^{(1)}}^2}{m_{W^{(1)}}^2}\right), \quad (3.13)$$

where V_{ij} is the relevant CKM element. The identical decay width, of course, applies to $u_L^{(1)} \rightarrow d_L W^{(1)}$ decays. The decay width into a KK-Z is given by

$$\Gamma(d_L^{(1)} \rightarrow d_L Z^{(1)}) = \frac{e^2 m_{d_L^{(1)}}}{128\pi \sin^2 \theta_W} \left(1 - \frac{m_{Z^{(1)}}^2}{m_{d_L^{(1)}}^2}\right)^2 \left(2 + \frac{m_{d_L^{(1)}}^2}{m_{Z^{(1)}}^2}\right). \quad (3.14)$$

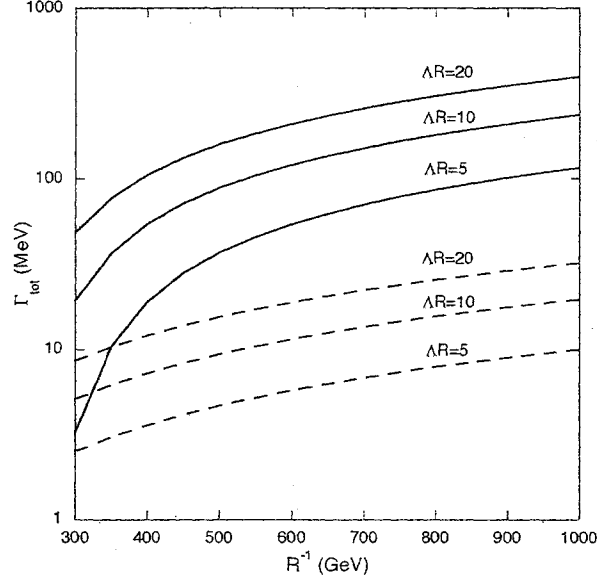


FIG. 3.3: The total decay width of $n = 1$ isosinglet and isodoublet down KK-quarks as a function of R^{-1} for fixed $\Delta R = 5, 10, 20$. The solid lines represent the total decay widths of isodoublet down KK-quarks for each corresponding ΔR value, respectively. The dashed lines are for the isosinglet case. The isodoublet up KK-quark total decay width is equal to that of the down and the isosinglet up KK-quark's width is four times larger than that of the isosinglet down.

We see that the branching ratio into the KK- W bosons are $2|V_{ij}|^2$ times that of the KK- Z bosons. The branching ratio into KK- γ bosons is negligible, always less than a few percent. These decays will give spectacular signatures. The decay into a KK- W boson, as shown in Fig. 3.2, leads to the decay chains $d_L^{(1)} \rightarrow u_L W^{(1)} \rightarrow u_L l \nu^{(1)}$ and $d_L^{(1)} \rightarrow u_L W^{(1)} \rightarrow u_L l^{(1)} \nu \rightarrow u_L l \nu \gamma^{(1)}$ leading to a monochromatic quark, a lepton, and missing energy. For example, for $1/R = 500$ GeV and $\Delta R = 20$, the quark energy will be 46 GeV. Assuming measurement of the quark jet allows reconstruction of the $W^{(1)}$ four-momentum, then the lepton energy can be completely determined¹. The decay into a KK- Z is even more spectacular, with the chain $d_L^{(1)} \rightarrow d_L Z^{(1)} \rightarrow d_L l l^{(1)} \rightarrow d_L l l \gamma^{(1)}$, where l is a charged lepton. Again, the initial quark jet energy is fixed, and the sequential two-body decays should allow for easy reconstruction of the event, and suppression of backgrounds. Of course, in both the KK- W and KK- Z cases, there will also be hadronic

¹Even if the $W^{(1)}$ four-momentum can't be reconstructed, the spread in the lepton energy will be $\mathcal{O}(10\%)$.

decays – we have focused on the leptonic because the signatures are much cleaner. The resulting total widths are plotted in Fig. 3.3; and the KK-W final state accounts for 2/3 of the widths (for the first two generations).

For the first two generations, generation-conserving decays are favored, since the CKM matrix is nearly the identity. However, for the third generation, a decay into a top quark is not kinematically allowed. For the KK-top quark, this means that only the decay into a KK-W is possible. Due to CKM suppression, decays of the KK-bottom into KK-Z and KK- γ are favored and thus the decay width of the KK-bottom is 1/3 of those shown in Fig. 3.3. For the isodoublet KK-top, the mass is somewhat larger than the other KK-quarks, and thus more phase space is available. For most of parameter-space, we find that the decay width of the KK-top (entirely through the KK-W chain) is approximately 80 percent of the widths shown in the figure.

isosinglet KK-top quarks

Due to radiative corrections the isodoublet and isosinglet KK-top quarks mix, with a mass matrix given by

$$\begin{pmatrix} 1/R + \delta m_{T^1} & m_{top} \\ m_{top} & -1/R - \delta m_{t^1} \end{pmatrix}$$

where the δm 's are small radiative corrections. The result is a mixing angle given by $\tan 2\theta_1 = 2m_{top}R/(2 + \delta m_{T^1}R + \delta m_{t^1}R)$, which leads to a coupling of the isosinglet top quark to a b-quark and a KK-W boson². The decay width is then [85]

$$\Gamma = \sin^2 \theta_1 \frac{G_F}{\sqrt{2}} \frac{M_W^2}{3\pi m_{t^1}^3 M_{W^1}^2} (m_{t^1}^2 - M_{W^1}^2)(m_{t^1}^2 + 2M_{W^1}^2). \quad (3.15)$$

For $1/R \sim 500$ GeV, the decay width is 10 MeV [85]. Therefore, the isodoublet KK-top quark can form a bound state whose decay signature is a monochromatic b-quark, a monochromatic lepton and missing energy.

²We thank Marc Sher for pointing this out.

3.3.2 Production cross-sections

The cross-section for production of a vector resonance, $e^+e^- \rightarrow V \rightarrow X$ is given by [86]

$$\sigma_V = \frac{12\pi(s/M_V^2)\Gamma_{ee}\Gamma_X}{(s - M_V^2)^2 + M_V^2\Gamma_V^2}, \quad (3.16)$$

where Γ_{ee} , Γ_X and Γ_V are the partial widths for $V \rightarrow e^+e^-$, for $V \rightarrow X$ and for the total width, respectively. Since we are interested in the total production cross-section, and since the partial width into Γ_{ee} is much smaller than the total width, we can set $\Gamma_X = \Gamma_V$ (this will be valid for all cases except the isosinglet KK-top quarkonia). At the peak resonance, the production cross-section is then given by

$$\sigma_V^{\text{peak}} = \frac{12\pi\Gamma_{ee}}{M_V^2\Gamma_V}. \quad (3.17)$$

We need the partial decay width of $V \rightarrow e^+e^-$. The decay width through a virtual photon is given by

$$\Gamma(V \rightarrow \gamma^* \rightarrow e^+e^-) \equiv \Gamma_\gamma = \frac{4\pi\alpha e_Q^2}{3M_V^3}|F_V|^2 \left[1 - \frac{16\alpha_s}{3\pi}\right], \quad (3.18)$$

where $|F_V|^2$ is related to the wave function at the origin, and is given by $12M_V|\Psi_V(0)|^2$.

The partial decay width including virtual Z exchange is related to this

$$\Gamma(V \rightarrow \gamma^*, Z^* \rightarrow e^+e^-) = (M_V^2/e^2e_Q)^2(|G_V|^2 + |G_A|^2)\Gamma_\gamma, \quad (3.19)$$

where

$$G_V = \frac{e^2e_Q}{M_V^2} + \frac{8G_F M_Z^2}{\sqrt{2}} \frac{g_V^e g_V^Q}{M_V^2 - M_Z^2 + i\Gamma_Z M_Z}, \quad (3.20)$$

and

$$G_A = \frac{8G_F M_Z^2}{\sqrt{2}} \frac{g_A^e g_V^Q}{M_V^2 - M_Z^2 + i\Gamma_Z M_Z}. \quad (3.21)$$

Here, g_V and g_A are the vector and axial vector couplings of the fermion to the Z, and $g_{V_L}^Q = g_{Q_L}$, $g_{V_R}^Q = (g_{Q_L} + g_{Q_R})/2$ with $g_Q = T_3 - e_Q \sin^2 \theta_W$. Finally, we need the wave

$M_V(\text{GeV})$	$\Gamma_{ee}(\bar{u}_L^{(1)}u_L^{(1)})(\text{keV})$	$\Gamma_{ee}(\bar{d}_L^{(1)}d_L^{(1)})(\text{keV})$	$\Gamma_{ee}(\bar{u}_R^{(1)}u_R^{(1)})(\text{keV})$	$\Gamma_{ee}(\bar{d}_R^{(1)}d_R^{(1)})(\text{keV})$
600	14.58	6.73	9.74	3.64
800	19.31	8.79	12.97	4.82
1000	24.06	10.89	16.21	6.01
1200	28.82	13.00	19.45	7.20
1400	33.59	15.13	22.68	8.39
1600	38.36	17.25	25.92	9.59
1800	43.14	19.39	29.16	10.78
2000	47.92	21.52	32.40	11.98

TABLE 3.1: The partial decay width of $V \rightarrow e^+e^-$ for both isodoublet and isosinglet KK-quark bound states .

function at the origin. At these high mass scales, one expects single gluon exchange to be fairly accurate, and in that approximation the wave function at the origin is given by

$$|\Psi(0)|^2 = \frac{1}{\pi} \left(\frac{2M_Q\alpha_s(M_Q)}{3n} \right)^3, \quad (3.22)$$

where n is the principle quantum number. Putting these together, we find that

$$\Gamma_{ee} = \frac{e^4\alpha_s^3(M_Q)}{27n^3\pi^2} M_V \left(1 - \frac{16\alpha_s}{3\pi} \right) \left(e_Q^2 + \frac{(g_V^Q)^2}{(1-\kappa_Z)^2 \sin^4 2\theta_W} \right), \quad (3.23)$$

where $\kappa_Z = m_Z^2/M_V^2$. To get Eq. (3.23) we assumed that g_V^e is negligible and $\Gamma_Z^2\kappa_Z \ll (1-\kappa_Z)^2 M_V^2$, even though we have used the exact expressions for numerical calculations.

In Table 3.1, we have listed the decay width, Γ_{ee} for a range of KK-quarkonia masses.

We can now determine, using Eq. (3.5), the peak production cross sections for isodoublet and isosinglet KK-quarkonia. The results are show in Figs. 3.4 and 3.5. The cross sections are substantial, between 1 and 100 picobarns.

We now turn to the mass splittings between the different KK-quarkonia levels.

3.3.3 Mass Splittings

To observe KK-quark bound states, the mass splitting between adjacent resonances must be larger than their typical decay widths. The KK-quark mass scale justifies a non-relativistic calculation of the binding energies. We therefore solve the radial Schrödinger

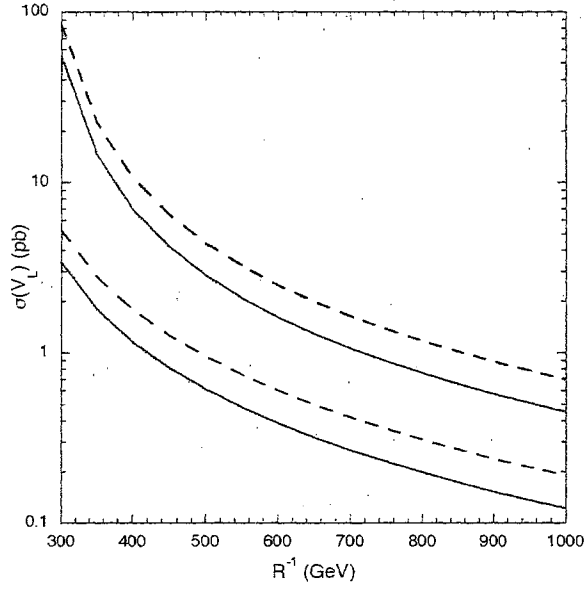


FIG. 3.4: The resonance production cross section for isodoublet KK-quarkonia states, except KK-toponium, as a function of R^{-1} for $\lambda R = 5, 20$. The solid lines represent down type KK-quarkonia states and the dashed ones represent up-type KK-quarkonia states, and the upper (lower) lines correspond to $\lambda R = 5$ (20).

equation,

$$-\frac{1}{2\mu} \frac{d^2 u}{dr^2} + [V(r) + \frac{1}{2\mu} \frac{l(l+1)}{r^2}] u = \Delta E u, \quad (3.24)$$

for a suitable phenomenological potential $V(r)$. Here $u(r) = rR(r)$ and the complete wave function is $\psi(r, \theta, \phi) = R(r)Y_{lm}(\theta, \phi)$. The wave function satisfies

$$\begin{aligned} u(0) &= 0, \\ u(r) &\rightarrow 0, \quad r \rightarrow \infty. \end{aligned} \quad (3.25)$$

Given a choice for $V(r)$, Eq.(3.24) is solved numerically to obtain the energy eigenvalues ΔE ; the mass for each bound state is then given by

$$M_n = 2M_{KK} + \Delta E_n, \quad (3.26)$$

where ΔE_n is the energy eigenvalue of the n^{th} level and M_{KK} is the mass of the KK-quark. Normalizing the wave function by

$$\int_0^\infty |u|^2 dr = 1, \quad (3.27)$$

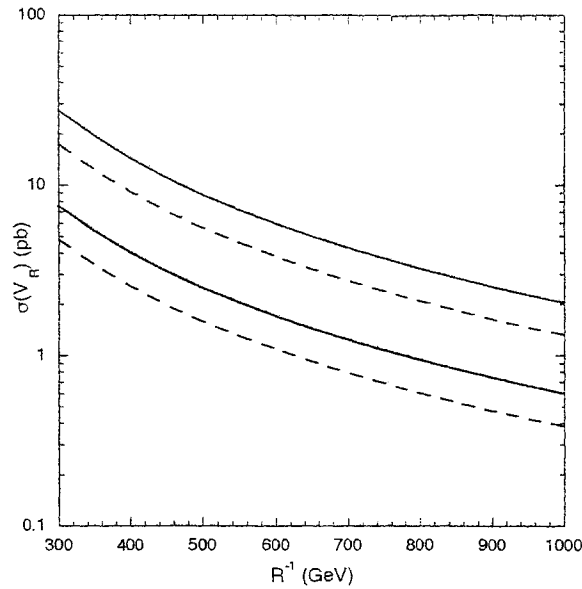


FIG. 3.5: The same as Fig. 3.4 but for isosinglet KK-quarkonia states. Here the upper (lower) lines correspond to $\lambda R = 20$ (5).

one may compute $R(0) = u'(0)$.

QCD motivates the following form for the potential:

$$V = -\frac{4}{3} \frac{\alpha_s}{r} + Ar. \quad (3.28)$$

The first term is Coulomb-like and is generated by one-gluon exchange, while the second is linear and models confinement. For $A \simeq 1 \text{ GeV fm}^{-1}$, this potential predicts energy level splittings in good agreement with the data for the Υ and J/ψ systems. At the typical energies of KK-quarkonia production, one would expect the Coulomb-like potential to dominate resulting in nearly hydrogen-like energy level splittings. However, hydrogen-like wave functions become more spread out at higher energy levels, suggesting a more significant contribution from the linear term in these cases. Note, however, that the level spacings for a hydrogen-like spectrum decrease roughly as $\Delta E_{n,n+1} \propto \frac{1}{n^3}$, where n is the radial quantum number. Therefore, only the first few energy levels will have splittings large enough to permit KK-quark bound states to be distinguished.

For $A = 1 \text{ GeV fm}^{-1}$ and $\alpha_s = 0.1$, the radial Schrödinger equation was solved numerically for the 1S, 2S, and 3S energy levels. The results are listed in Table 3.3.3 for KK-quark masses of 300 GeV and 500 GeV, along with the predictions of a hydrogen-like

M_{KK}	level	ΔE (GeV)	$a_0^{3/2} R(0)$	ΔE_H (GeV)	$a_0^{3/2} R(0)_H$
300	1S	-1.319	3.096	-1.334	3.079
300	2S	-0.276	1.173	-0.333	1.089
300	3S	-0.030	0.763	-0.149	0.593
500	1S	-2.213	3.085	-2.223	3.079
500	2S	-0.521	1.122	-0.555	1.089
500	3S	-0.171	0.670	-0.248	0.593

TABLE 3.2: Energy shifts and radial wave functions at the origin computed numerical assuming the potential in Eq. (3.28). The parameter a_0 here is $1/(\mu\alpha_s)$, where $\mu = M_{KK}/2$ is the reduced mass. The last two columns show the result obtained when neglecting the linear term in the potential.

potential. As expected, both the energy eigenvalues and $R(0)$ are nearly hydrogen-like, justifying the use of Eq. (3.10) in the decay rate calculations.

We see that the mass splittings, especially between the 1S and 2S states, are substantially larger than the width of these states, and thus will be discernible in a collider with sufficient energy resolution. We now turn to experimental detection of these states.

3.4 Detection

The production cross section for KK-quarkonia at a linear collider can now be discussed. For definitiveness, we first consider the isosinglet KK-quarks, assuming $1/R = 500$ GeV and $\Lambda R = 20$. The masses of the $d_R^{(1)}$ and $s_R^{(1)}$ are then 572.14 GeV, the $b_R^{(1)}$ is 572.16 GeV, and the $u_R^{(1)}$ and $c_R^{(1)}$ are 573.84 GeV. (The mass of the $t_R^{(1)}$ is actually a few GeV lighter, but its decay signature, as noted in the last section, is completely different.)

Putting these together, we find the cross section as a function of \sqrt{s} given in Fig. 3.6. The signature is very dramatic—one expects two monochromatic (in this case, 67 GeV) quarks and large missing energy. Clearly, the splitting between the resonances is large enough to separate the states. In the case of the top KK-quark, the resulting cross section looks identical to those of the up and charm KK-quark, but now the signature would be a fermion-antifermion pair, each with an energy of 570 GeV.

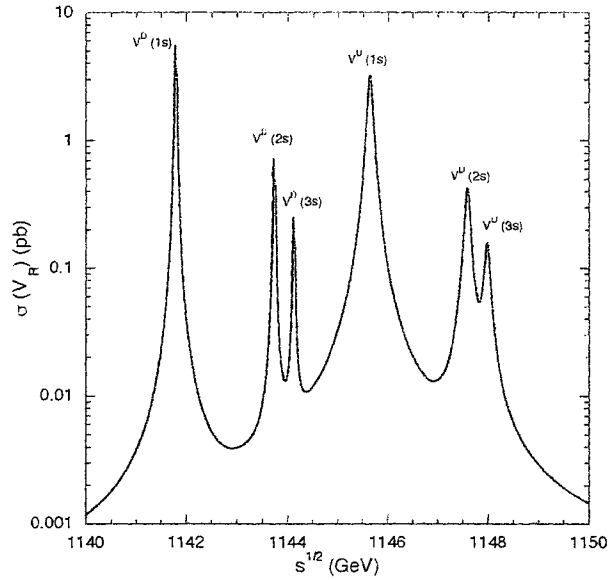


FIG. 3.6: The cross section for KK-quarkonia formed by isosinglet KK-quarks as a function of \sqrt{s} for $1/R = 500$ GeV and $\Lambda R = 20$. The labels V^D refer to the bound states of isosinglet KK-down, KK-strange and KK-bottom quarks, while V^U refers to the bound states of isosinglet KK-up and KK-charm quarks.

The masses of the isodoublet KK-quarks, except for the top, are nearly degenerate at 585.7 GeV. The cross section is plotted in Fig. 3.7. Again, the splitting between the resonances is large enough to separate the low-lying states. Here, the signatures are also dramatic, with two monochromatic quarks (in this case with energies of 46 GeV) and, depending on the decay chain, charged leptons, as discussed earlier. The isodoublet top KK-quark has a similar cross section, but is approximately 12 GeV heavier.

These center-of-mass energies are rather high. However, the lower bound on the size of the extra dimensions is approximately 300 GeV. Using this value of $1/R$, we find the results in Figs 3.8 and 3.9, which are similar to the $1/R = 500$ GeV case. Note that one can discern the fact that the KK-bottom quark is slightly heavier than the KK-down and KK-strange quarks, leading to some substructure in the resonances. Of course, in all of these cases, the $n = 2$ modes will be out of reach of a TeV scale linear collider.

Of course, it will still not be possible to detect these structures if the beam resolution is too large. At a muon collider, this will not be a problem, since mass resolution of

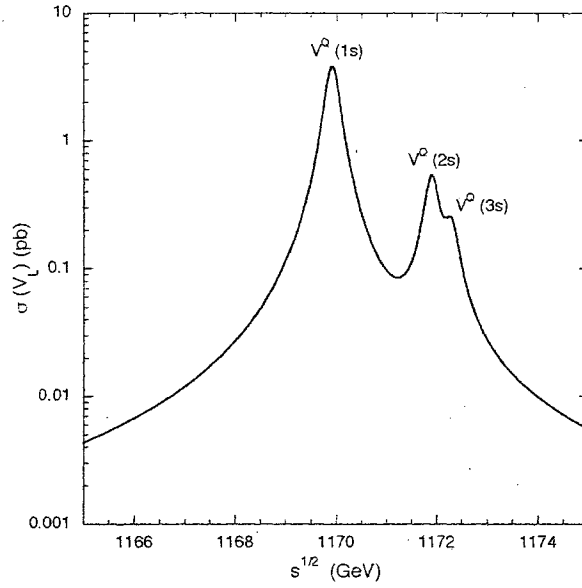


FIG. 3.7: The cross section for KK-quarkonia formed by isodoublet KK-quarks as a function of \sqrt{s} for $1/R = 500$ GeV and $\Lambda R = 20$. The label V^Q refers to all of the isodoublet KK-quarks, except for the KK-top.

a few MeV is possible after deconvolution of the beamstrahlung and initial state radiation [87, 88]. Resolution is a potential problem for electron-positron colliders, however, since one expects the average energy loss at $\sqrt{s} = 500$ GeV to be approximately 1.5% [89]. This energy loss comes from initial state radiation and beamstrahlung. However, the spectrum for each is well known and it is expected [89, 90] that the resulting mass resolution after deconvolution will be better than 10^{-4} , possibly a few times 10^{-5} , or 50 MeV for a $\sqrt{s} = 1000$ GeV. Such a mass resolution would easily allow the states to be detected (although precise width measurements would require better resolution). Clearly, a dedicated simulation would be needed to determine the capabilities of a linear collider (such a simulation would also be relevant for long-lived fourth generation quarkonia, and other s-channel resonances) for detection of KK-quarkonia states.

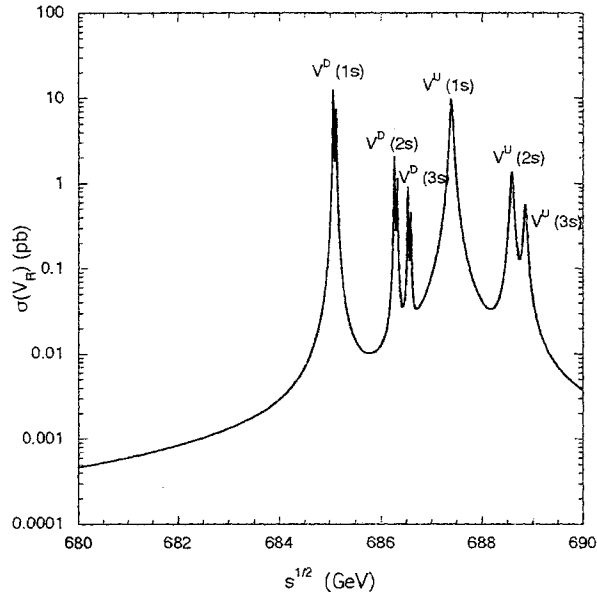


FIG. 3.8: The cross section for KK-quarkonia formed by isosinglet KK-quarks as a function of \sqrt{s} for $1/R = 300$ GeV and $\Lambda R = 20$. The labels are the same as in the previous figures.

3.5 Conclusions

If the simple model of Universal Extra Dimensions that we have considered is realized in nature, the mass splittings between the $n = 1$ KK-quarks and the lightest KK particle will be substantially smaller than the splitting between the top and bottom quarks. As a consequence, KK-quarks can be sufficiently long lived to form bound states, that we call KK-quarkonia, for a wide range of model parameters. With boundary mass corrections renormalized to vanish at an $\mathcal{O}(\text{TeV})$ cutoff scale Λ , we show that the KK-quark decay widths are in the 10-100 MeV range. We find that the peak cross sections for the 1S KK-quarkonia states are of the order of a few picobarns, and that the production cross sections near threshold show very clear and distinctive 1S, 2S and 3S resonant peaks. The decay signatures are very dramatic and nearly background-free: each isosinglet KK-quark (except the top) will decay into missing energy and a monochromatic quark (whose energy is determined solely by the KK-quark masses), and each isodoublet KK-quark will decay into missing energy, a monochromatic quark, and one or more leptons arising

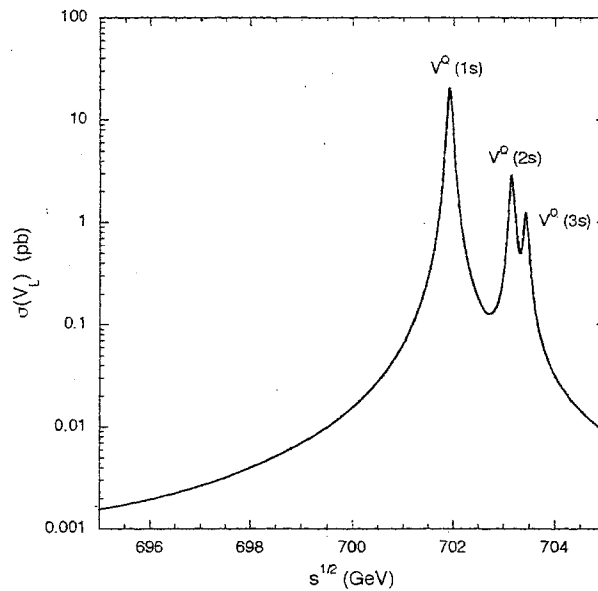


FIG. 3.9: The cross section for KK-quarconia formed by isodoublet KK-quarks as a function of \sqrt{s} for $1/R = 300$ GeV and $\Lambda R = 20$. The labels are the same as in the previous figures.

from subsequent two-body decays. The key issue for experimental detection is achieving sufficient energy resolution. This will not be a difficulty for a muon collider, and not impossible for an electron-positron machine. However, determining the resolution in the later case will require simulations to deconvolve the beamstrahlung and initial state radiation energy loss mechanisms.

3.6 Decay Width Formulae

In this appendix, we give the partial decay width expressions for the decays of $n = 1$ KK-quarks by retaining all fermion masses and the mixing angle θ_1 . For the decays of isosinglet KK-quarks, the partial decay widths can be expressed as

$$\begin{aligned}
\Gamma(d_R^{(1)} \rightarrow d_R \gamma^{(1)}) &= \frac{e^2 m_{d_R^{(1)}} \cos^2 \theta_1}{288\pi \cos^2 \theta_W} \lambda^{1/2}(\kappa_\gamma, \kappa_d) \left[\frac{1}{\kappa_\gamma} \lambda(\kappa_\gamma, \kappa_d) + 3(-\kappa_\gamma + \kappa_d + 1) \right], \\
\Gamma(u_R^{(1)} \rightarrow u_R \gamma^{(1)}) &= \frac{e^2 m_{u_R^{(1)}} \cos^2 \theta_1}{72\pi \cos^2 \theta_W} \lambda^{1/2}(\kappa_\gamma, \kappa_u) \left[\frac{1}{\kappa_\gamma} \lambda(\kappa_\gamma, \kappa_d) + 3(-\kappa_\gamma + \kappa_d + 1) \right], \\
\Gamma(d_R^{(1)} \rightarrow d_R Z^{(1)}) &= \frac{e^2 m_{d_R^{(1)}} \sin^2 \theta_1}{288\pi \cos^2 \theta_W} \lambda^{1/2}(\kappa_Z, \kappa_d) \left[\frac{1}{\kappa_\gamma} \lambda(\kappa_\gamma, \kappa_d) + 3(-\kappa_\gamma + \kappa_d + 1) \right], \\
\Gamma(u_R^{(1)} \rightarrow u_R Z^{(1)}) &= \frac{e^2 m_{u_R^{(1)}} \sin^2 \theta_1}{72\pi \cos^2 \theta_W} \lambda^{1/2}(\kappa_Z, \kappa_u) \left[\frac{1}{\kappa_\gamma} \lambda(\kappa_\gamma, \kappa_d) + 3(-\kappa_\gamma + \kappa_d + 1) \right] \quad (3.29)
\end{aligned}$$

and those for isodoublet case are

$$\begin{aligned}
\Gamma(d_L^{(1)} \rightarrow d_L \gamma^{(1)}) &= \frac{e^2 m_{d_L^{(1)}}}{128\pi} \left[\frac{1 \cos \theta_1}{3 \cos \theta_W} - \frac{\sin \theta_1}{\sin \theta_W} \right]^2 \lambda^{1/2}(\kappa_\gamma, \kappa_d) \\
&\quad \times \left[\frac{1}{\kappa_\gamma} \lambda(\kappa_\gamma, \kappa_d) + 3(-\kappa_\gamma + \kappa_d + 1) \right], \\
\Gamma(u_L^{(1)} \rightarrow u_L \gamma^{(1)}) &= \frac{e^2 m_{u_L^{(1)}}}{128\pi} \left[\frac{1 \cos \theta_1}{3 \cos \theta_W} + \frac{\sin \theta_1}{\sin \theta_W} \right]^2 \lambda^{1/2}(\kappa_\gamma, \kappa_u) \\
&\quad \times \left[\frac{1}{\kappa_\gamma} \lambda(\kappa_\gamma, \kappa_d) + 3(-\kappa_\gamma + \kappa_d + 1) \right], \\
\Gamma(d_L^{(1)} \rightarrow d_L Z^{(1)}) &= \frac{e^2 m_{d_L^{(1)}}}{128\pi} \left[\frac{\cos \theta_1}{\sin \theta_W} + \frac{1 \sin \theta_1}{3 \cos \theta_W} \right]^2 \lambda^{1/2}(\kappa_Z, \kappa_d) \\
&\quad \times \left[\frac{1}{\kappa_\gamma} \lambda(\kappa_\gamma, \kappa_d) + 3(-\kappa_\gamma + \kappa_d + 1) \right], \\
\Gamma(u_L^{(1)} \rightarrow u_L Z^{(1)}) &= \frac{e^2 m_{u_L^{(1)}}}{128\pi} \left[\frac{\cos \theta_1}{\sin \theta_W} - \frac{1 \sin \theta_1}{3 \cos \theta_W} \right]^2 \lambda^{1/2}(\kappa_Z, \kappa_u) \\
&\quad \times \left[\frac{1}{\kappa_\gamma} \lambda(\kappa_\gamma, \kappa_d) + 3(-\kappa_\gamma + \kappa_d + 1) \right], \\
\Gamma(u_L^{(1)} \rightarrow d_L W^{(1)}) &= \frac{e^2 m_{u_L^{(1)}}}{64\pi \sin^2 \theta_W} |V_{ij}|^2 \lambda^{1/2}(\kappa_Z, \kappa_d) \\
&\quad \times \left[\frac{1}{\kappa_\gamma} \lambda(\kappa_\gamma, \kappa_d) + 3(-\kappa_\gamma + \kappa_d + 1) \right], \quad (3.30)
\end{aligned}$$

where

$$\lambda(x, y) = (1 - x - y)^2 - 4xy, \quad \kappa_q = \frac{M_q^2}{M_{KK}^2}, \quad \kappa_\gamma = \frac{M_{\gamma^{(1)}}^2}{M_{KK}^2}, \quad \kappa_Z = \frac{M_{Z^{(1)}}^2}{M_{KK}^2}, \quad \kappa_W = \frac{M_{W^{(1)}}^2}{M_{KK}^2}. \quad (3.31)$$

and $q = u, d, s, c$ or b .

CHAPTER 4

Higgsless GUT Breaking and Trinification

4.1 Introduction

Extra spatial dimensions allow for the possibility of gauge symmetry breaking by the appropriate choice of boundary conditions on the fields. The relevance of this point to model building was first realized by Kawamura [91, 92, 93], in the context of SU(5) grand unified theories (GUTS), and was developed substantially afterwards by a number of authors [94, 95, 96, 97, 98]. In the simplest case of an S^1/Z_2 orbifold, the matrix representing the action of the Z_2 symmetry in field space may not commute with all the generators of the gauge symmetry. Boundary conditions may be chosen so that different components of the gauge multiplet have different Z_2 parities, leaving only some with zero modes after the theory is dimensionally reduced. The fact that the zero-mode spectrum includes incomplete multiplets of the gauge group indicates that the symmetry has been broken. Although no Higgs fields are involved, longitudinal gauge boson scattering amplitudes are well behaved at high energies [99]. The same approach may be employed to

project away the zero-modes [100] of the color-triplet Higgs in SU(5) GUTS, naturally resolving the doublet-triplet splitting problem [91, 92, 93, 94, 95, 96, 97, 98].

In the simplest orbifold constructions, the orbifold parity commutes with the diagonal generators of the original gauge symmetry, so that the unbroken subgroup has the same rank. For symmetry breakings like $SU(5) \rightarrow SU(3)_C \times SU(2)_W \times U(1)_Y$, [91, 92, 93, 94, 95, 96, 97, 98] or $SU(3)_W \rightarrow SU(2)_W \times U(1)_Y$ [101, 102], the breaking by orbifold boundary conditions provides an economical approach for constructing models. However, larger groups, like E_6 or E_8 can only be broken directly to the standard model gauge group and, at best, a product of additional U(1) factors [103]. One must then rely on the conventional Higgs mechanism to complete the breaking of the residual GUT symmetry. In this chapter, we will consider the use of more general boundary conditions to break such unified symmetries directly to the standard model gauge group, and hence, to reduce the rank of the original group. This approach has been discussed in the context of Higgsless electroweak symmetry breaking [99, 104, 105, 106, 107, 108, 109, 110]; here we will employ the same technique at a high scale, while retaining the ordinary Higgs mechanism for the breaking of electroweak symmetry. This choice allows us to eliminate the often complicated and problematic GUT-breaking Higgs sector, while allowing for the easy generation of light fermion masses.

The unified theory we consider is based on the ‘trinified’ gauge group $G_T = SU(3)_C \times SU(3)_L \times SU(3)_R \rtimes Z_3$ [111, 112, 113, 114, 115, 116, 117, 118]. The semidirect product (indicated by the symbol \rtimes) provides for a symmetry that cyclically permutes the gauge group labels C , L , and R . Hence, the $SU(3)^3$ representation (rep) $(\mathbf{1}, \mathbf{3}, \bar{\mathbf{3}})$ is part of the trinified rep

$$\mathbf{27} = (\mathbf{1}, \mathbf{3}, \bar{\mathbf{3}}) \oplus (\bar{\mathbf{3}}, \mathbf{1}, \mathbf{3}) \oplus (\mathbf{3}, \bar{\mathbf{3}}, \mathbf{1}) . \quad (4.1)$$

Moreover, the Z_3 symmetry assures the equality of the three SU(3) gauge couplings at the GUT scale. As originally pointed out in Ref. [111], an appropriate embedding of

$U(1)_Y$ in $SU(3)_L \times SU(3)_R$ yields the familiar GUT-scale prediction $\sin^2 \theta = 3/8$. We review this construction in Section 4.2. We will work with a supersymmetric trinified theory in which the G_T gauge multiplet may propagate in a single extra dimensional interval. We first consider the simplest case in which all the matter and Higgs fields are confined to a brane on which G_T is broken. Working in an effective theory of gauge-symmetry-breaking ‘spurions’ on this brane, we establish the boundary conditions necessary to break the bulk gauge group to that of the standard model, $G_T \rightarrow G_{SM}$. We also include the couplings of these spurions to the matter multiplets of the theory. In the limit in which the symmetry breaking parameters are taken to infinity, we obtain the Higgsless limit of the GUT-breaking sector. In particular, the mass scale for the heavy gauge multiplets becomes determined by the compactification radius, and all exotic matter fields are decoupled from the theory. The low-energy theory is simply that of the minimal supersymmetric standard model (MSSM), with a set of massive gauge multiplets at a scale lower than that of conventional supersymmetric unification, 2×10^{16} GeV. We show that unification is nonetheless preserved. Above the compactification scale, the differential gauge running (*i.e.*, $\alpha_i^{-1}(\mu) - \alpha_j^{-1}(\mu)$ for $i \neq j$) is logarithmic, a feature that has been noted before in the case of $SU(5)$ GUTS broken on a boundary [119]. We then show that viable alternative theories exist in which the Higgs and/or matter multiplets are allowed to propagate in the bulk space, and we discuss the boundary conditions on these fields. In this case, the exotic matter fields remain part of the theory, but with large masses set by the compactification radius.

This chapter is organized as follows. In Section 4.2, we review the symmetry breaking in conventional trinification models, and describe some of the main phenomenological features of these theories. In Section 4.3, we give the extra-dimensional construction of supersymmetric $SU(3)^3$, determine the boundary conditions necessary to break the gauge group down to that of the standard model, and study the Higgsless limit of the GUT-breaking sector. In Section 4.4, we study gauge unification in our minimal model, while

in Section 4.5 we discuss the possibility of allowing chiral multiplets in the bulk. In Section 4.6, we summarize our conclusions.

4.2 Framework

Trinification [111, 112, 113, 114, 115, 116, 117, 118] is based on the gauge group $G_T = \text{SU}(3)_C \times \text{SU}(3)_L \times \text{SU}(3)_R \ltimes Z_3$, where \ltimes indicates a semidirect product. The Z_3 symmetry cyclically permutes the gauge group labels C , L and R , ensuring a single unified coupling at the GUT scale. G_T reps consist of the sum of cyclically permuted $\text{SU}(3)^3$ reps. For example, the gauge fields are in the 24-dimensional rep

$$A_T^\mu(24) = A_C^\mu(8, 1, 1) + A_L^\mu(1, 8, 1) + A_R^\mu(1, 1, 8). \quad (4.2)$$

Here, A_C^μ represent the eight gluon fields of the standard model, while only some of the A_L^μ and A_R^μ above correspond to electroweak gauge bosons. The $\text{SU}(2)_W$ gauge group of the standard model is contained entirely in $\text{SU}(3)_L$; writing $A = A^a T^a$, then the $\text{SU}(2)_W$ gauge bosons W^a correspond to A_L^a for $a = 1 \dots 3$. On the other hand, the hypercharge gauge boson is a linear combination of A_L^8 , A_R^3 and A_R^8 . The choice

$$A_Y^\mu = -\frac{1}{\sqrt{5}}(A_L^8 + \sqrt{3}A_R^3 + A_R^8)^\mu, \quad (4.3)$$

yields the standard GUT-scale prediction $\sin^2 \theta_W = 3/8$. The pattern of gauge symmetry breaking is achieved via one or more Higgs fields in the 27-dimensional rep,

$$\phi(27) = \phi(1, 3, \bar{3}) + \phi(3, \bar{3}, 1) + \phi(\bar{3}, 1, 3). \quad (4.4)$$

Only the first $\text{SU}(3)^3$ factor in this rep allows for color-singlet vacuum expectation values (vevs) that may break $\text{SU}(3)^3$ down to $\text{SU}(3)_C \times \text{SU}(2)_L \times U(1)_Y$:

$$\phi(1, 3, \bar{3}) = \begin{pmatrix} \hat{0} & 0 & 0 \\ 0 & \hat{0} & \hat{0} \\ 0 & v_2 & v_1 \end{pmatrix}. \quad (4.5)$$

Here, v_i represent the GUT-scale vevs, while hatted entries denote components capable of eventually breaking the electroweak gauge group. Spontaneous symmetry breaking renders twelve of the original gauge bosons with masses of order the GUT scale. Interestingly, these massive gauge bosons are integrally charged and cannot generate dimension-six operators that contribute to proton decay. Depending on the number of Higgs multiplets and their couplings to the matter fields, proton decay may still occur via color-triplet Higgs exchange.

Standard model fermions are embedded economically in the 27-dimensional representation. In SU(5) language, the 27 decomposes as

$$27 = [10 \oplus \bar{5}] \oplus 5 \oplus \bar{5} \oplus 1 \oplus 1 . \quad (4.6)$$

The reps in brackets correspond to a full standard model generation, while the remaining reps are exotic. Thus the exotic fields include left- and right-handed fermions with the quantum numbers of a charge $-1/3$ weak singlet quark (B), a hypercharge $-1/2$ weak doublet lepton (E^0, E^-) and an electroweak singlet (N). Using the notation

$$\psi(27) = \psi(1, 3, \bar{3}) + \psi(\bar{3}, 1, 3) + \psi(3, \bar{3}, 1) \quad (4.7)$$

$$\equiv \psi_C + \psi_L + \psi_R , \quad (4.8)$$

we may choose an $SU(2)_W$ basis in which the fermion reps take the matrix form

$$\psi_C = \begin{pmatrix} E^{0c} & E & e \\ -E^c & E^0 & \nu \\ e^c & N^c & N \end{pmatrix}, \quad \psi_L = \begin{pmatrix} u_{\bar{r}}^c & u_{\bar{g}}^c & u_{\bar{b}}^c \\ d_{\bar{r}}^c & d_{\bar{g}}^c & d_{\bar{b}}^c \\ B_{\bar{r}}^c & B_{\bar{g}}^c & B_{\bar{b}}^c \end{pmatrix}, \quad \psi_R = \begin{pmatrix} u_r & d_r & B_r \\ u_g & d_g & B_g \\ u_b & d_b & B_b \end{pmatrix} \quad (4.9)$$

where all entries are left-handed. In supersymmetric trinification, these matrices are composed of left-handed chiral superfields, with each entry indicating the fermionic component. Yukawa couplings necessarily involve invariants formed by taking the product of three 27's. These come in two types,

$$Z_3[\psi_R \psi_L \phi_{Ci}] , \quad (4.10)$$

and

$$Z_3[\psi_C\psi_C\phi_{Cj}] . \quad (4.11)$$

We use the symbol Z_3 to represent the cyclic permutation of R , L and C , *e.g.*,

$$Z_3[\psi_R\psi_L\phi_C] = \psi_R\psi_L\phi_C + \psi_C\psi_R\phi_L + \psi_L\psi_C\phi_R. \quad (4.12)$$

The index on the field ϕ_C takes into account the possibility that there may be more than one 27-plet Higgs field. If there is only one Higgs 27, then both the up- and down-type quark Yukawa couplings for a given generation originate from a single G_T -invariant interaction, of the form shown in Eq. (4.10). This implies the incorrect GUT-scale mass relation [111]

$$\frac{m_u}{m_d} = \frac{m_c}{m_s} = \frac{m_t}{m_b}. \quad (4.13)$$

Therefore, at least two Higgs 27's must couple to the quarks via Eq. (4.10). Generally, the same set of Higgs fields will couple to the leptons via Eq. (4.11) and proton decay may proceed via color-triplet Higgs exchange. If a third Higgs 27-plet is introduced that couples to the leptons only, then proton decay can be prevented by imposing a global symmetry on the Higgs sector that prevents mixing between the third Higgs and the other two. This, however, leads to a symmetry-breaking sector that seems somewhat contrived.

It is conventionally assumed that the vevs v_1 and v_2 arise in separate Higgs 27-plets:

$$\phi(\mathbf{1}, \mathbf{3}, \bar{\mathbf{3}}) = \begin{pmatrix} 0 & 0 & 0 \\ 0 & 0 & 0 \\ 0 & 0 & v_1 \end{pmatrix}, \quad \chi(\mathbf{1}, \mathbf{3}, \bar{\mathbf{3}}) = \begin{pmatrix} 0 & 0 & 0 \\ 0 & 0 & 0 \\ 0 & v_2 & 0 \end{pmatrix}. \quad (4.14)$$

The superpotential terms responsible for quark and lepton masses can now be determined from the invariants Eq.(4.10) and Eq.(4.11),

$$W_Q = (\psi_L)_i^j (\psi_R)_k^i [g_1 (\phi_C)_j^k + g_2 (\chi_C)_j^k], \quad (4.15)$$

$$W_L = \frac{1}{2} h (\psi_C)_\alpha^i (\psi_C)_\beta^j [h_1 (\phi_C)_\gamma^k + h_2 (\chi_C)_\gamma^k] \epsilon_{ijk} \epsilon^{\alpha\beta\gamma}. \quad (4.16)$$

These may be expanded, yielding

$$W = g_2 v_2 d^c B + g_1 v_1 B^c B + v_1 h_1 \epsilon_{ij} L_H^c L_H^j - v_2 h_2 \epsilon_{ij} L_H^c L^j, \quad (4.17)$$

where the lepton doublets are defined by $L_H = (E^0, E)$, $L = (\nu, e)$, and $L_H^c = (-E^c, E^{c0})$. Clearly, one linear combination of B^c and d^c , and of L_H and L , remain unaffected by GUT symmetry breaking¹, and should be identified with the physical right-handed down quark and lepton doublet superfields:

$$\begin{aligned} d_{phys}^c &= (-g_2 v_2 B^c + g_1 v_1 d^c) / \sqrt{g_1^2 v_1^2 + g_2^2 v_2^2} \\ L_{phys} &= (h_2 v_2 L_H + h_1 v_1 L) / \sqrt{h_1^2 v_1^2 + h_2^2 v_2^2}. \end{aligned} \quad (4.18)$$

The masses of the heavy quark and lepton states remaining in Eq. (4.17) are given by

$$m_{B, B_{phys}^c} = (g_1^2 v_1^2 + g_2^2 v_2^2)^{1/2}, \quad (4.19)$$

$$m_{L_H^c, L_{H, phys}} = (h_1^2 v_1^2 + h_2^2 v_2^2)^{1/2}. \quad (4.20)$$

For this minimal choice of symmetry breaking, the singlets N^c and N remain massless. However, as we discuss in the next section, vevs in other Higgs field representations can give masses to these states as well.

We will not discuss the structure of the Higgs sector in conventional trinified theories since our goal is to dispense with this sector entirely. We henceforth consider supersymmetric trinified theories embedded in $4 + 1$ spacetime dimensions. As in Ref. [99], we assume that the extra spatial dimension is compact, and runs over the interval $y = 0$ to $y = \pi R$. We will always assume that the G_T gauge multiplet propagates in the bulk, and we will consider consistent boundary conditions that allow us to break this gauge group directly to that of the standard model upon compactification. The radius of compactification is a free parameter that we will determine based on the condition that supersymmetric

¹Ref. [112] states that no light lepton eigenstate will remain if $h_2 \neq 0$. This is not correct, since unbroken electroweak symmetry assures that a massless eigenstate must remain.

gauge unification is preserved. We first consider the simplest case in which all matter and Higgs fields are placed on the $y = \pi R$ brane, and afterwards discuss the possibility of placing chiral multiplets in the bulk.

In all cases, we will treat the symmetry breaking on the πR brane in an effective theory approach. We will introduce G_T breaking spurions $\{\Phi_i\}$ on this brane and consider both their couplings to brane-localized fields, as well as their effect on the 5D wave function of fields in the bulk. Historically, the term ‘‘spurion’’ refers to a symmetry-breaking parameter that is taken to transform as a spurious field, so that it may be included consistently in an effective Lagrangian. In the present case, one may think of the spurions as a collection of brane Higgs vevs, that can plausibly arise in some ultraviolet completion. Since we will focus on the limit in which these vevs are taken to infinity, we will not defend any particular ultraviolet theory. Partial examples will be given only to justify the consistency of the boundary conditions that we assume. In a few instances, we will require higher-dimension operators involving the spurions, which necessarily involve some cut off Λ . In the decoupling limit, we will take both Φ and Λ to infinity in fixed ratio. In other words, we do not assign Λ to some physical scale, but use this limiting procedure to obtain a consistent Higgsless low-energy effective theory that could otherwise be defined *ab initio*.

4.3 Symmetry Breaking

We choose to break the trinified gauge group at the $y = \pi R$ brane. For a generic gauge field A^μ , the boundary conditions

$$\partial_5 A^\mu(x^\nu, 0) = 0 \quad \text{and} \quad \partial_5 A^\mu(x^\nu, \pi R) = V A^\mu(x, \pi R) \quad (4.21)$$

lead to a mode expansion of the form

$$f_k(y) = N_k \cos(M_k y) \quad , \quad (4.22)$$

where M_k is given by the transcendental equation

$$M_k \tan(M_k \pi R) = -V , \quad (4.23)$$

and where the normalization

$$N_k = \frac{\sqrt{2}}{\sin(M_k \pi R)} [\pi R(1 + M_k^2/V^2) - 1/V]^{-1/2} \quad (4.24)$$

assures that $\int_0^{\pi R} f^2 = 1$ [99]. Note that the symmetry breaking parameter V has dimensions of mass. The nontrivial boundary condition in Eq. (4.21) can be realized in an ultraviolet completion of the theory in which a brane localized Higgs field σ is responsible for the symmetry breaking. The brane equations of motion for the field A^μ includes terms localized at $y = \pi R$ from the start, as well as surface terms obtained from integrating the bulk action by parts. In particular, the kinetic terms

$$S_{KE} \supset \int d^4x \int_0^{\pi R} dy \left[-\frac{1}{2} F_{5\nu} F^{5\nu} + D^\mu \sigma^\dagger D_\mu \sigma \delta(y - \pi R) \right] \quad (4.25)$$

include

$$S_{KE} \supset \int d^4x \int_0^{\pi R} dy \left[-\partial_5 A_\nu \partial_5 A^\nu + \frac{g_5^2}{2} \langle \sigma \rangle^\dagger \langle \sigma \rangle A^\mu A_\mu \delta(y - \pi R) \right] . \quad (4.26)$$

Variation of this portion of the action with respect to A^ν yields a constraint at $y = \pi R$,

$$-\partial_5 A_\nu + \frac{g_5^2}{2} \langle \sigma \rangle^\dagger \langle \sigma \rangle A^\nu = 0 , \quad (4.27)$$

which corresponds to the desired boundary condition if one identifies $V \equiv g_5^2 \langle \sigma \rangle^\dagger \langle \sigma \rangle / 2$. Since the 5D gauge coupling g_5 has mass dimension $-1/2$, one finds that V has dimensions of mass, as before.

Csáki, Grojean, Murayama, Pilo, and Terning [99], have demonstrated that the boundary conditions given in Eq. (4.21) require a brane-localized Higgs field to cancel contributions to scattering amplitudes that grow with energy as E^2 . However, a remarkable feature of brane-localized breaking of gauge symmetries is that one can decouple the Higgs field

without decoupling the massive gauge multiplets as well. In the limit that $\langle\sigma\rangle$, and hence V , are taken to infinity, one finds from Eq. (4.23) that the KK mass spectrum becomes

$$M_n \approx \frac{M_c}{2}(2n+1)\left(1 + \frac{M_c}{\pi V} + \dots\right), \quad (4.28)$$

where M_c is the compactification scale $1/R$. Thus, the low-energy theory has no Higgs fields, and the KK tower for the gauge fields is shifted by $+M_c/2$ relative to the tower one would obtain if V were set to zero.

In the case of G_T , the first SU(3) factor corresponds to the unbroken color group, so we may immediately write down the boundary conditions on the gluon fields A_C^μ ,

$$\partial_5 A_C^\mu(x, 0) = \partial_5 A_C^\mu(x, \pi R) = 0. \quad (4.29)$$

Similarly, an SU(2) subgroup of the second SU(3) factor remains unbroken, so that

$$\partial_5 A_L^a(x, 0) = \partial_5 A_L^a(x, \pi R) = 0 \text{ for } a = 1 \dots 3 \quad (4.30)$$

Since the only remaining unbroken group is a U(1) factor, all gauge fields corresponding to off-diagonal generators must become massive. Thus, we require that

$$\partial_5 A_L^a(x, 0) = 0, \partial_5 A_L^a(x, \pi R) = V_L A_L^a(x, \pi R) \text{ for } a = 4 \dots 7, \quad (4.31)$$

$$\partial_5 A_R^a(x, 0) = 0, \partial_5 A_R^a(x, \pi R) = V_R A_R^a(x, \pi R) \text{ for } a = 1, 2, 4 \dots 7. \quad (4.32)$$

The remaining U(1) factors are more interesting. As we showed in the previous section, the embedding of hypercharge within $SU(3)_L \times SU(3)_R$ that leads to the prediction $\sin^2 \theta = 3/8$ requires that the hypercharge gauge boson be identified with the linear combination

$$A_Y^\mu = -\frac{1}{\sqrt{5}}(A_L^8 + \sqrt{3}A_R^3 + A_R^8)^\mu \quad (4.33)$$

Thinking in terms of an ultraviolet completion, suitable Higgs fields must generate a brane gauge boson mass matrix with a zero eigenvalue corresponding to the eigenvector $(-1/\sqrt{5}, -\sqrt{3}/\sqrt{5}, -1/\sqrt{5})$. The only other necessary constraint on this matrix is that

the remaining eigenvalues must be non-vanishing. Restricting ourselves to real entries, for the sake of simplicity, we may parameterize the remaining boundary conditions as follows:

$$\partial_5 A_L^8(x, 0) = \partial_5 A_R^3(x, 0) = \partial_5 A_R^8(x, 0) = 0, \quad (4.34)$$

$$\partial_5 \begin{bmatrix} A_L^8(x, \pi R) \\ A_R^3(x, \pi R) \\ A_R^8(x, \pi R) \end{bmatrix} = \begin{pmatrix} V_1 & -\frac{1}{2\sqrt{3}}(V_1+V_3) & -\frac{1}{2}(V_1-V_3) \\ -\frac{1}{2\sqrt{3}}(V_1+V_3) & \frac{1}{6}(V_2+V_3) & \frac{1}{2\sqrt{3}}(V_1-V_2) \\ -\frac{1}{2}(V_1-V_3) & \frac{1}{2\sqrt{3}}(V_1-V_2) & \frac{1}{2}(V_2-V_3) \end{pmatrix} \begin{bmatrix} A_L^8(x, \pi R) \\ A_R^3(x, \pi R) \\ A_R^8(x, \pi R) \end{bmatrix} \quad (4.35)$$

Finally, we consider the A^5 components. In a nonsupersymmetric theory, we could impose the boundary conditions $A^5(x, 0) = A^5(x, \pi R) = 0$ on all the gauge fields so that no additional light scalar states remain in the 4D theory. In the supersymmetric case, A^μ and A^5 live within a vector V and chiral Φ_V superfield, respectively. Since supersymmetry is unbroken, the fermionic components of V and Φ_V (say, λ and ψ) must form Dirac spinors with the same mass spectrum as the gauge fields [119]. Since these masses originate from terms of the form $\partial_5 \lambda \psi$, the 5D wave function of Φ_V must be proportional to $\sin M_k y$, with M_k given as before.

If one were to assume an ultraviolet completion involving only the minimal Higgs content of conventional 4D trinified theories (localized on the πR brane) one would find that

$$\begin{aligned} V_1 &= \frac{2}{3}(v_1^2 + v_2^2)g_5^2 \\ V_2 &= \frac{1}{3}(2v_1^2 + 5v_2^2)g_5^2 \\ V_3 &= -\frac{1}{3}(2v_1^2 - 4v_2^2)g_5^2. \end{aligned} \quad (4.36)$$

The more general values of the parameters V_i may be thought of as arising in some arbitrarily complicated GUT-breaking Higgs sector, which decouples as one takes V_L, V_R and $V_i \rightarrow \infty$. However, we will not wed ourselves to any particular interpretation of the physics responsible for generating the symmetry-breaking parameters on the boundary.

We will proceed with an effective field theory analysis of the possible symmetry breaking on the πR brane. We will introduce the symmetry breaking systematically in terms of constant spurion fields that we may treat as transforming in irreducible reps of $SU(3)^3$. When we obtain operators that are nonrenormalizable, we will introduce powers of a cutoff, Λ to obtain the proper mass dimension, as discussed at the end of Section 4.2.

A given spurion representation may contribute to the symmetry breaking parameterized by Eq. (4.35) provided that it contains standard model singlet components, with hypercharge defined as in Eq. (4.33), that develop vevs. We know immediately of one possibility from the minimal 4D trinified theory, namely a $\mathbf{27}$ with vevs in the $(\mathbf{1}, \mathbf{3}, \bar{\mathbf{3}})$ component,

$$\Phi(\mathbf{1}, \mathbf{3}, \bar{\mathbf{3}}) \sim \begin{pmatrix} 0 & 0 & 0 \\ 0 & 0 & 0 \\ 0 & v_2 & v_1 \end{pmatrix}. \quad (4.37)$$

As described in Section 4.2, these vevs give mass to the heavy fields B , B^c , L_H and L_H^c while contributing to the boundary condition on the gauge fields via Eq. (4.36). This rep, however, does not contribute to the mass of the new singlet leptons, N^c and N . Since we wish to retain only the particle content of the MSSM at the electroweak scale, we will be more general. The set of $SU(3)^3$ representations that appear in the product of two $\mathbf{27}$'s and that are color singlet are $(\mathbf{1}, \mathbf{3}, \bar{\mathbf{3}})$, $(\mathbf{1}, \bar{\mathbf{6}}, \mathbf{3})$, $(\mathbf{1}, \mathbf{3}, \mathbf{6})$, and $(\mathbf{1}, \bar{\mathbf{6}}, \mathbf{6})$. For each, we may isolate the components that are $SU(2)_W \times U(1)_Y$ singlets. The results are shown in Table 4.1. While the reps $(\mathbf{1}, \bar{\mathbf{6}}, \mathbf{3})$ and $(\mathbf{1}, \mathbf{3}, \mathbf{6})$ contain standard model singlet components, it turns out that these do not split the $\mathbf{27}$ matter multiplets. For example, the coupling of the $(\mathbf{1}, \bar{\mathbf{6}}, \bar{\mathbf{3}})$ to two $\mathbf{27}$ matter superfields may be written

$$W = \Psi_\alpha^a \Psi_\beta^b \Phi_{ab,\gamma}^{(\mathbf{1}, \bar{\mathbf{6}}, \bar{\mathbf{3}})} \epsilon^{\alpha\beta\gamma} \quad (4.38)$$

which vanishes for $a = b = 3$ and $\gamma = 1$, because of the antisymmetry of the $SU(3)_R$ epsilon tensor. Of the three new spurion reps in Table 4.1, only the $(\mathbf{1}, \bar{\mathbf{6}}, \mathbf{6})$ gives us

TABLE 4.1: $SU(3)^3$ reps in the product of two trified $\mathbf{27}$ -plets containing Standard Model singlet components, with hypercharge defined as in Eq. (4.33). Parentheses delimit indices that are symmetric.

$SU(3)^3$ rep	$SU(3)_L \times SU(3)_R$ tensor	SM singlet components
$(\mathbf{1}, \mathbf{3}, \bar{\mathbf{3}})$	Φ_α^a	$a = 3, \alpha = 2, 3$
$(\mathbf{1}, \bar{\mathbf{6}}, \bar{\mathbf{3}})$	$\Phi_{(ab)\alpha}$	$a = b = 3, \alpha = 1$
$(\mathbf{1}, \mathbf{3}, \mathbf{6})$	$\Phi^{a(\alpha\beta)}$	$a = 3, (\alpha\beta) = (12), (13)$
$(\mathbf{1}, \bar{\mathbf{6}}, \mathbf{6})$	$\Phi_{(ab)}^{(\alpha\beta)}$	$(ab) = (33), (\alpha\beta) = (22), (23), (33)$

something new,

$$\begin{aligned}
 W &= \Psi_\alpha^a \Psi_\beta^b \Phi_{ab}^{\alpha\beta} \\
 &= v_{22} N_R^2 + 2v_{23} N_R N_L + v_{33} N_L^2 .
 \end{aligned} \tag{4.39}$$

Here v_{ij} corresponds to vevs for the standard model singlet components of the $(\mathbf{1}, \bar{\mathbf{6}}, \mathbf{6})$ spurion, as given in Table 4.1. Hence, we arrive at Majorana and Dirac masses for the exotic neutral leptons, which may be decoupled from the theory if the v_{ij} are taken to infinity. Thus we reach the following conclusion:

Gauge symmetry breaking spurions localized at the πR brane in the $\mathbf{27}$ and $\mathbf{108}$ irreducible reps of the trinification group, and with nonvanishing standard model singlet entries in their $(\mathbf{1}, \mathbf{3}, \bar{\mathbf{3}})$ and $(\mathbf{1}, \bar{\mathbf{6}}, \mathbf{6})$ components, respectively, break the trinification gauge group down to the standard model, and yield the MSSM matter content at low energies. In the limit that all the symmetry breaking parameters are taken to infinity, we obtain Higgsless trinification breaking with an incomplete matter multiplet located at the πR brane.

This picture is pleasing since any physics on the brane associated with an ultraviolet completion that might lead to proton decay has been decoupled away. The only issue we have not taken into account is the mechanism for breaking electroweak symmetry and the generation of light fermion masses. We may easily incorporate the standard Higgs mech-

anism for electroweak symmetry breaking by introducing $\mathbf{27}$ and $\overline{\mathbf{27}}$ Higgs superfields on the πR brane, Ψ_H and $\Psi_{\bar{H}}$, respectively. (These are distinguished from matter superfields by unbroken matter or R-parity, which we assume throughout.) We identify H (\bar{H}) as the doublet Higgs field with hypercharge $1/2$ ($-1/2$) living inside the multiplet Ψ_H ($\Psi_{\bar{H}}$). We also introduce another spurion rep, the $\mathbf{192}$, which includes the color singlet rep $\Omega \sim (\mathbf{1}, \mathbf{8}, \mathbf{8})$. Assuming that the nonvanishing, standard model singlet components of Ω are given by

$$\Omega_{ab}^{\alpha\beta} = v_\Omega T_b^{8a} T_\beta^{3\alpha} \quad (4.40)$$

then the couplings

$$W = H_\alpha^a (\mu \delta_\beta^\alpha \delta_a^b + h \Omega_{a\alpha}^{b\beta}) \bar{H}_b^\beta \quad (4.41)$$

will provide high-scale μ terms for all members of the Higgs multiplet, except for the weak doublets H and \bar{H} , providing that $\mu = -4\sqrt{3} h v_\Omega$. Thus, in this approach, we simply impose a fine-tuning of the parameters to arrange for a doublet-triplet splitting². However, since we ultimately take the limit in which $v_\Omega \rightarrow \infty$, as with the other symmetry-breaking spurions, there is no sign of this fine-tuning in the low-energy theory. From a low-energy perspective, it is completely consistent to assign two electroweak Higgs doublets to the brane in the GUT-Higgsless limit.

One feature of this solution that needs clarification is the coupling of these Higgs doublets to the matter fields. While the up-quark Higgs fields H lives in a $\mathbf{27}$ and couples to the matter fields via the conventional cubic interactions of 4D trinified theories, the down-type Higgs fields \bar{H} lies in a $\overline{\mathbf{27}}$ and does not couple directly. Nonetheless, we may arrange for a suitable down quark Yukawa matrix by introducing a $\overline{\mathbf{27}}$ spurion with the same nonvanishing components as the $\mathbf{27}$ spurion that we have already considered. Then the down quark Yukawa matrix will originate via a higher-dimension operator

$$\frac{1}{\Lambda} Z_3 [\Phi(\mathbf{1}, \bar{\mathbf{3}}, \mathbf{3}) \bar{H}(\mathbf{1}, \bar{\mathbf{3}}, \mathbf{3}) \Psi(\bar{\mathbf{3}}, \mathbf{1}, \mathbf{3}) \Psi(\mathbf{3}, \bar{\mathbf{3}}, \mathbf{1})] \quad (4.42)$$

²Higher order combinations of the other spurions may generate a $(\mathbf{1}, \mathbf{8}, \mathbf{8})$; we assume a fine tuning of the sum of all such contributions.

We may generate the down quark Yukawa couplings by fixing the ratio of the spurion vev to Λ , and taking both to infinity in the Higgsless limit.

4.4 Gauge Unification

By breaking the GUT gauge group through boundary conditions, the heavy vector superfields that have GUT-scale masses in 4D trinified theories instead have zero-modes with mass $M_c/2$ in the exact Higgsless limit. The $SU(3)_C \times SU(2)_W \times U(1)_Y$ quantum numbers of these states are given by

$$V_H \sim (\mathbf{1}, \mathbf{2}, 1/2) \oplus (\mathbf{1}, \mathbf{1}, 1) \oplus (\mathbf{1}, \mathbf{1}, 1) \oplus (\mathbf{1}, \mathbf{1}, 0) \oplus (\mathbf{1}, \mathbf{1}, 0) , \quad (4.43)$$

where the hypercharges are shown here with their standard, rather than their GUT, normalization. KK modes of the ordinary MSSM vector superfields begin at M_c . The two towers of massive states are thus uniformly shifted with respect to each other by $M_c/2$. Each KK level in these towers consists of an $N = 2$ supersymmetric multiplet, which includes both a vector and a chiral superfield. The beta function contributions from these towers are indicated in Table 4.2. Notice that the sum of all the KK gauge multiplet contributions to the beta functions is $(-6, -6, -6)$; if the two massive towers were degenerate level by level, they would affect gauge coupling running universally and have no effect on the quality of unification. However, the $M_c/2$ splitting separates these states into two subsets, each contributing nonuniversally to the beta functions. The shifted towers therefore provide a large number of threshold corrections to the differential gauge coupling running $\alpha_i^{-1}(\mu) - \alpha_j^{-1}(\mu)$. There is no reason *a priori* to assume that these corrections will preserve gauge unification. In our trinified theory, we will see that they do.

While the individual α_i^{-1} experience power-law running above $M_c/2$, a remarkable feature of this tower of threshold corrections is that the $\alpha_i^{-1}(\mu) - \alpha_j^{-1}(\mu)$ evolve logarithmically. This behavior was pointed out by Nomura, Smith and Weiner [119] in the

	(b_1, b_2, b_3)	$(\tilde{b}_1, \tilde{b}_2, \tilde{b}_3)$
$(V, \Phi)_{321}$	(0,-6,-9)	(0,-4,-6)
$(V, \Phi)_{heavy}$	-	(-6,-2,0)
H, \bar{H}	$(\frac{3}{5}, 1, 0)$	-
Matter	(6,6,6)	-
Total	$(\frac{33}{5}, 1, -3)$	(-6,-6,-6)

TABLE 4.2: Contributions to the beta function coefficients from the zero modes (b_i) and the KK levels (\tilde{b}_i) in our minimal scenario. Here Φ represents a chiral multiplet in the adjoint rep.

context of a supersymmetric SU(5) GUT broken on a brane. Thus, theories of this type unify logarithmically, in contrast to the first examples of higher-dimensional gauge unification discussed in Refs. [75, 120, 121]. For our analysis, we follow the conventions of Ref. [119]: We first define gauge coupling differences with respect to α_1^{-1} ,

$$\delta_i(\mu) = \tilde{\alpha}_i^{-1}(\mu) - \alpha_1^{-1}(\mu). \quad (4.44)$$

Unification occurs when $\delta_2 = \delta_3 = 0$. Above $M_c/2$, Eq.(4.44) can be written as

$$\delta_i(\mu) = \delta_i(M_c/2) - \frac{1}{2\pi} R_i(\mu) \quad (4.45)$$

where $R_i(\mu)$ represents the differential logarithmic running between all the thresholds from $M_c/2$ up to the renormalization scale μ . For trinified gauge multiplets in the bulk only, we find

$$R_2(\mu) = -\frac{28}{5} \log\left(\frac{\mu}{M_c/2}\right) - 4 \sum_{0 < n M_c < \mu} \log\left(\frac{\mu}{n M_c}\right) + 4 \sum_{0 < (n+1/2) M_c < \mu} \log\left(\frac{\mu}{[n + 1/2] M_c}\right), \quad (4.46)$$

$$R_3(\mu) = -\frac{48}{5} \log\left(\frac{\mu}{M_c/2}\right) - 6 \sum_{0 < n M_c < \mu} \log\left(\frac{\mu}{n M_c}\right) + 6 \sum_{0 < (n+1/2) M_c < \mu} \log\left(\frac{\mu}{[n + 1/2] M_c}\right). \quad (4.47)$$

If the two towers of massive modes were degenerate, the last two terms in each of the equations above would have exactly canceled, and the R_i 's would be the same as in the MSSM. The overall effect of the threshold corrections is to delay unification, as shown in Fig. 4.1.

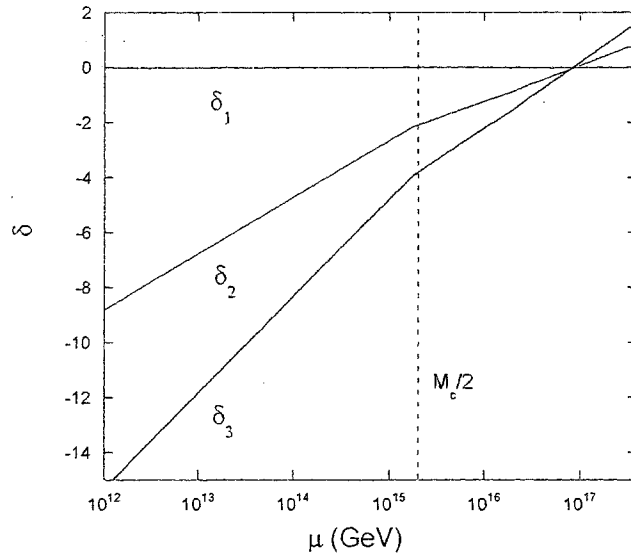


FIG. 4.1: Gauge unification for $M_c = 4 \times 10^{15}$ GeV.

The shallower slopes above $M_c/2$ in Fig. 4.1 can be understood by rewriting Eq. (4.45) in the form.

$$\delta_i(\mu) = \delta_i(M_c/2) - \frac{1}{2\pi} \delta b_i \log\left(\frac{\mu}{M_c/2}\right) - \frac{1}{2\pi} \Delta \tilde{b}_{321} \sum_{nM_c/2 < \mu} (-1)^n \log\left(\frac{\mu}{nM_c/2}\right) \quad (4.48)$$

where we have used the fact that the difference in KK gauge multiplet beta functions $\Delta \tilde{b}_{321} = -\Delta \tilde{b}_{heavy}$. The first and second terms are negative and positive, respectively, and cancel in the MSSM at the unification point. The new term has positive coefficient $-\frac{1}{2\pi} \Delta \tilde{b}_{321}$. However, one may estimate the sum via integration, and one finds it is well approximated by $-(1 + \log(\mu/M_c))/2$. Thus, the new threshold corrections serve to reduce the effect of the second term (the MSSM differential logarithmic running) so that unification is delayed.

In the Higgsless limit, there are two significant physical scales in the theory: the compactification scale $1/R$, which determines the masses of the super-heavy states in the theory, and the 5D Planck scale, $M_*(5D)$, which determines where gravity becomes important. In Fig. 4.2, we show both the unification scale M_{GUT} , defined as the point at which $\alpha_1^{-1} = \alpha_2^{-1}$, and $M_*(5D)$, as a function of the compactification scale M_c . These scales are identical when $M_c \sim 2 \times 10^{15}$ GeV. For larger M_c , the 5D Planck

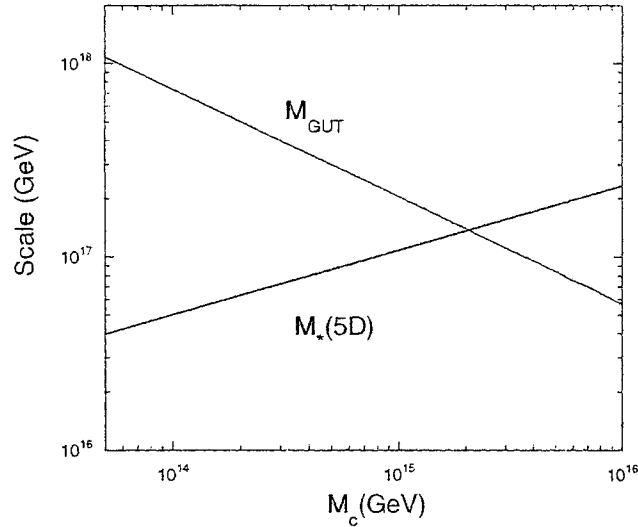


FIG. 4.2: Unification and 5D Planck scales as functions of M_c . For definitions of scales, see the text.

scale is higher; in this case, one could introduce other, purely gravitational extra dimensions that again bring the higher-dimensional Planck scale in coincidence with M_{GUT} . For $M_c 2 \times 10^{15}$ GeV, $M_*(5D)$ is lower than M_{GUT} and a field theoretic calculation of gauge coupling unification can no longer be trusted. For all values of M_c larger than 2×10^{15} GeV, the unification scale is increased relative to that of the 4D MSSM, *i.e.*, 2×10^{16} GeV. At its maximum value, 1.4×10^{17} GeV, the accuracy of gauge unification is $\sim 1\%$. This estimate assumes that brane-localized, higher-dimension kinetic energy operators have a negligible effect on the equality of the gauge couplings at the unification scale. Such an assumption is reasonable since these effects are volume suppressed by a factor of $\sim \pi M_*(5D)/M_c$ [119], which is generally large. Of course, the precise values of the operator coefficients are unknown, and one cannot rule out the possibility that such operators are simply not present in the theory.

4.5 Other Possibilities

In the previous sections, we have allowed all exotic chiral superfields to be perfectly decoupled in the Higgsless limit. This was accomplished by restricting matter and Higgs

multiplets to the $y = \pi R$ brane, and including the most general set of couplings to the symmetry breaking parameters. In this section, we discuss the alternative possibility that some (or all) of the 27 's propagate in the bulk, along with the gauge multiplets. Assuming the same set of symmetry-breaking parameters on the πR brane, exotic fields now acquire masses of order the compactification scale, leaving the MSSM at low energies.

In general, a bulk matter field consists of an $N = 2$ hypermultiplet $\Psi = (\psi, \psi^c)$, where ψ and ψ^c are each left-handed, 4D $N = 1$ chiral superfields; in our case, these fields transform as a 27 and a $\overline{27}$, respectively. We wish to argue that it is consistent within our framework to apply the following simple boundary conditions to elements of the 27 (and conjugate elements in the $\overline{27}$) that we require to become massive:

$$\partial_5 \phi|_{y=0} = \phi^c|_{y=0} = \phi|_{y=\pi R} = \partial_5 \phi^c|_{y=\pi R} = 0 . \quad (4.49)$$

Here, ϕ and ϕ^c represented the scalar components of Ψ and Ψ^c , respectively. These boundary conditions are satisfied for

$$\begin{aligned} \phi &= \sum_k N_k \cos(M_k y) \phi^{(k)} \\ \phi^c &= \sum_k N_k \sin(M_k y) \phi^{c(k)} , \end{aligned} \quad (4.50)$$

where $N_k = (\pi R/2)^{-1/2}$, and $M_k = (k + 1/2) M_c$, for integer k . Of course, Eq. (4.50) solve the bulk equations of motion $\partial_M \partial^M \phi = 0$ provided that the KK modes satisfy the on-shell relation $p_k^2 = M_k^2$. Since supersymmetry is unbroken, the same conditions apply to the fermionic components as well.

To show that these boundary conditions are consistent, let us consider one possible ultraviolet completion. First, let us generalize our boundary conditions to

$$\begin{aligned} \partial_5 \phi|_{y=0} = 0 \quad , \quad \phi^c|_{y=0} = 0 \\ (-\sin \eta \phi^c + \cos \eta \phi)|_{y=\pi R} = 0 \quad , \quad \partial_5(\cos \eta \phi^c + \sin \eta \phi)|_{y=\pi R} = 0 \end{aligned} \quad (4.51)$$

which are satisfied by Eq. (4.50), if

$$\tan(M_k \pi R) = \cot \eta . \quad (4.52)$$

Notice that one linear combination of the fields in Eq. (4.51) satisfies Dirichlet boundary conditions at $y = \pi R$, while the orthogonal satisfies has Neumann boundary conditions. The precise linear combination is determined by the mixing angle η , which is a free parameter. Our desired boundary conditions are obtained from Eq. (4.51) in the limit that $\eta \rightarrow 0$.

Now consider the following 5D Lagrangian, with a brane-localized μ -term

$$\mathcal{L}_5 = \int d^4\theta [\psi^\dagger \psi + \psi^{c\dagger} \psi^c] + \int d^2\theta [\psi^c \partial_5 \psi + \frac{1}{2} \cot \eta \psi^2 \delta(y - \pi R)] \quad (4.53)$$

Here we have displayed the effective $N = 1$ supersymmetric Lagrangian, following the construction described in Ref. [122]. Extracting the purely scalar components, one finds

$$\begin{aligned} \mathcal{L}_5 &= F^\dagger F + \partial_\mu \phi^\dagger \partial^\mu \phi + F^{c\dagger} F^c + \partial_\mu \phi^{c\dagger} \partial^\mu \phi^c \\ &+ [\phi^c \partial_5 F + F^c \partial_5 \phi + \cot \eta \phi F \delta(y - \pi R) + \text{h.c.}] \end{aligned} \quad (4.54)$$

Aside from the bulk equations of motion for the auxiliary fields $F = \partial_5 \phi^{c\dagger}$ and $F^c = -\partial_5 \phi^\dagger$, one finds from the nonvanishing surface terms the boundary condition

$$-\phi^c \delta F|_{y=0} + (\phi^c + \cot \eta \phi) \delta F|_{y=\pi R} = 0 \quad (4.55)$$

which is clearly satisfied by the boundary conditions in Eq (4.51). Substituting out the auxiliary fields, one is left with the Lagrangian

$$\begin{aligned} \mathcal{L} &= \partial_5 \phi^{c\dagger} \partial_5 \phi^c - \partial_5^2 \phi^{c\dagger} \phi^c + \phi_c^\dagger \partial_5^2 \phi_c + \partial_\mu \phi^{c\dagger} \partial^\mu \phi^c \\ &+ \partial_\mu \phi^\dagger \partial^\mu \phi - \partial_5 \phi^\dagger \partial_5 \phi - \cot \eta \delta(y - \pi R) (\partial_5 \phi^{c\dagger} \phi + \phi^\dagger \partial_5 \phi^c) . \end{aligned} \quad (4.56)$$

Variation of the action with respect to ϕ leads to the further brane constraint

$$\partial_5 \phi^\dagger \delta \phi|_{y=0} + \partial_5 (-\phi^\dagger + \cot \eta \phi^{c\dagger}) \delta \phi|_{y=\pi R} = 0 \quad (4.57)$$

which is satisfied by the remaining boundary conditions in Eq (4.51). Thus, our more general set of boundary conditions are consistent with this explicit brane Lagrangian. In

particular, the simpler boundary conditions in Eq. (4.49) arise in the limit that the coupling $\cot \eta$ is allowed to become nonperturbatively large.

In the context of our previous discussion, the dimensionless brane coupling proportional to $\cot \theta$ arises at some order in the symmetry breaking spurions Φ . Generically,

$$W = -\frac{1}{2}\lambda(\Phi/\Lambda)\psi\psi\delta(y-\pi R) , \quad (4.58)$$

where, λ is a dimensionless coupling, and $\cot \eta$ is identified with $\lambda\Phi/\Lambda$. Any exotic field that decoupled in our earlier construction, will receive a brane coupling proportional to $\cot \eta$ in the present one. Thus, in the $\eta \rightarrow 0$ limit, we recover the boundary conditions of Eq. (4.49) applied to that particular field, whose zero mode obtains a mass of $M_C/2$.

If we take this completion literally, then we would want to restrict $\cot \eta$ by the condition that the coupling λ remain perturbative. However, we are not wedding ourselves to any particular origin for the boundary conditions. We will take the example just discussed as motivation for the consistency of Eq. (4.49), and work in the exact $\eta = 0$ limit. The reader who disagrees with this approach may simply consider our results an approximation to the explicit ultraviolet completion discussed above when $\cot \eta$ is taken to be somewhat strongly coupled.

In the case where the bulk $\mathbf{27}$'s are the three standard model generations, the exotic N , E and B fields will become massive given our choice of brane spurions. Our results for gauge unification will not be affected since these fields form the complete $SU(5)$ reps $5 \oplus \bar{5} \oplus \mathbf{1} \oplus \mathbf{1}$. Another possibility is to place the $\mathbf{27}$ and $\bar{\mathbf{27}}$ Higgs multiplets in the bulk. In this case, we have a tower of KK modes beginning at $M_C/2$ for the massive components, and a tower beginning at M_C for those components with massless zero modes. This leads to an additional threshold correction of the type discussed in Section IV. We find that this tends to spoil unification for values of $1/R$ that are significantly smaller than the conventional supersymmetric unification scale, $M_u = 2 \times 10^{16}$ GeV. Thus, this possibility may be realized if $1/R$ and M_u are within a factor of a few of each other so that unification

is preserved to good approximation.

4.6 Conclusions

The breaking of gauge symmetries through the choice of consistent boundary conditions on an extra dimensional interval provides a powerful new tool for model building. Unlike the orbifold case, a more general choice of boundary conditions allows one to reduce the rank of the bulk gauge group. Aside from the breaking of electroweak symmetry [99, 104, 105, 106, 107, 108, 109, 110], this approach is naturally of interest in the breaking of grand unified and other gauge extensions of the standard model that have gauge groups with rank greater than four. We have demonstrated this explicitly in the case of gauge trinification. We obtained boundary conditions necessary to break the trinified gauge group directly down to that of the standard model, while preserving the GUT-scale relation $\sin^2 \theta_W = 3/8$. Symmetry breaking was introduced consistently in terms of spurions localized on the πR brane. In the Higgsless limit, in which these spurions are taken to infinity, the massive gauge multiplets have zero-modes at $M_c/2$, where M_c is the compactification scale. In the same limit, all exotic matter and Higgs fields are decoupled from the theory, and Higgs-mediated proton decay is avoided. We retain the light Higgs doublets of the MSSM, so that light fermion masses may be easily obtained. By placing the gauge multiplets in the bulk, there is power law running due to the KK modes. As in other 5D unified theories with gauge symmetries broken on a boundary [119], we find that the running of the differences $\alpha_i^{-1} - \alpha_j^{-1}$ remains logarithmic. For the massive gauge fields in our trinified theory, we find that unification is preserved, and that the scale at which the couplings unify is increased. For $M_c \sim 2 \times 10^{15}$ GeV, the gauge couplings unify at the 5D Planck mass 1.4×10^{17} GeV, with a percent accuracy at the one-loop level.

CHAPTER 5

Improved Trinification in 5D

5.1 Introduction

Extra dimensions provide a variety of new tools for building realistic Grand Unified Theories (GUTs). In orbifold compactifications, for example, different components of a GUT multiplet may be assigned different parities under reflections about the orbifold fixed points. Judicious choices can yield a particle spectrum in which all unwanted states (for example, color-triplet Higgs fields) appear at or near the compactification scale $1/R$. A related technique that has received some attention in the context of electroweak symmetry breaking is the Higgsless mechanism [99, 123, 124, 125]. In this approach, a more general set of boundary conditions are employed, allowing for the reduction in the rank of the gauge group. These boundary conditions can be thought of as arising from a boundary Higgs sector that has been decoupled from the theory. Interestingly, in this decoupling limit, the spectrum of massive gauge fields is determined by $1/R$ rather than the boundary vacuum expectation values (vevs) [119]. While electroweak symmetry breaking clearly necessitates the reduction in rank of the gauge group, the same is true of GUTs with rank greater than four. This was the motivation for the study of boundary breaking in trinified

theories [126], one of the simplest unified theories of rank six. Other recent work on trinified theories in extra dimensions appears in Ref. [127, 128, 129, 115, 130].

While Ref. [126] explored the usefulness of generalized boundary conditions in breaking a simple unified theory of rank greater than four, the models presented there had a number of shortcomings: electroweak symmetry breaking was still accomplished by introducing chiral Higgs multiplets and a fine-tuning was required to keep these fields in the low-energy spectrum. In this chapter, we present simpler models that avoid these problems. Electroweak Higgs doublets will be identified as components of gauge fields, an economical approach known as gauge-Higgs unification in the literature [31, 32, 33, 34, 35], and these Higgs fields will remain light down to the weak scale due to an R-symmetry [131]. In addition, we present one construction in which an additional gauge group factor provides both for a unified boundary condition on the standard model gauge couplings and also serves as an origin for the electroweak Higgs fields. This yields a trinified theory without the cumbersome (though entirely conventional) cyclic symmetry whose only purpose is to maintain the equality of GUT-scale gauge couplings. The two models we present are consistent with the constraints from proton decay and gauge coupling unification.

5.2 $SU(3)^3 \times \mathbf{Z}_3$

Conventional trinification is based on the gauge group $G_T = SU(3)_C \times SU(3)_L \times SU(3)_R \times \mathbf{Z}_3$. The discrete symmetry cyclically permutes the group labels C, L, and R, which maintains a single gauge coupling g at the unification scale. Gauge and matter fields transform under the 24- and 27-dimensional representations, respectively, with

decompositions

$$\begin{aligned}
24 &= (8, 1, 1) \oplus (1, 8, 1) \oplus (1, 1, 8) , \\
27 &= (1, 3, \bar{3}) \oplus (\bar{3}, 1, 3) \oplus (3, \bar{3}, 1) ,
\end{aligned} \tag{5.1}$$

under the C, L, R gauge factors. In the usual Gell-Mann basis, weak SU(2) is generated by T_L^a for $a = 1 \dots 3$, while hypercharge, in its standard model normalization, is generated by

$$Y = -\frac{1}{\sqrt{3}}(T_L^8 + \sqrt{3}T_R^3 + T_R^8) . \tag{5.2}$$

With the hypercharge gauge coupling identified as $\sqrt{3/5}g$, the choices above yield the standard GUT-scale prediction $\sin^2 \theta_W = 3/8$. This is phenomenologically acceptable in the present context, given the new boundary corrections to unification [119] that we expect generically in extra-dimensional models.

We first consider a model in five dimensions (5D) with G_T chosen as the bulk gauge symmetry. We compactify the extra dimension on an $S^1/(Z_2 \times Z'_2)$ orbifold, labelled by the coordinate y . Defining $y' \equiv y + \pi R/2$, points related by the translation $y \rightarrow y + 2\pi R$ and by the reflections $y \rightarrow -y$ and $y' \rightarrow -y'$, are identified. The physical region in y is thus reduced to the interval $[0, \pi R/2]$. In addition, we assume $\mathcal{N} = 1$ supersymmetry in 5D. Bulk gauge fields thus form $\mathcal{N} = 2$ 4D hypermultiplets consisting of $\mathcal{N} = 1$ vector $V(A^\mu, \lambda)$ and chiral $\Phi(\sigma + iA_5, \lambda')$ multiplets at each Kaluza-Klein (KK) level. All matter fields are placed on the $\pi R/2$ brane for simplicity.

We now show that the electroweak Higgs doublets of the minimal supersymmetric standard model (MSSM) can be identified with some of the A_5 components of the gauge multiplets. Under the two orbifold parities, we assume the bulk fields transform as follows:

$$\begin{aligned}
V(x^\mu, -y) &= P V(x^\mu, y) P^{-1}, & V(x^\mu, -y') &= P' V(x^\mu, y') P'^{-1} \\
\Phi(x^\mu, -y) &= -P \Phi(x^\mu, y) P^{-1}, & \Phi(x^\mu, -y') &= -P' \Phi(x^\mu, y') P'^{-1} .
\end{aligned} \tag{5.3}$$

Here P and P' are 3×3 matrices that act in gauge group space and have eigenvalues of ± 1 . Noting that the supersymmetric bulk action requires the terms $\mathcal{S}_{5D} \supset \int d^4\theta \frac{2}{g^2} \text{Tr}(\sqrt{2}\partial_5 + \Phi^\dagger)e^{-V}(-\sqrt{2}\partial_5 + \Phi)e^V$ [122], one sees that $\partial_5 V$ and Φ should have the same transformation properties under the orbifold parities. Therefore, although components within a gauge multiplet can transform differently under the parity operations, the relative sign of the vector and chiral multiplets is uniquely determined. With the notation $(P, P') = (P_C \oplus P_L \oplus P_R, P'_C \oplus P'_L \oplus P'_R)$ we choose

$$\begin{aligned} P_C &= \text{diag}(1, 1, 1), & P_L &= \text{diag}(1, 1, -1), & P_R &= \text{diag}(1, 1, -1), \\ P'_C &= \text{diag}(1, 1, 1), & P'_L &= \text{diag}(1, 1, -1), & P'_R &= \text{diag}(1, 1, 1). \end{aligned} \quad (5.4)$$

Parity assignments for the component fields immediately follow:

$$V_C : \left(\begin{array}{cc|c} (+, +) & (+, +) & (+, +) \\ (+, +) & (+, +) & (+, +) \\ \hline (+, +) & (+, +) & (+, +) \end{array} \right), \quad \Phi_C : \left(\begin{array}{cc|c} (-, -) & (-, -) & (-, -) \\ (-, -) & (-, -) & (-, -) \\ \hline (-, -) & (-, -) & (-, -) \end{array} \right), \quad (5.5)$$

$$V_L : \left(\begin{array}{cc|c} (+, +) & (+, +) & (-, -) \\ (+, +) & (+, +) & (-, -) \\ \hline (-, -) & (-, -) & (+, +) \end{array} \right), \quad \Phi_L : \left(\begin{array}{cc|c} (-, -) & (-, -) & (+, +) \\ (-, -) & (-, -) & (+, +) \\ \hline (+, +) & (+, +) & (-, -) \end{array} \right), \quad (5.6)$$

$$V_R : \left(\begin{array}{cc|c} (+, +) & (+, +) & (-, +) \\ (+, +) & (+, +) & (-, +) \\ \hline (-, +) & (-, +) & (+, +) \end{array} \right), \quad \Phi_R : \left(\begin{array}{cc|c} (-, -) & (-, -) & (+, -) \\ (-, -) & (-, -) & (+, -) \\ \hline (+, -) & (+, -) & (-, -) \end{array} \right). \quad (5.7)$$

As we will see shortly, fields that are odd under P have vanishing wave functions at $y = 0$, while those that are odd under P' vanish at $y = \pi R/2$. It follows that the gauge symmetry that is operative at the $\pi R/2$ fixed point is $SU(3)_C \times SU(2)_L \times U(1)_L \times SU(3)_R$, a fact that we will use later. Only fields that are even under both P and P' have massless zero modes, from which we conclude that the total effect of the orbifold projection is to reduce the bulk gauge symmetry to $SU(3)_C \times SU(2)_L \times U(1)_L \times SU(2)_R \times U(1)_R$. Crucially,

two $SU(2)_L$ doublets in the chiral multiplet Φ_L retain massless zero modes, and it follows immediately from Eq. (5.2) that these have hypercharges $Y = \pm\frac{1}{2}$. We identify these superfields with the MSSM Higgs doublets.

We break the remaining gauge symmetry down to that of the MSSM using generalized boundary conditions. To illustrate this approach consider a gauge field A^μ that is even under reflections about $y = 0$. This implies that the 5D wave function for the k^{th} mode has the form

$$A_\mu(x^\nu, y) \sim \cos(M_k y) A_\mu^{(k)}(x^\nu) , \quad (5.8)$$

for y in the interval $0 \leq y \leq \pi R/2$. Imposing the boundary condition

$$\partial_5 A^\mu(y = \pi R/2) = V A^\mu(y = \pi R/2) , \quad (5.9)$$

one obtains the following transcendental equation for M_k

$$M_k \tan(M_k \pi R/2) = -V . \quad (5.10)$$

In the large V limit the KK spectrum is well approximated by

$$M_k \approx M_c \frac{(2k+1)}{2} \left(1 + \frac{M_c}{\pi V} + \dots\right), \quad k = 0, 1, \dots , \quad (5.11)$$

where we define the compactification scale $M_c \equiv 2/R$. Thus, in the limit $V \rightarrow \infty$, the spectrum reduces to a tower whose low lying states are $M_c/2, 3M_c/2, 5M_c/2, \text{etc.}$ This is shifted by $M_c/2$ relative to the tower one would obtain if V were set to zero. The symmetry breaking parameter V has dimensions of mass and can be associated with products of the form $g^2 v^2$, where g is a five-dimensional gauge coupling and v a boundary vev. Since v generically sets the scale of the physical states in the boundary symmetry-breaking sector, the limit $V \rightarrow \infty$ corresponds to the decoupling of the boundary Higgs fields from the theory. It is worth noting that in the supersymmetric case, the spectrum of the additional scalar and fermionic components of Φ and V are the same as in Eq. (5.11), as a consequence of gauge invariance and unbroken supersymmetry [119].

In the present context, we could introduce two 27 boundary Higgs fields, whose $(\mathbf{1}, \mathbf{3}, \bar{\mathbf{3}})$ components have appropriate vevs to break $SU(3)^3$ down to the standard model gauge group. However, we have already noted that the orbifold projection has reduced the gauge symmetry to $SU(3)_C \times SU(2)_L \times U(1)_L \times SU(3)_R$ at the $\pi R/2$ brane. This allows us to choose much simpler Higgs representations at this boundary to implement the symmetry breaking:

$$\chi_1 = \bar{\chi}_1 = (0 \ 0 \ v_1) \quad \chi_2 = \bar{\chi}_2 = (0 \ v_2 \ v_3). \quad (5.12)$$

Here the field χ is an $SU(3)_R$ triplet with $U(1)_L$ charge $+1/\sqrt{3}$, and $\bar{\chi}$ has conjugate quantum numbers. Both χ_i and $\bar{\chi}_i$ are singlets under color and $SU(2)_L$, and are together anomaly free. They represent the one relevant row of the $(\mathbf{1}, \mathbf{3}, \bar{\mathbf{3}})$ representation used to break the unified symmetry in conventional trinified models. The real vevs shown in χ_1 and χ_2 are completely general choices, while we assume the same vevs for the barred fields. (The latter choice is consistent with D -flatness.) These vevs are sufficient to break the remaining gauge symmetry down to that of the standard model. Note, however, that a realistic potential may require additional fields.

How do these boundary vevs affect the spectra of fields transforming as $(+, +)$, $(-, -)$, $(-, +)$, and $(+, -)$ under our orbifold reflections? First, the fields $A^\mu(x^\nu, y)$ whose wave functions are odd at the $y = \pi R/2$ brane (corresponding to parities $(\pm, -)$), vanish at that endpoint. Therefore, these KK towers are unaffected by the boundary vevs, and are given by $M_n(-, -) = (n+1)M_c$ and $M_n(+, -) = (n+1/2)M_c$, for $n = 0, 1, \dots$. As discussed above, the $(+, +)$ fields acquire a massive tower $M_n(+, +, V \rightarrow \infty) = (n+1/2)M_c$. Finally, consider the $(-, +)$ fields. Since these wave functions are odd at the $y = 0$ brane they have the general form

$$A_\mu(x^\nu, y) \sim \sin(M_k y) A_\mu^{(k)}(x^\nu). \quad (5.13)$$

Imposing the boundary condition in Eq. (5.9) yields the transcendental equation

$$M_k \cot(M_k \pi R/2) = V, \quad (5.14)$$

which implies a KK tower

$$M_k \approx M_c k \left(1 + \frac{M_c}{\pi V} + \dots\right), \quad k = 1, 2, \dots, \quad (5.15)$$

in the large V limit.

In the present case, the boundary conditions following from the existence of the χ and $\bar{\chi}$ vacuum expectation values may be written

$$\partial_5 A_\mu^i(x^\nu, \pi R/2) = V_{ij} A_\mu^j(x^\nu, \pi R/2), \quad (5.16)$$

where V_{ij} is a matrix in the space of the $SU(3)_L \times SU(3)_R$ gauge fields. The entries of this matrix were considered explicitly in Ref. [126], and have the form $\sum_i c_i g^2 v_i^2$, where the v_i are defined in Eq. (5.12) and the c_i are numerical coefficients. The precise form of V_{ij} and the values of the c_i are irrelevant for the present analysis since we will always take the $g^2 v_i^2$ to be large compared to M_c . In this limit, the spectra of KK modes become independent of these details, and we obtain one of six possible towers already discussed: $(+, -)$, $(-, -)$, $(+, +, V = 0)$, $(+, +, V \rightarrow \infty)$, $(-, +, V = 0)$, and $(-, +, V \rightarrow \infty)$.

As noted earlier, matter fields are located at the $\pi R/2$ fixed point. Although the $SU(3)^3$ $\mathbf{27}$ s decompose into a direct sum of representations under the unbroken gauge symmetry at $\pi R/2$, all of these components must be retained in order to have an anomaly-free theory that reproduces complete MSSM generations in the low-energy theory. We now show that the exotic matter content of the $\mathbf{27}$ s become massive via couplings to the boundary Higgs fields χ and $\bar{\chi}$, and decouple from the theory as the vevs v_i are taken large. We first decompose the $\mathbf{27}$ under the unbroken $SU(3)_C \times SU(2)_L \times U(1)_L \times SU(3)_R$ symmetry at $y = \pi R/2$,

$$\mathbf{27} = L(\mathbf{1}, \mathbf{2}, \bar{\mathbf{3}})_q + e^c(\mathbf{1}, \mathbf{1}, \bar{\mathbf{3}})_{-2q} + q^c(\bar{\mathbf{3}}, \mathbf{1}, \mathbf{3})_0 + Q(\mathbf{3}, \mathbf{2}, \mathbf{1})_{-q} + B(\mathbf{3}, \mathbf{1}, \mathbf{1})_{2q}, \quad (5.17)$$

where the $U(1)_L$ charge $q = 1/(2\sqrt{3})$. The notation serves as a reminder of the embedding of standard model fields. In addition, the L multiplet contains a vector-like pair of exotic lepton doublets, (E^0, E^-) and (E^+, E^{0c}) , e^c contains a pair of exotic singlets, N^c and N , while q^c contains the right-handed partners of the exotic left-handed, charge $-1/3$ quarks that make up the multiplet B in its entirety. GUT scale mass terms arise via the superpotential couplings

$$W = h_L(L_\alpha^i L_\beta^j \bar{\chi}_\gamma \epsilon^{\alpha\beta\gamma} \epsilon_{ij}) + \frac{1}{2} h_Q(q_i^{c\alpha} B^j \bar{\chi}_\beta \delta_j^i \delta_\alpha^\beta). \quad (5.18)$$

Expanding Eq.(5.18) produces the low-energy matter content of minimal trinified theories. The right-handed d and B quarks mix leaving one linear combination massless to be identified with the physical d_R quark. Similarly, only one linear combination of the left-handed lepton doublets receives a mass from the first term in Eq. (5.18). Thus, the low-energy spectrum consists of the particle content of the MSSM, as well as the singlets N and N^c . These can be made massive as well by including higher-dimension operators in the superpotential of the form, $(e^c \chi_i)^2/\Lambda$, where Λ is the cutoff of the effective theory. Thus, unlike the model in Ref. [126], no additional fields need to be included at the boundary to rid the low-energy theory of the singlets.

Having recovered the MSSM particle content, we now consider how to obtain Yukawa couplings involving the electroweak Higgs doublets. Since we have identified the Higgs doublets with components of the bulk adjoint chiral superfield Φ , which transforms nonlinearly under a gauge transformation (*i.e.*, $\Phi \rightarrow e^\Lambda(\Phi - \sqrt{2}\partial_5)e^{-\Lambda}$), no local Yukawa couplings are possible. However, the solution to this problem is well known in the literature on 5D gauge-Higgs unification models: one may couple the Higgs doublets to the matter fields at the fixed point via Wilson loop operators [35, 131]. The Wilson line operator $\mathcal{H} = \mathcal{P} \exp(\int_{y_i}^{y_f} \frac{1}{\sqrt{2}} \Phi dy)$, where \mathcal{P} represents the path ordered product, is a non-local object that transforms linearly under the 5D gauge transformation at points y_i and y_f , $\mathcal{H} \rightarrow e^\Lambda|_{y_f} \mathcal{H} e^{-\Lambda}|_{y_i}$. Choosing $y_i = y_f = \pi R/2$ and a path that wraps around the extra di-

mension, one obtains a Wilson loop operator that transforms linearly at the orbifold fixed point where our matter fields are located: $\mathcal{H} \rightarrow e^\Lambda \mathcal{H} e^{-\Lambda}$, with $\Lambda \equiv \Lambda(x^\mu, y = \pi R/2)$. We focus on the doublet components of \mathcal{H} , which we call $H(\mathbf{1}, \mathbf{2}, \mathbf{1})_{3q}$ and $\bar{H}(\mathbf{1}, \mathbf{2}, \mathbf{1})_{-3q}$, using the notation of Eq. (5.17). Yukawa couplings originate at the $\pi R/2$ brane via the interactions

$$W = \frac{1}{\Lambda} \bar{\chi} L e^c H + \frac{1}{\Lambda} \bar{\chi} Q q^c H + \frac{1}{\Lambda^2} \chi_1 \chi_2 Q q^c \bar{H} \quad , \quad (5.19)$$

after the χ and $\bar{\chi}$ fields develop vevs. Here Λ is a cutoff of the effective theory. Note that in the decoupling limit $v_i \rightarrow \Lambda \rightarrow \infty$, none of the terms in Eq. (5.19) are suppressed; this is an indication that the low-energy theory is restricted only by standard model gauge symmetry at $y = \pi R/2$.

We resolve the μ problem in our model by using the $U(1)_R$ symmetry of the bulk action. Under this symmetry, the superspace coordinate θ transforms with charge $+1$, while V and Φ are neutral. An $H\bar{H}$ term is not allowed since the superpotential must have R -charge -2 . We may induce a small μ parameter by coupling the Higgs fields to a singlet X with R -charge -2 , via the superpotential coupling $XH\bar{H}$. The μ parameter is generated if the X field develops a vev, which can happen naturally due to supersymmetry-breaking effects, as in the next-to-minimal supersymmetric standard model. Note that this mechanism works assuming we impose only a discrete subgroup of $U(1)_R$, which avoids any unwanted R -axions. Assuming the χ and $\bar{\chi}$ have R -charge zero and each matter field -1 , then the Yukawa couplings in Eq. (5.19) are allowed and a Z_4 subgroup of $U(1)_R$ is sufficient.

Finally, we consider the issue of gauge coupling unification. The possible towers of KK modes are described by either $(n + 1/2)M_c > 0$ or $nM_c > 0$, for n an integer. The supersymmetric beta functions for the fields charged under the standard model gauge groups are shown in Table 5.1. Note that only two exotic (V, Φ) multiplets, with charges $(\mathbf{1}, \mathbf{1}, \mathbf{1})$ and $(\mathbf{1}, \mathbf{1}, -\mathbf{1})$, respectively, under $SU(3)_C \times SU(2)_W \times U(1)_Y$ have KK towers

	(b_3, b_2, b_1)	$(\bar{b}_3, \bar{b}_2, \bar{b}_1)$
$(V, \Phi)_{321}$	$(-9, -6, 0)$	$(-6, -4, 0)$
$(V, \Phi)_{(1,2,\pm 1/2)}$	$(0, 1, \frac{3}{5})$	$(0, -2, -\frac{6}{5})$
$(V, \Phi)_{(1,1,\pm 1)}$	-	$(0, 0, -\frac{24}{5})$
Matter	$(6, 6, 6)$	-
Total	$(-3, 1, \frac{33}{5})$	$(-6, -6, -6)$

TABLE 5.1: Contributions to the beta function coefficients from the zero modes (b_i) and the KK levels (\bar{b}_i). Here the Φ represent chiral multiplets in the adjoint representation. Results in the second and third lines represent sums over all fields with the stated quantum numbers.

that are shifted down by $M_c/2$ due to the boundary Higgs vevs. Notice that if all the KK towers were aligned, they would contribute universally to the gauge running. As first pointed out in Ref. [119], the shifted spectra contribute as a tower of threshold corrections; while the power-law running is still universal, the running of the differences $\alpha_i^{-1} - \alpha_j^{-1}$ is logarithmic. With the notation $\delta_i(\mu) \doteq \alpha_i^{-1}(\mu) - \alpha_1^{-1}(\mu)$, for $i = 2$ or 3 , the differential running above the first KK threshold is given by

$$\delta_i(\mu) = \delta_i(M_c/2) - \frac{1}{2\pi} R_i(\mu) \quad , \quad (5.20)$$

where

$$R_2(\mu) = -\frac{28}{5} \log\left(\frac{\mu}{M_c/2}\right) - \frac{12}{5} \sum_{0 < n M_c < \mu} \log\left(\frac{\mu}{n M_c}\right) + \frac{12}{5} \sum_{0 < (n+1/2) M_c < \mu} \log\left(\frac{\mu}{[n+1/2] M_c}\right), \quad (5.21)$$

$$R_3(\mu) = -\frac{48}{5} \log\left(\frac{\mu}{M_c/2}\right) - \frac{12}{5} \sum_{0 < n M_c < \mu} \log\left(\frac{\mu}{n M_c}\right) + \frac{12}{5} \sum_{0 < (n+1/2) M_c < \mu} \log\left(\frac{\mu}{[n+1/2] M_c}\right). \quad (5.22)$$

Note that the last two terms in each equation above would cancel if the KK-towers were aligned, and one would obtain the differential running of the MSSM. Numerical study of these equations reveal that unification is preserved, but that the scale of unification M_U is delayed. For example, for $M_C = 4 \times 10^{14}$ GeV we find $M_U \approx 8 \times 10^{16}$ GeV, which is approximately the 5D Planck scale. For $M_C = 2 \times 10^{16}$ GeV we find $M_U = 2.8 \times 10^{16}$ GeV, which simply demonstrates that there is a limit in which most of the KK

towers do not contribute and MSSM unification is recovered. For $4 \times 10^{14} \text{ GeV} < M_U < 2 \times 10^{16} \text{ GeV}$ we find that the α^{-1} unify at well below the 1% level, ignoring possible boundary effects. Thus, our extra-dimensional construction does not lead to any problems with successful gauge unification. Discussion of other possible corrections to unification may be found in Ref. [126] and will not be discussed further here.

Finally, we note that there is no proton decay in this model. In ordinary trinification, proton decay is mediated by colored Higgses that are part of a **27**. In our model, the smaller gauge symmetry at the $\pi R/2$ fixed point allowed us to include symmetry breaking fields in much smaller representations, without dangerous colored components. Since there is no proton decay from the gauge sector of trinified theories, our model is safe from these effects.

5.3 $SU(9) \times SU(3)^3$

Before concluding, we wish briefly to present an alternative starting point that can provide a common origin for the GUT-scale equality of gauge couplings (without the Z_3 symmetry) and the existence of the electroweak Higgs doublets. We consider an $SU(9) \times SU(3)^3$ bulk gauge theory on a $S^1/(Z_2 \times Z'_2)$ orbifold. The $SU(3)_C \times SU(3)_L \times SU(3)_R$ symmetry of our previous model is identified with the diagonal subgroup of an $SU(3)^3$ living within $SU(9)$ and the other $SU(3)^3$ factor, so that

$$\frac{1}{g_{(C,L,R)}^2} = \frac{1}{g_{SU(9)}^2} + \frac{1}{g_{(C',L',R')}^2}. \quad (5.23)$$

Here C', L' , and R' refer to the three $SU(3)$ factors present before symmetry breaking. If these $SU(3)$ gauge groups are somewhat strongly coupled, then Eq. (5.23) leads to an approximate unified boundary condition for the diagonal subgroup. This is precisely the idea of “unification without unification” described in Ref. [132]. Note that the bulk gauge symmetry can be thought of as a two-site deconstructed sixth dimension, with symmetry

broken at a boundary. Generalizations to replicated $SU(9)$ factors are also interesting, since the primed gauge couplings do not have to be made particularly large. In any case, the $SU(9)$ vector multiplet decomposes under the diagonal $SU(3)^3$ subgroup as

$$V_9 : \left(\begin{array}{c|c|c} (8, \mathbf{1}, \mathbf{1}) & (\mathbf{3}, \bar{\mathbf{3}}, \mathbf{1}) & (\mathbf{3}, \mathbf{1}, \bar{\mathbf{3}}) \\ \hline (\bar{\mathbf{3}}, \mathbf{3}, \mathbf{1}) & (\mathbf{1}, \mathbf{8}, \mathbf{1}) & (\mathbf{1}, \mathbf{3}, \bar{\mathbf{3}}) \\ \hline (\bar{\mathbf{3}}, \mathbf{1}, \mathbf{3}) & (\mathbf{1}, \bar{\mathbf{3}}, \mathbf{3}) & (\mathbf{1}, \mathbf{1}, \mathbf{8}) \end{array} \right) . \quad (5.24)$$

We know from ordinary trinification that fields with the quantum numbers of Higgs doublets live in the $(\mathbf{1}, \mathbf{3}, \bar{\mathbf{3}})$ representation and its conjugate. We therefore wish to find parity assignments that preserve these elements of the chiral adjoint Φ as well. With parity transformations defined as in Eq. (5.3), we choose

$$\begin{aligned} P_{SU(9)} &= \text{diag}(1, 1, 1, 1, 1, 1, 1, -1, 1), & P'_{SU(9)} &= \text{diag}(1, 1, 1, -1, -1, 1, 1, 1, 1) , \\ P_C &= \text{diag}(1, 1, 1), & P_L &= \text{diag}(1, 1, -1), & P_R &= \text{diag}(1, 1, -1), \\ P'_C &= \text{diag}(1, 1, 1), & P'_L &= \text{diag}(1, 1, 1), & P'_R &= \text{diag}(1, 1, 1). \end{aligned} \quad (5.25)$$

One finds, for example, that the $(\mathbf{1}, \mathbf{3}, \bar{\mathbf{3}})$ components of the $SU(9)$ chiral adjoint Φ_9 has parities

$$\Phi_9(\mathbf{1}, \mathbf{3}, \bar{\mathbf{3}}) : \left(\begin{array}{ccc} (-, +) & (+, +) & (-, +) \\ (-, +) & (+, +) & (-, +) \\ (-, -) & (+, -) & (-, -) \end{array} \right) , \quad (5.26)$$

which indicates the location of one of the Higgs doublets. Aside from the corresponding $(+, +)$ entries in the $(\mathbf{1}, \bar{\mathbf{3}}, \mathbf{3})$ block, all other components of Φ_9 have no zero modes.

The orbifold parities in Eq. (5.25) break the $SU(9)$ symmetry to $SU(8) \times U(1)$ at the $y = 0$ fixed point, $SU(7) \times SU(2) \times U(1)$ at $y = \pi R/2$ and to $SU(6) \times SU(2) \times U(1) \times U(1)'$ overall. The $SU(3)^3$ factors are broken to $SU(3)_C \times SU(2)_L \times SU(2)_R \times U(1)_L \times U(1)_R$ overall, but are unbroken at $y = \pi R/2$. Thus, the most natural way to include matter fields is by introducing complete 27 's at the $\pi R/2$ fixed point.

The breaking of the remaining gauge symmetry down to that of the MSSM can be done with a boundary Higgs sector, as in our previous model. To determine the necessary representations, we may pretend the $SU(3)^3$ factor is embedded in another $SU(9)$, and use the fact that a Higgs $\Sigma \sim (9, \bar{9})$ with diagonal vevs will leave a diagonal $SU(9)$ unbroken. A straightforward decomposition of Σ in terms of the actual gauge symmetry at $\pi R/2$, $SU(7) \times SU(2) \times U(1) \times SU(3)^3$, gives the desired representations. These break the remaining symmetry down to the diagonal subgroup $SU(3)_C \times SU(2)_L \times U(1)_L \times SU(2)'_R \times U(1)'_R$. We may recover the standard model gauge group by including $SU(9)$ singlet, $(1, 3, \bar{3})$ and $(1, \bar{3}, 3)$ boundary Higgs fields, with the same pattern of vevs found in conventional trinified theories. Yukawa couplings can arise via higher dimension operators involving the boundary Higgs fields, and are unsuppressed in the Higgsless limit, as shown in the previous model; the decoupling of exotic matter fields also works in the same way. Color-triplet components of Φ_9 exist, so that proton decay is not absent, but doublet-triplet splitting is explained naturally via the orbifold projection.

5.4 Conclusions

We have presented improved models of 5D trinification. In the first model, unified symmetry was broken by a combination of orbifold projections and a boundary Higgs sector that could be decoupled from the theory. Electroweak Higgs fields appeared economically as the fifth components of gauge fields. The model demonstrated the existence of a consistent low-energy theory in which no chiral Higgs fields needed to be added to the theory in an ad hoc way. This model is free of proton decay and consistent with gauge unification. In the second model, we showed that an additional $SU(9)$ gauge factor could provide a common origin for the unified boundary condition on the standard model gauge couplings, and the origin of the electroweak Higgs, via gauge-Higgs unification. Both models provide new and explicit realizations of 5D trinified GUTs, and demonstrate a

Higgsless approach that can be applied to other unified theories with rank greater than four.

BIBLIOGRAPHY

- [1] M. Acciarri et al. (L3), Phys. Lett. **B479**, 101 (2000), hep-ex/0002034.
- [2] H.-C. Cheng, K. T. Matchev, and M. Schmaltz, Phys. Rev. **D66**, 036005 (2002), hep-ph/0204342.
- [3] M. Peskin and D. Schroeder, An Introduction to Quantum Field Theory, Perseus Books (1995).
- [4] S. Eidelman et al. (Particle Data Group), Phys. Lett. **B592**, 1 (2004).
- [5] E. Kolb and M. Turner, The Early Universe, Perseus Books (1993).
- [6] S. Pokorski (2005), hep-ph/0502132.
- [7] H. Georgi and S. L. Glashow, Phys. Rev. Lett. **32**, 438 (1974).
- [8] N. Arkani-Hamed, S. Dimopoulos, and G. R. Dvali, Phys. Lett. **B429**, 263 (1998), hep-ph/9803315.
- [9] I. Antoniadis, N. Arkani-Hamed, S. Dimopoulos, and G. R. Dvali, Phys. Lett. **B436**, 257 (1998), hep-ph/9804398.
- [10] N. Arkani-Hamed, S. Dimopoulos, and G. R. Dvali, Phys. Rev. **D59**, 086004 (1999), hep-ph/9807344.
- [11] C. D. Hoyle et al., Phys. Rev. **D70**, 042004 (2004), hep-ph/0405262.

- [12] E. G. Adelberger, B. R. Heckel, and A. E. Nelson, *Ann. Rev. Nucl. Part. Sci.* **53**, 77 (2003), hep-ph/0307284.
- [13] L. Randall and R. Sundrum, *Phys. Rev. Lett.* **83**, 3370 (1999), hep-ph/9905221.
- [14] L. Randall and R. Sundrum, *Phys. Rev. Lett.* **83**, 4690 (1999), hep-th/9906064.
- [15] T. Appelquist, H.-C. Cheng, and B. A. Dobrescu, *Phys. Rev.* **D64**, 035002 (2001), hep-ph/0012100.
- [16] H.-C. Cheng, J. L. Feng, and K. T. Matchev, *Phys. Rev. Lett.* **89**, 211301 (2002), hep-ph/0207125.
- [17] D. Majumdar, *Mod. Phys. Lett. A* **18**, 1705 (2003).
- [18] D. Hooper and G. D. Kribs, *Phys. Rev.* **D67**, 055003 (2003), hep-ph/0208261.
- [19] G. Servant and T. M. P. Tait, *Nucl. Phys.* **B650**, 391 (2003), hep-ph/0206071.
- [20] A. J. Buras, A. Poschenrieder, M. Spranger, and A. Weiler, *Nucl. Phys.* **B678**, 455 (2004), hep-ph/0306158.
- [21] N. Seiberg and E. Witten, *JHEP* **09**, 032 (1999), hep-th/9908142.
- [22] F. Ardalan, H. Arfaei, and M. M. Sheikh-Jabbari, *JHEP* **02**, 016 (1999), hep-th/9810072.
- [23] F. Ardalan, H. Arfaei, and M. M. Sheikh-Jabbari, *Nucl. Phys.* **B576**, 578 (2000), hep-th/9906161.
- [24] J. D. Prestage, J. J. Bollinger, W. M. Itano, and D. J. Wineland, *Phys. Rev. Lett.* **54**, 2387 (1985).
- [25] S. K. Lamoreaux, J. P. Jacobs, B. R. Heckel, F. J. Raab, and E. N. Fortson, *Phys. Rev. Lett.* **57**, 3125 (1986).

- [26] R. L. Walsworth and D. F. Phillips (1999), physics/0007062.
- [27] D. Bear, R. E. Stoner, R. L. Walsworth, V. A. Kostelecky, and C. D. Lane, Phys. Rev. Lett. **85**, 5038 (2000), physics/0007049.
- [28] C. E. Carlson, C. D. Carone, and N. Zobin, Phys. Rev. **D66**, 075001 (2002), hep-th/0206035.
- [29] S. Doplicher, K. Fredenhagen, and J. E. Roberts, Commun. Math. Phys. **172**, 187 (1995), hep-th/0303037.
- [30] S. Doplicher, K. Fredenhagen, and J. E. Roberts, Phys. Lett. **B331**, 39 (1994).
- [31] I. Antoniadis, K. Benakli, and M. Quiros, New J. Phys. **3**, 20 (2001), hep-th/0108005.
- [32] N. Haba and Y. Shimizu, Phys. Rev. **D67**, 095001 (2003), hep-ph/0212166.
- [33] G. Burdman and Y. Nomura, Nucl. Phys. **B656**, 3 (2003), hep-ph/0210257.
- [34] I. Gogoladze, Y. Mimura, and S. Nandi, Phys. Lett. **B560**, 204 (2003), hep-ph/0301014.
- [35] C. Csaki, C. Grojean, and H. Murayama, Phys. Rev. **D67**, 085012 (2003), hep-ph/0210133.
- [36] J. Madore, S. Schraml, P. Schupp, and J. Wess, Eur. Phys. J. **C16**, 161 (2000), hep-th/0001203.
- [37] M. Hayakawa, Phys. Lett. **B478**, 394 (2000), hep-th/9912094.
- [38] A. Armoni, Nucl. Phys. **B593**, 229 (2001), hep-th/0005208.
- [39] Y. Liao, JHEP **11**, 067 (2001), hep-th/0110112.

- [40] M. Chaichian, P. Presnajder, M. M. Sheikh-Jabbari, and A. Tureanu, *Eur. Phys. J.* **C29**, 413 (2003), hep-th/0107055.
- [41] M. Chaichian, P. Presnajder, M. M. Sheikh-Jabbari, and A. Tureanu, *Phys. Lett.* **B526**, 132 (2002), hep-th/0107037.
- [42] B. Jurco, L. Moller, S. Schraml, P. Schupp, and J. Wess, *Eur. Phys. J.* **C21**, 383 (2001), hep-th/0104153.
- [43] X. Calmet, B. Jurco, P. Schupp, J. Wess, and M. Wohlgenannt, *Eur. Phys. J.* **C23**, 363 (2002), hep-ph/0111115.
- [44] X. Calmet and M. Wohlgenannt, *Phys. Rev.* **D68**, 025016 (2003), hep-ph/0305027.
- [45] X.-G. He, *Eur. Phys. J.* **C28**, 557 (2003), hep-ph/0202223.
- [46] I. Mocioiu, M. Pospelov, and R. Roiban, *Phys. Lett.* **B489**, 390 (2000), hep-ph/0005191.
- [47] M. Chaichian, M. M. Sheikh-Jabbari, and A. Tureanu, *Phys. Rev. Lett.* **86**, 2716 (2001), hep-th/0010175.
- [48] I. Hinchliffe and N. Kersting, *Phys. Rev.* **D64**, 116007 (2001), hep-ph/0104137.
- [49] S. M. Carroll, J. A. Harvey, V. A. Kostelecky, C. D. Lane, and T. Okamoto, *Phys. Rev. Lett.* **87**, 141601 (2001), hep-th/0105082.
- [50] C. E. Carlson, C. D. Carone, and R. F. Lebed, *Phys. Lett.* **B518**, 201 (2001), hep-ph/0107291.
- [51] A. Anisimov, T. Banks, M. Dine, and M. Graesser, *Phys. Rev.* **D65**, 085032 (2002), hep-ph/0106356.

- [52] C. E. Carlson, C. D. Carone, and R. F. Lebed, Phys. Lett. **B549**, 337 (2002), hep-ph/0209077.
- [53] V. Nazaryan, Phys. Rev. **D67**, 017704 (2003), hep-ph/0210300.
- [54] I. Hinchliffe, N. Kersting, and Y. L. Ma, Int. J. Mod. Phys. **A19**, 179 (2004), hep-ph/0205040.
- [55] J. L. Hewett, F. J. Petriello, and T. G. Rizzo, Phys. Rev. **D64**, 075012 (2001), hep-ph/0010354.
- [56] S. Godfrey and M. A. Doncheski, Phys. Rev. **D65**, 015005 (2002), hep-ph/0108268.
- [57] C. E. Carlson and C. D. Carone, Phys. Rev. **D65**, 075007 (2002), hep-ph/0112143.
- [58] E. O. Iltan, Phys. Rev. **D66**, 034011 (2002), hep-ph/0204332.
- [59] E. O. Iltan, New J. Phys. **4**, 54 (2002), hep-ph/0204129.
- [60] K. Morita, Prog. Theor. Phys. **108**, 1099 (2003), hep-th/0209234.
- [61] H. Kase, K. Morita, Y. Okumura, and E. Umezawa, Prog. Theor. Phys. **109**, 663 (2003), hep-th/0212176.
- [62] H. S. Snyder, Phys. Rev. **71**, 38 (1947).
- [63] A. Connes and J. Lott, Nucl. Phys. Proc. Suppl. **18B**, 29 (1991).
- [64] A. Connes, J. Math. Phys. **36**, 6194 (1995).
- [65] A. Connes, Commun. Math. Phys. **182**, 155 (1996), hep-th/9603053.

- [66] A. Connes, M. R. Douglas, and A. Schwarz, JHEP **02**, 003 (1998), hep-th/9711162.
- [67] M. Acciarri et al. (L3), Phys. Lett. **B384**, 323 (1996).
- [68] M. Acciarri et al. (L3), Phys. Lett. **B413**, 159 (1997).
- [69] M. Acciarri et al. (L3), Phys. Lett. **B475**, 198 (2000), hep-ex/0002036.
- [70] P. Achard et al. (L3), Phys. Lett. **B531**, 28 (2002), hep-ex/0202025.
- [71] P. Abreu et al. (DELPHI), Phys. Lett. **B491**, 67 (2000), hep-ex/0103005.
- [72] O. J. P. Eboli, A. A. Natale, and S. F. Novaes, Phys. Lett. **B271**, 274 (1991).
- [73] I. Antoniadis, Phys. Lett. **B246**, 377 (1990).
- [74] K. R. Dienes, E. Dudas, and T. Gherghetta, Phys. Lett. **B436**, 55 (1998), hep-ph/9803466.
- [75] K. R. Dienes, E. Dudas, and T. Gherghetta, Nucl. Phys. **B537**, 47 (1999), hep-ph/9806292.
- [76] P. Nath and M. Yamaguchi, Phys. Rev. **D60**, 116006 (1999), hep-ph/9903298.
- [77] P. Nath and M. Yamaguchi, Phys. Rev. **D60**, 116004 (1999), hep-ph/9902323.
- [78] M. Masip and A. Pomarol, Phys. Rev. **D60**, 096005 (1999), hep-ph/9902467.
- [79] A. Strumia, Phys. Lett. **B466**, 107 (1999), hep-ph/9906266.
- [80] R. Casalbuoni, S. De Curtis, D. Dominici, and R. Gatto, Phys. Lett. **B462**, 48 (1999), hep-ph/9907355.
- [81] C. D. Carone, Phys. Rev. **D61**, 015008 (2000), hep-ph/9907362.

- [82] T. G. Rizzo and J. D. Wells, Phys. Rev. **D61**, 016007 (2000), hep-ph/9906234.
- [83] D. Majumdar, Phys. Rev. **D67**, 095010 (2003), hep-ph/0209277.
- [84] H.-C. Cheng, K. T. Matchev, and M. Schmaltz, Phys. Rev. **D66**, 056006 (2002), hep-ph/0205314.
- [85] E. De Pree and M. Sher (2005), hep-ph/0507313.
- [86] V. Barger and R. Phillips, Frontiers in Physics **71** (1996).
- [87] G. G. Hanson, Nucl. Instrum. Meth. **A503**, 96 (2003).
- [88] C. M. Ankenbrandt et al., Phys. Rev. ST Accel. Beams **2**, 081001 (1999), physics/9901022.
- [89] K. Monig, LC-PHSM-2000-60-TESLA (available at <http://www-flc.desy.de/lcnotes/>).
- [90] G. Wilson, LC-PHSM-2001-009-TESLA (available at <http://www-flc.desy.de/lcnotes/>).
- [91] Y. Kawamura, Prog. Theor. Phys. **103**, 613 (2000), hep-ph/9902423.
- [92] Y. Kawamura, Prog. Theor. Phys. **105**, 999 (2001), hep-ph/0012125.
- [93] Y. Kawamura, Prog. Theor. Phys. **105**, 691 (2001), hep-ph/0012352.
- [94] A. Hebecker and J. March-Russell, Nucl. Phys. **B613**, 3 (2001), hep-ph/0106166.
- [95] A. Hebecker and J. March-Russell, Nucl. Phys. **B625**, 128 (2002), hep-ph/0107039.
- [96] L. J. Hall, Y. Nomura, T. Okui, and D. R. Smith, Phys. Rev. **D65**, 035008 (2002), hep-ph/0108071.

- [97] L. J. Hall and Y. Nomura, Phys. Rev. **D65**, 125012 (2002), hep-ph/0111068.
- [98] L. J. Hall and Y. Nomura, Phys. Rev. **D66**, 075004 (2002), hep-ph/0205067.
- [99] C. Csaki, C. Grojean, H. Murayama, L. Pilo, and J. Terning, Phys. Rev. **D69**, 055006 (2004), hep-ph/0305237.
- [100] I. Antoniadis, C. Munoz, and M. Quiros, Nucl. Phys. **B397**, 515 (1993), hep-ph/9211309.
- [101] I. Antoniadis and K. Benakli, Phys. Lett. **B326**, 69 (1994), hep-th/9310151.
- [102] L. J. Hall and Y. Nomura, Phys. Lett. **B532**, 111 (2002), hep-ph/0202107.
- [103] C.-S. Huang, J. Jiang, T.-j. Li, and W. Liao, Phys. Lett. **B530**, 218 (2002), hep-th/0112046.
- [104] R. Foadi, S. Gopalakrishna, and C. Schmidt, JHEP **03**, 042 (2004), hep-ph/0312324.
- [105] J. Hirn and J. Stern, Eur. Phys. J. **C34**, 447 (2004), hep-ph/0401032.
- [106] G. Cacciapaglia, C. Csaki, C. Grojean, and J. Terning, Phys. Rev. **D70**, 075014 (2004), hep-ph/0401160.
- [107] S. Gabriel, S. Nandi, and G. Seidl, Phys. Lett. **B603**, 74 (2004), hep-ph/0406020.
- [108] R. S. Chivukula, E. H. Simmons, H.-J. He, M. Kurachi, and M. Tanabashi, Phys. Rev. **D70**, 075008 (2004), hep-ph/0406077.
- [109] C. Schwinn, Phys. Rev. **D69**, 116005 (2004), hep-ph/0402118.
- [110] T. Ohl and C. Schwinn, Phys. Rev. **D70**, 045019 (2004), hep-ph/0312263.

- [111] S. Glashow, 5th workshop on grand unification:proceedings Workshop on Grand Unification,Eds. K. Kang, H. Fried, P. Frampton **5**, 10 (1984).
- [112] K. S. Babu, X.-G. He, and S. Pakvasa, Phys. Rev. **D33**, 763 (1986).
- [113] G. Lazarides and C. Panagiotakopoulos, Phys. Lett. **B336**, 190 (1994), hep-ph/9403317.
- [114] G. Lazarides and C. Panagiotakopoulos, Phys. Rev. **D51**, 2486 (1995), hep-ph/9407286.
- [115] K.-S. Choi and J. E. Kim, Phys. Lett. **B567**, 87 (2003), hep-ph/0305002.
- [116] J. E. Kim, Phys. Lett. **B564**, 35 (2003), hep-th/0301177.
- [117] S. Willenbrock, Phys. Lett. **B561**, 130 (2003), hep-ph/0302168.
- [118] G. R. Dvali and Q. Shafi, Phys. Lett. **B339**, 241 (1994), hep-ph/9404334.
- [119] Y. Nomura, D. R. Smith, and N. Weiner, Nucl. Phys. **B613**, 147 (2001), hep-ph/0104041.
- [120] D. Ghilencea and G. G. Ross, Phys. Lett. **B442**, 165 (1998), hep-ph/9809217.
- [121] C. D. Carone, Phys. Lett. **B454**, 70 (1999), hep-ph/9902407.
- [122] N. Arkani-Hamed, T. Gregoire, and J. Wacker, JHEP **03**, 055 (2002), hep-th/0101233.
- [123] G. Cacciapaglia, C. Csaki, C. Grojean, and J. Terning, Phys. Rev. **D71**, 035015 (2005), hep-ph/0409126.
- [124] C. Schwinn, Phys. Rev. **D71**, 113005 (2005), hep-ph/0504240.

- [125] G. Cacciapaglia, C. Csaki, C. Grojean, M. Reece, and J. Terning (2005), hep-ph/0505001.
- [126] C. D. Carone and J. M. Conroy, Phys. Rev. **D70**, 075013 (2004), hep-ph/0407116.
- [127] A. Demaria and R. R. Volkas, Phys. Rev. **D71**, 105011 (2005), hep-ph/0503224.
- [128] C. D. Carone, Phys. Rev. **D71**, 075013 (2005), hep-ph/0503069.
- [129] J. E. Kim, Phys. Lett. **B591**, 119 (2004), hep-ph/0403196.
- [130] I. Gogoladze, Y. Mimura, and S. Nandi, Phys. Rev. **D69**, 075006 (2004), hep-ph/0311127.
- [131] L. J. Hall, Y. Nomura, and D. R. Smith, Nucl. Phys. **B639**, 307 (2002), hep-ph/0107331.
- [132] N. Weiner (2001), hep-ph/0106097.

VITA

Justin Morgan Conroy

Justin Morgan Conroy was born on November 12, 1977 in Plainfield, New Jersey. He graduated from Mary Washington College, Fredericksburg, Virginia in 2000 with a bachelor's degree in Physics and Mathematics. He entered the graduate program at the College of William Mary, Williamsburg, Virginia in August 2000.